Ground Penetrating Radar-based Deterioration Assessment of Bridge Decks

Ahmad Shami

A Thesis

in

The Department

of

Building, Civil and Environmental Engineering

Presented in Partial Fulfillment of the Requirements

for the Degree of Master of Science (Civil Engineering) at

Concordia University

Montreal, Quebec, Canada

July 2015

CONCORDIA UNIVERSITY

School of Graduate Studies

This is to certify that the thesis prepared

By: **Ahmad Shami**

Entitled: **Ground Penetrating Radar-based Deterioration Assessment of Bridge Decks**

and submitted in partial fulfillment of the requirements for the degree of

Master of Science (Civil Engineering)

complies with the regulations of the University and meets the accepted standards with respect to originality and quality.

Signed by the final examining committee:

_____Chair
Dr. O. Moselhi

_____External Examiner
Dr. G. Gopakumar

_____BCEE Examiner
Dr. A. Bagchi

_____BCEE Examiner
Dr. T. Zayed

_____Supervisor
Dr. T. Zayed

Approved by

_____
Chair of Department or Graduate Program Director

July 8th 2015   _____
Dean of Faculty

ABSTRACT

GROUND PENETRATING RADAR-BASED DETERIORATION ASSESSMENT OF BRIDGE DECKS

Ahmad Shami

The ASCE report card 2013 rated bridges at a grade of C+, implying their condition is moderate and require immediate attention. Moreover, the Federal Highway Administration reported that it is required to invest more than $20.5 billion each year to eliminate the bridge deficient backlog by 2028. In Canada 2012, more than 50% of bridges fall under fair, poor, and very poor categories, where more than $90 billion are required to replace these bridges. Therefore, government agencies should have an accurate way to inspect and assess the corrosiveness of the bridges under their management.

Numerical Amplitude method is one of the most common used methods to interpret Ground Penetrating Radar (GPR) outputs, yet it does not have a fixed and informative numerical scale that is capable of accurately interpreting the condition of bridge decks. To overcome such problem, the present research aims at developing a numerical GPR-based scale with three thresholds and build deterioration models to assess the corrosiveness of bridge decks. Data, for more than 60 different bridge decks, were collected from previous research works and from surveys of bridge decks using a ground-coupled antenna with the frequency of 1.5 GHz. The amplitude values of top reinforcing rebars of each bridge deck were classified into four categories using k-means clustering technique. Statistical analysis was performed on the collected data to check the best-fit

probability distribution and to choose the most appropriate parameters that affect thresholds of different categories of corrosion and deterioration. Monte-Carlo simulation technique was used to validate the value of these thresholds. Moreover, a sensitivity analysis was performed to realize the effect of changing the thresholds on the areas of corrosion. The final result of this research is a four-category GPR scale with numerical thresholds that can assess the corrosiveness of bridge decks. The developed scale has been validated using a case study on a newly constructed bridge deck and also by comparing maps created using the developed scale and other methods. The comparison shows sound and promising results that advance the state of the art of GPR output interpretation and analysis. In addition, deterioration models and curves have been developed using Weibull Distribution based on GPR outputs and corrosion areas. The developed new GPR scale and deterioration models will help the decision makers to assess accurately and objectively the corrosiveness of bridge decks. Hence, they will be able to take the right intervention decision for managing these decks.

ACKNOWLEDGMENTS

TABLE OF CONTENTS

LIST OF TABLES

LIST OF FIGURES

CHAPTER 1 INTRODUCTION

1.1 OVERVIEW

Bridges are vital elements of the infrastructure system in terms of mobility, environment, economy, and development of communities. However, maintaining bridges at a functional and safe levels is not an easy task. The process of assessing and monitoring bridges should be cost effective, efficient, and fit for the purpose (Alani et al. 2013). Therefore, inspectors use many techniques to assess accurately and effectively the corrosion of the bridge decks. These techniques are divided into two main categories: destructive and non-destructive. Destructive techniques (DTs) provide accurate and direct results, but they also cause damage to the element under investigation, and they are expensive and time-consuming. Non-destructive techniques (NDTs) are inexpensive and quick, but they do not provide direct information about the element under inspection.

Visual inspection is one the most common methods used in bridge deck inspection because it is inexpensive and requires a minimal level of experience. However, this inspection method is subjective and can only assess the condition of the bridge deck surface. It cannot assess the condition under the surface of the bridge deck. The other commonly used technique, half-cell potential, can only detect the potential of corrosion and is somewhat expensive. Although the chain drag technique is easy to apply and inexpensive, it can detect only the delimitation in bridge decks. Therefore, this will make ground-penetrating radar (GPR) one of the NDTs whose advantages outweigh its limitations. GPR is an NDT first developed in the 1970s for military purposes, and was then used by construction companies for locating pipes and utility lines (Morey 1998). The first

1

GPR system was sold in 1985 and was first comprehensively documented in the 1990s (Wollny 1998). Today, much research has been done on GPR to develop and widen its usage, especially in assessing the condition of concrete structures. In many ways, GPR is considered one of the best NDTs: it can detect reinforcing bar corrosion, it is inexpensive, its inspection process does not require expertise, and it can be used to survey large areas in a short time. Therefore, this research focuses on the GPR technology and tries to solve one of its limitations.

1.2   PROBLEM STATEMENT

This research attempts to solve a problem associated with GPR results generated by using a numerical amplitude method to assess bridge deck corrosion. The problem is that the scale of GPR is relative (i.e., it varies from one bridge to another). There is no fixed or even general range for thresholds that define the limits of categories (good, fair, poor, and critical). Martino et al. (2014) try to solve this issue by developing a model based on statistical parameters such as mean, standard deviation, variance, kurtosis, and skew. From these parameters, they invent a formula to calculate the area of the corroded area by multiplying the mean with the skew. When the area of corrosion is calculated, the threshold can be found by trial and error. However, this method is unsuitable for healthy or much corroded bridge decks. Also, the thresholds determined by this method are not constant for all bridge decks. During data collection from several bridges, one bridge showed that it was improving over time, for which no plausible explanation could be found. It had been found that the scale of the bridge in each survey is distributed based on the range of the amplitude values in

that specific time of survey, regardless of the amplitude value itself. A comparison of two maps of the same bridge, one old (Figure 1-1) and one new (Figure 1-2), shows that the condition of the bridge in Figure 1-1 is better than that in Figure 1-2. However, this is not the case because a comparison of the amplitude of the two maps demonstrates the second to be better, which is the real case. Both maps have the same scale but with different numbers (amplitudes). However, the first one has a range of about 48 dB, while the second one has just 13 dB. For example, the value of -7 dB in Figure 1-1 falls into the "good" category, while the same value in Figure 1-2 falls under the very critical category. Therefore, it is confusing for the person who is dealing with the maps to identify the exact and real corrosion of the bridge under investigation. In order to overcome this problem, this study attempts to find a way to create a standardized scale that is applicable to all bridges.
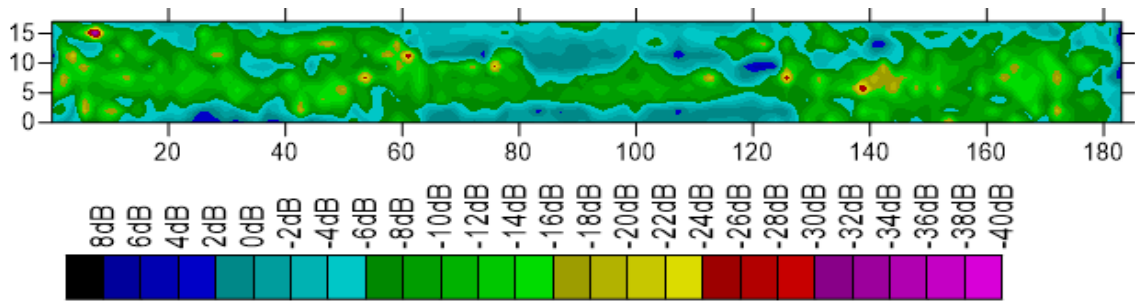
Figure 1-1. Old map
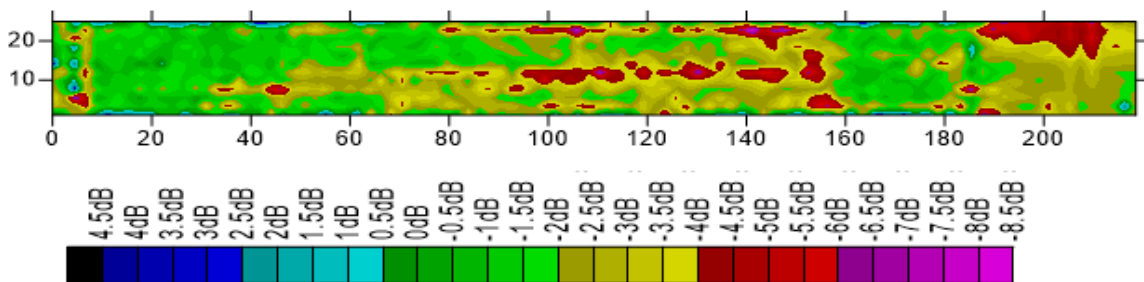
Figure 1-2. New map

1.3 OBJECTIVES

This study's main objective is to develop a numerical fixed GPR scale that can assess bridge deck corrosion accurately and precisely. To achieve this objective, several sub-objectives have been performed as follows:

1. Identify and study GPR data analysis and corrosion assessment scale.

2. Build various deterioration thresholds of GPR amplitudes.

3. Develop a standard corrosion scale and model.

4. Develop GPR-based deterioration models for the bridge deck.

1.4 METHODOLOGY

The methodology for achieving the objectives of this research is explained in the following points.

1. Collect data on different bridge decks in two ways, either by surveying bridge decks or from previous research works.

2. Perform a depth correction on the top reinforcing bars to make a normalization for the amplitude.

3. Divide the data into clusters to identify the limits and the thresholds of different categories of corrosion.

4. Execute a statistical analysis to find the best-fit probability distribution of these thresholds and test these distributions by a statistical test.

5. Simulate the thresholds of each category using Monte Carlo simulation to verify the value of these thresholds.

6. Perform a sensitivity analysis for each bridge deck by changing the scale one unit at a time to check the effect of changing the thresholds on the areas of corrosion.

7. Validate the developed scale using a case study and comparing it with other GPR interpretation methods, such as image-based analysis.

8. Build deterioration models for the bridge deck using Weibull distribution and considering the GPR results in thresholds and corrosion areas.

1.5   THESIS ORGANIZATION

Chapter One introduces the research and describes the problem that it addresses; it also includes the main objective, the methodology of the research, and the organization of the thesis. Chapter Two presents the literature review of the advantages and limitations of GPR and investigate the principle, components, and types of GPR machines. In addition, it describes the different methods and techniques used to assess the bridge decks with GPR. Brief explanations are also provided for the techniques used in this research, such as K-means clustering, statistical tests used, and Monte Carlo simulation. Chapter Three shows the methodology followed to achieve the objectives and explains how this research is executed. Chapter Four discusses the data sources used in this research and the method of data collection. Chapter Five presents the processes of analyzing the data and developing the model. The method by which these processes are executed and the results of each process are also shown. Also, the case study and model implementation are shown to validate the resulting scale. Chapter Six is a summary and a conclusion of the work

performed, its limitations and contributions, and recommendations for future work.

CHAPTER 2 LITERATURE REVIEW

2.1 INTRODUCTION

This chapter explains the literature review conducted for this research. Figure 2-1 illustrates the conducted literature review. First, it explains the four different categories of NDT used to assess the condition of bridge decks and examples for each category, but it focuses more on GPR technique; it elaborates its advantages and limitations, then presents a clear explanation of the GPR principle: how it works, the electromagnetic properties that have effects of the GPR, the most relevant GPR parameters and and their interrelationships, the types of GPR scans and the differences among them, and different types of GPR equipment and their respective usage. Moreover, this study explains in detail the most common methods used to analyze GPR data, including the underlying principle of each method and its limitations. Furthermore, the several techniques used in this research are also explained, such as the clustering technique used to divide the amplitude values into groups, the statistical tests used to find and test the best fit distribution, and statistical parameters such as mean, maiden, skew, and kurtosis. Then there is a section that describes the Monte Carlo simulation and its specific application.
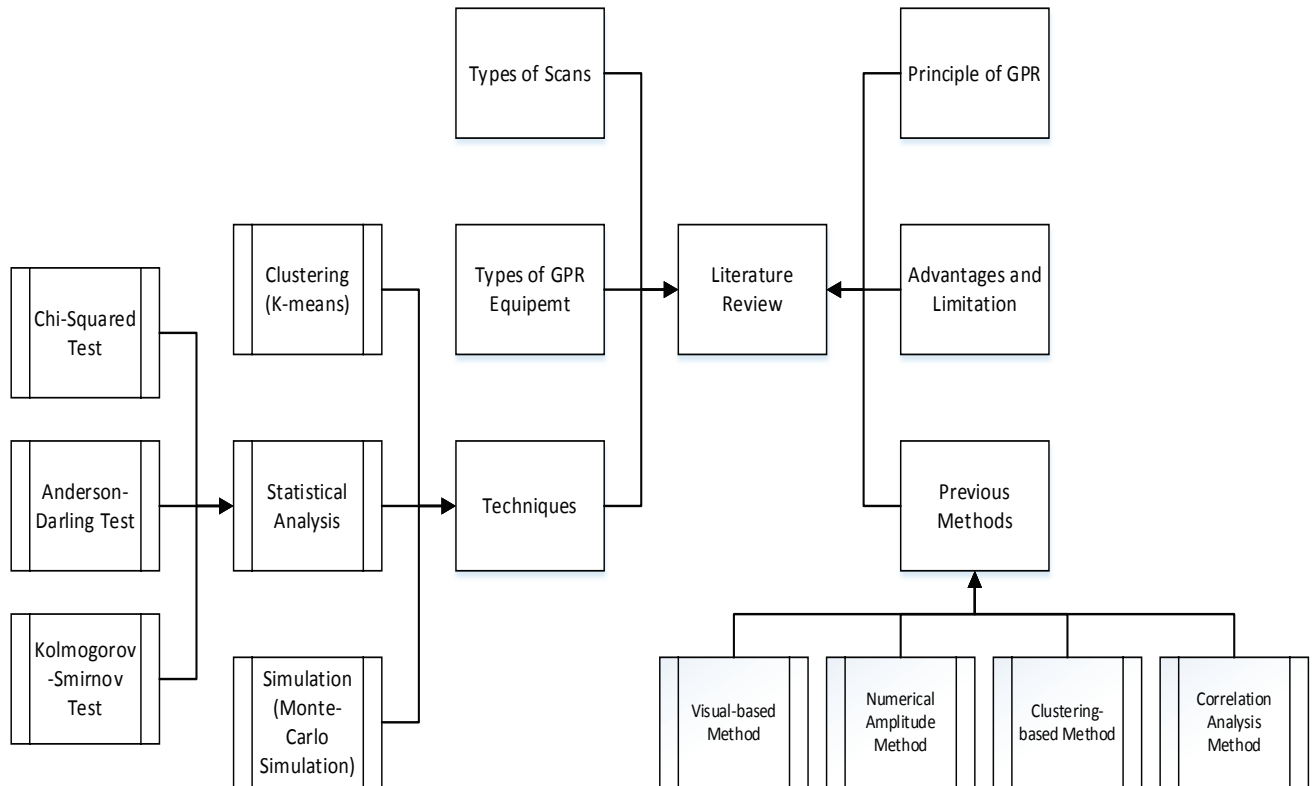
Figure 2-1. **Literature review flow chart**

2.2 CATEGORIES OF NON-DESTRUCTIVE TECHNIQUES

Currently, much research focuses on non-destructive techniques (NDTs) for assessing and monitoring the condition of bridges. Research shows that NDTs can be divided into four categories: acoustic, electrochemical, visual inspection, and electromagnetic techniques.

The acoustic technique uses the sound of the reflected wave to detect defects via two methods: chain drag and impact-echo (IE). The chain drag method involves dragging a chain over the bridge deck surface and listening to changes in the sound response; it is quick and inexpensive, but its results are qualitative. IE, which uses an acoustic transducer to detect, record, and

subsequently analyze an impact response for anomalies, is more expensive and time consuming but provides a quantitative result (Scott et al. 2003).

The electrochemical techniques address the interaction between electrical energy and chemical changes. The most common method for this technique is the half-cell potential, used to determine the location of the active corrosion by connecting to the bar on one side and measuring the potential difference in different locations, as shown in Figure 2-2. However, this technique is considered expensive and time consuming (Scott et al. 2003).
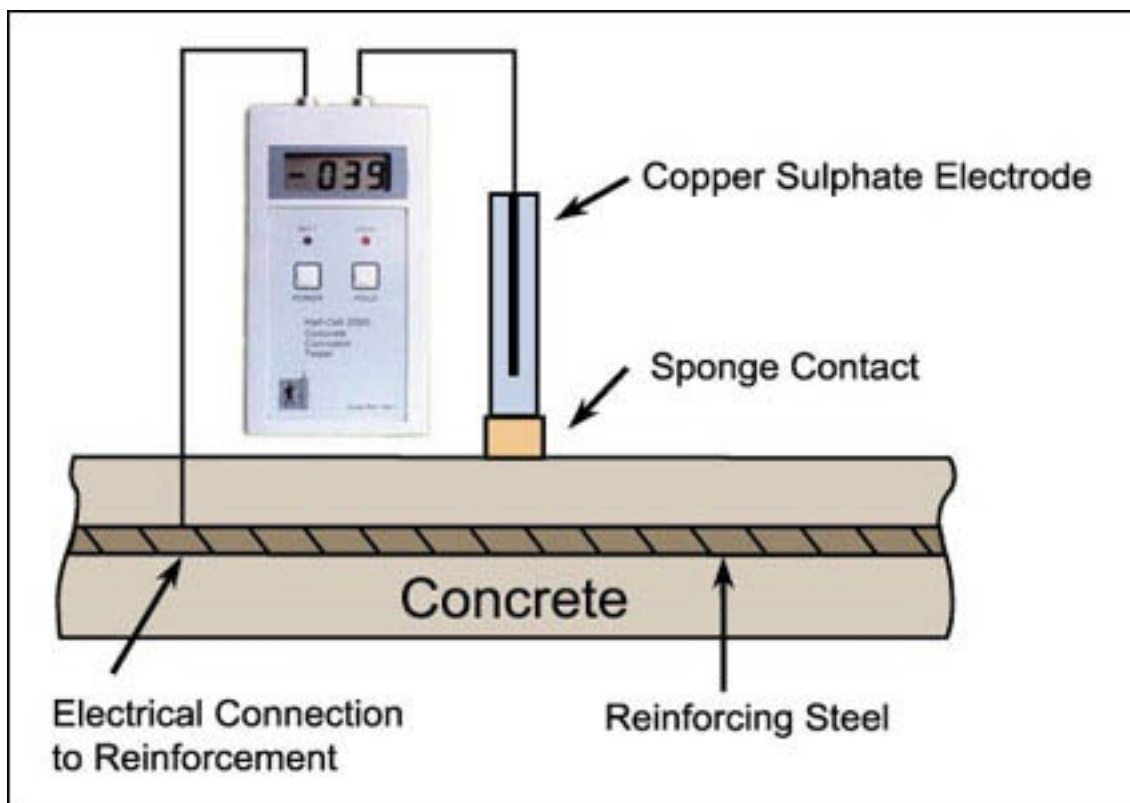
Figure 2-2. Half-cell potential principle (http://civil-online2010.blogspot.ca/2010/09/half-cell-electrical-potential-method.html)

Visual inspection is the technique used most to assess bridge deck surface conditions. This technique is very simple, requiring few tools and minimal

training; however, it cannot evaluate the subsurface or internal defects (Scott et al. 2003).

The fourth category includes electromagnetic techniques. Ground-penetrating radar (GPR) and infrared thermography (IR) are the most commonly used methods to assess bridge deck corrosion. GPR results give information about the bridge deck's material properties and its level of corrosion, whereas IR can be used to detect delamination. Because IR is very sensitive to the surrounding environment, factors such as diurnal temperature variation, rain, wind, and shadow can lead to error in results (Scott et al. 2003). Table 2-1 summarizes the techniques mentioned above (Lim et al. 2011; Dinh 2014).

2.3   GROUND-PENETRATING RADAR (GPR)

Radar is used to detect an object based on radio waves. The concept of detecting buried objects using radar was established in the early 1900s. The underlying principle is the transmission of electromagnetic (EM) waves and reception of those reflected from the object across their path (Loulizi 2001). GPR is a geophysical technique that uses EM waves to detect objects buried beneath a surface and image the subsurface. In the last 30 years, this technique has proved an effective way to identify objects that are shallowly buried (Luo et al. 2005). It is considered as a non-invasive and non-destructive technique that has many uses in site and ground investigation (Sato et al. 2008).

Table 2-1. Summary of various NDT techniques and their applications, advantages and limitations (Lim et al. 2011) (Dinh 2014)

Technique	Application	Advantage	Limitation
Impact Echo (IE)	• Measure thickness • Detect delamination	• Precise and immediate result	• Suitable only for plate-like structure • Reinforcement has an effect on the result • Requires expert to interpret the result
Chain Drag	• Detect delamination	• Easy to carry and use	• Depends on the experience of the inspector (subjective) • Cannot be used on bridge covered with asphalt • Detect only up to 3" depth
Half-Cell Potential	• Give an indication of the probability of correction	• Portable equipment.	• Requires an expert to perform the test and interpret the result • Time consuming • Applicable to moist concrete • Cannot be applied to bars coated with epoxy
Visual Inspection	• Detect defects such as spalling	• Easily executed • Inexpensive • Minimal equipment required	• Detects only surface defects • Results depend on the experience of the inspector (subjective)
Infrared Thermography (IR)	• Detect delamination near the surface	• Can be used to survey a large area quickly • Can be done remotely without closing the structure	• Affected by weather conditions • Limited to shallow defects, effective only up to about 3" • Equipment is expensive • Expertise required to perform the test
Ground-Penetrating Radar (GPR)	• Detect the location of the reinforcing bars • Measure slab thickness • Map the underneath utility • Assess the corrosion of bridge decks	• Fast surveying if air-couple antenna used • Easily detecting metal objects	• Data require some expertise for analyzing • Moisture content has a great effect • The congested reinforcing bar may affect the results

The ability of GPR to detect the object is based on the difference in permittivity of the object itself and the surrounding medium. When there is a discontinuity in the medium's dielectric, the GPR will record the difference (Zhao et al. 2005). Because of its sensitivity to changes in EM properties, GPR can detect metallic and non-metallic materials (Daniels 1996). A review of previous research reveals a focus on geophysical inversion and modeling, image and signal processing, and hardware design and radar systems (Al-Nuaimy 1999). However, research focusing on the corrosion scale of GPR is limited.

Over the past 20 years, GPR theory, technique, and technology have developed significantly (Jol 2009). GPR is considered a non-destructive technique that emits EM pulses to locate and evaluate the depth of a buried object that cannot be seen visually (Maser 1996). Usually, a GPR system includes data collection units and antennas, of which there are two types: mono-static and bi-static. Mono-static antennas consist of one antenna that performs both transmitting and receiving functions, while bi-static antennas include separate antennas for transmitting pulses and receiving those that are reflected (Belli 2008).

The basic elements of a GPR system are listed below and shown in Figure 2-3:

- The display unit, such as a laptop used to display the recorder data
- The control unit, which controls the operation of transmitting and recording EV pulses
- An antenna that performs the task of transmitting EM waves and receiving reflected waves

- A cart used to carry all GPR elements
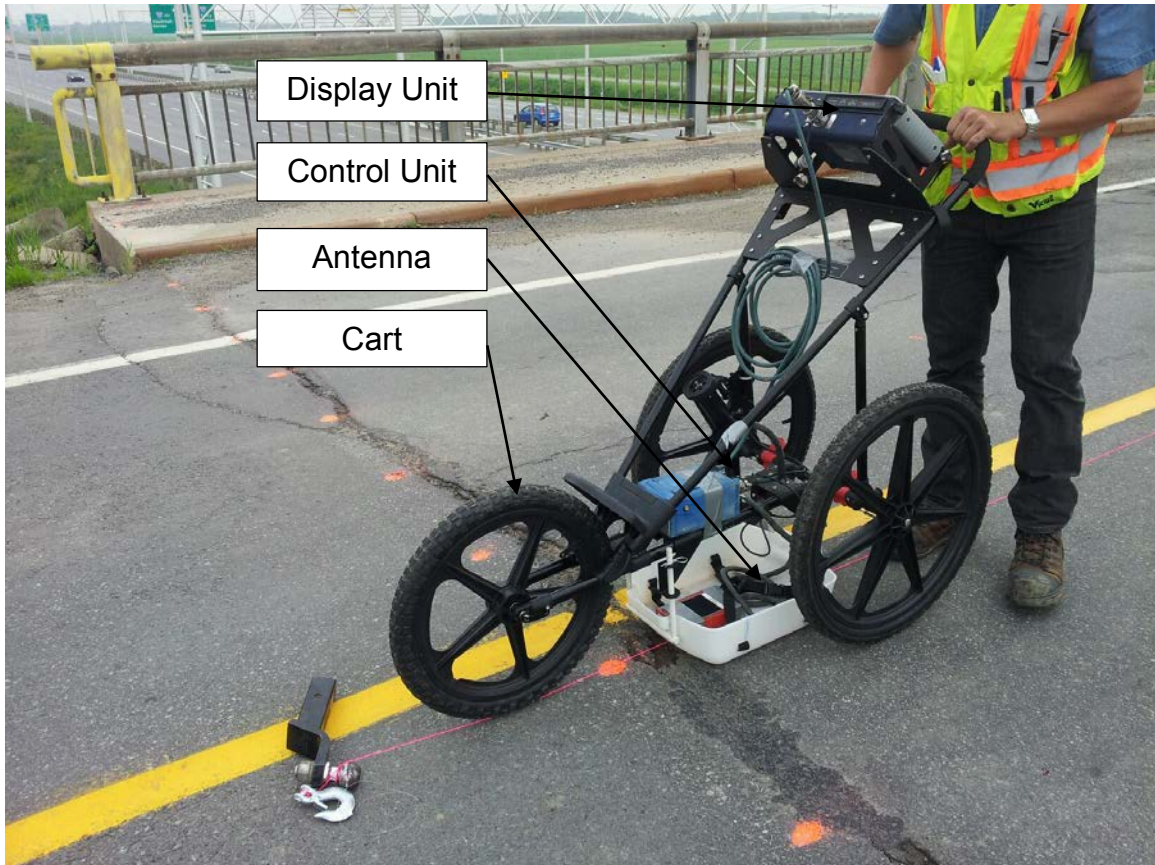
Figure 2-3. GPR system components

EM wave properties, such as propagation depth and reflected wave resolution, have a great influence on GPR operation. Electric conductivity (σ), permittivity (ε), and permeability (μ) are the parameters that have the greatest effect on the EM properties (Scheele 2011). GPR signal penetration is affected by the electrical conductivity of the objects penetrated. Moreover, conductivity is affected by the moisture content of the surface under investigation, i.e., the higher the moisture content, the higher the conductivity, resulting in shallower GPR signal penetration depth (Deniels 2004). Relative permeability does not provide useful information in engineering surveys because most of the materials poor in iron oxide have low magnetic permeability, which leads to little contrast in

13

the EM waves. However, a dielectric contrast related to permittivity provides a high contrast in the reflected waves (Abujarad 2007).

GPR systems are used mainly to determine the size, location, and shape of subsurface objects that cannot be seen visually. Its principle is similar to that of regular radar. A transmitter antenna emits EM pulses from the surface being investigated, and then these pulses propagate through the surface. The receiving antenna collects the reflected pulses and records their properties, including wavelength, two-way travel time, and amplitude, to analyze and interpret subsurface corrosion (Dojack 2012). The changes reported between transmitted and reflected pulses indicate a change in the materials' properties. The principle of GPR system is illustrated in Figure 2-4 (Bostanudin 2013).

The evaluation of GPR system performance depends on the ability of the signals to propagate to the depth required and the resolution of the results (images). The propagation depth and the resolution are both based on the wavelength of the transmitted signal. To obtain high-quality images, the wavelength should be short, which means the frequency will be high. In other words, the higher the frequency, the better the resolution, the shallower the propagation depth, and vice versa (Abujarad 2007).
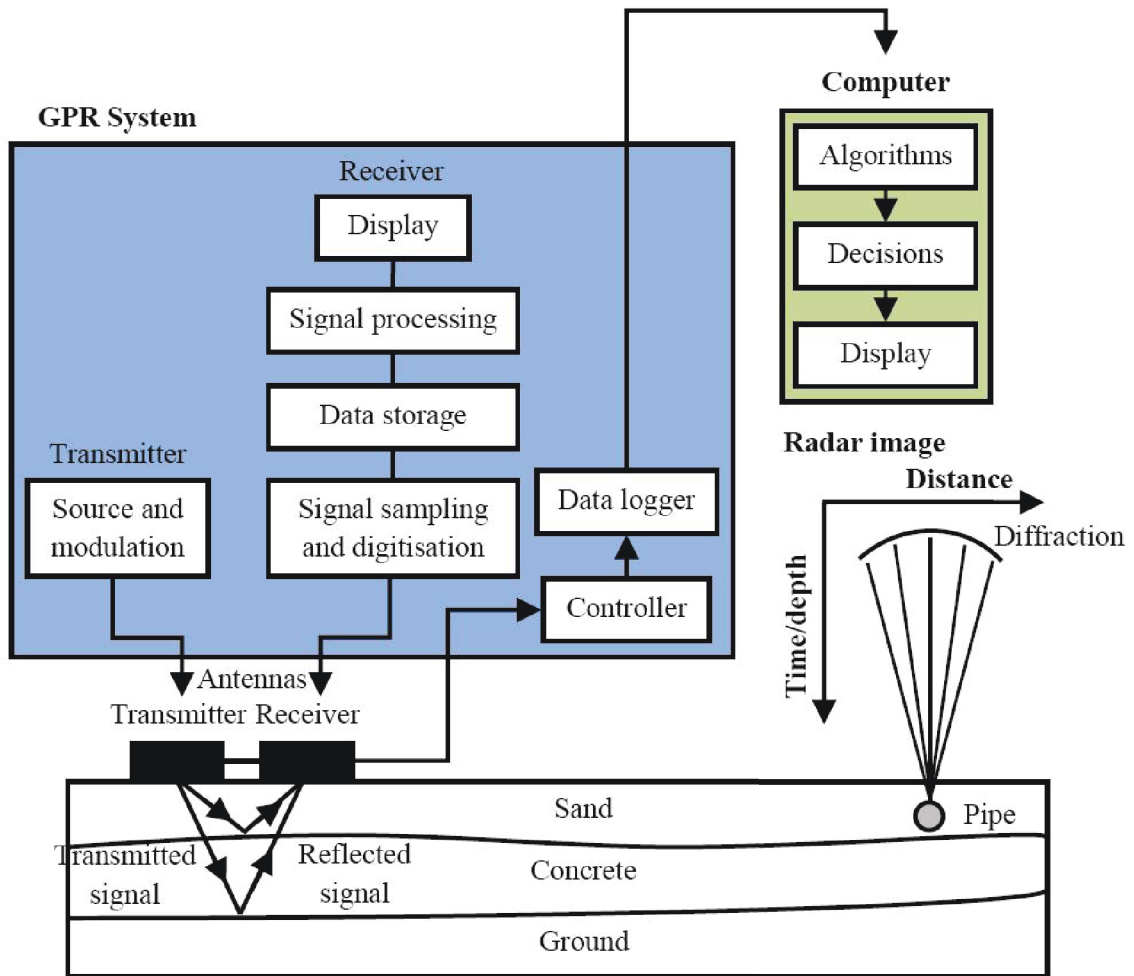
Figure 2-4. Basic functional principle of a GPR device (Bostanudin 2013)

2.4 ADVANTAGES AND LIMITATIONS OF GPR

The GPR system has many advantages that cannot be found in other techniques for assessing subsurface corrosion. These advantages can be summarized as the following (Abujarad et al. 2005; Dojack 2012):

- It can be used to detect both metallic and non-metallic objects.

- It can be used to survey a large area in a short time.

- It is a non-destructive technique, which means it does not damage the structure under investigation.

- It is considered less expensive than other techniques.

However, despite its valuable advantages, GPR has some limitations (Abujarad et al. 2005), which much ongoing research is focused on overcoming:

- There are no exact thresholds for the GPR scale to identify the corrosion of the structure under investigation.

- EM waves from radio, microwave, television, and mobile phones can cause unwanted signals (noise) in GPR results because GPR is sensitive to these types of waves.

- A high level of experience is required to interpret the GPR data and results.

2.5 BASIC PRINCIPLES OF GPR

The factors on which the quality of the data obtained from GPR depends can be divided into two groups (Orlando 2007; Conyers 2013):

- The characteristics of the materials in which EM waves propagate, such as permeability, electrical conductivity, and permeability

- GPR parameters that control the transmitted waves into the surface and subsurface such as wave velocity, wave length, the relation between the frequency with depth, and resolution

2.5.1 Electromagnetic Properties in Dielectric Materials

- Permeability: The ability of the material to become magnetized in the presence of an EM field, measured in henry per meter (H/m) (Belli 2008) (Annan 2009).

- Electrical conductivity: The ability of a material to conduct the electric portion of an EM wave, measured in Siemens per meter (S/m).

- Permittivity: The ability of a material to store and transmit an electric charge induced by an EM field, measured in Farads per meter (F/m) (GSSI 2006).

2.5.2 GPR Parameters

The required depth and resolution of the GPR results are controlled by some parameters that significantly affect the resultant images of the GPR. These parameters include

- Wave velocity: The velocity with which a wave travels through the material depends on the angular frequency, which is related to the frequency of the machine used during the survey, as we can see from Equation 2-1

$$\boldsymbol{\omega = 2\pi f}$$ Equation 2-1

The velocity of the wave is measured in meters per sec (m/s), the angular frequency is measured in radians per second (rad/s), and the frequency in Hertz (Belli 2008).

- Wavelength: The distance over which the propagating wave repeat itself is called a wavelength, measured in meters (m). The wavelength could be calculated if the velocity and frequency are known, as shown in Equation 2-2

$$\lambda = \frac{v}{f}$$ Equation 2-2

2.5.3 Relationship between Frequency, Depth, and Resolution

Frequency has an inverse relationship with both the wavelength and the penetrating depth. This means that, with low frequency, waves will penetrate deeper into the material and vice versa. It also has a direct relationship with the resolution: the higher the frequency, the better the resolution. This is because the frequency is related inversely to the wavelength, such that a higher frequency will have shorter wavelengths that produce a narrow cone of transmitted waves that can focus on smaller areas (Conyers 2004). Therefore, the GPR machine's frequency is a critical parameter that should be chosen in an appropriate manner (Grealy 2006; Neubauer et al. 2002; Prakash et al. 2007).

2.6   TYPES OF SCANS

The purpose of the GPR data is to provide a resultant image that visualizes the real situation of the scanned subsurface after performing analysis and interpretation for these data. Collected data from GPR could be divided into three types as following:

- A-scan: this type is a one-dimensional plot, representing amplitude vs. time.

- B-scan: a two-dimensional image created from a gathering A-scan. The horizontal axis represents the position of the scan, while the vertical axis represents the two-way travel time. Usually, GPR data analysis is based on interpretation of many B-scans.

- C-scan: a three-dimensional presentation of GPR data formed from a collection of B-scans. C-scans provide a block view for GPR data and are helpful for providing a good image for specific targets. It is

easier to identify specific targets in C-scans (three-dimensional images) than in B-scans. (Bostanudin 2013).

2.7 TYPES OF GPR EQUIPMENT

Based on their operation methods, GPR systems are divided into two types. Air-coupled GPR systems (Figure 2-5A) are connected directly to a moving vehicle, which reduces the quality of the scanned images. Usually, the air-couple antenna is used to survey highways, railroads, and other large areas in a short time. Ground-coupled GPR systems are used for better quality scans; they require direct contact with the surface under investigated. Ground-coupled GPR is used to survey bridge decks. One GPR machine consists of a hand-held antenna (Figure 2-5B) and is used when it is difficult to survey the surface with the regular machine, especially for vertical elements such as columns, walls, and piers.

Figure 2-5 A) GPR air-coupled machine (Al-Qadi 2003). B) Handheld GPR machine

2.8   METHODS OF GPR DATA ANALYSIS

2.8.1 NUMERICAL AMPLITUDE METHOD

The most common analysis method, the numerical amplitude method, depends on the value of the amplitude of the reflected waves from the top layer of reinforcing bars. The GPR maps developed by this method are based on the relative difference between the amplitude values of the reinforcing bars. The higher the amplitude value, the better the condition of the bar, and vice versa (Gucunski et al. 2011). Moreover, the color variations in the maps generated by using this method are due not only to deterioration but also to variation in rebar depth (Parrillo et al. 2006). The required adjustment, depth correction, was invented by Barnes et al. (2008). This method's main limitation is its lack of a clear value for the thresholds that define the different categories of corrosion. In other words, the scale used to assess bridge deck corrosion varies from bridge to bridge. For example, the profiles of one bridge deck may have amplitude values from 10 dB to -5 dB, where 10 dB represents the best condition and -5 dB represents the worst for that bridge. Meanwhile, another of Bridges' profiles may have amplitude values that range from -5 dB to -40 dB, where -5 dB represents the best condition and -40 dB represents the worst. The -5 dB value is classified as "good" for one bridge deck but "critical" for the other. This can be the case for any value from the profiles and is not unique to -5 dB. This means that the thresholds are changing from one bridge to another. Therefore, this method could result in wrongly interpreting the condition of a bridge deck because the amplitude values of the top layer of reinforcing bars are affected by several

factors, such as surface anomalies, reinforcing bar spacing, reinforcing bar depth, reinforcing bar configuration, and polarization effects (Tarussov et al. 2013).

2.8.2 IMAGE-BASED METHOD

To eliminate the disadvantages and shortcomings of the numerical amplitude method related to relativity in the scale, Tarussov et al. (2013) tried to solve this problem via the image-based method, which primarily detects defects in the bridge deck by visually inspecting the B-scan profiles of the bridge. As shown in Figure 2-6, while surveying, the analyst will mark the anomalies based on the shape and the brightness of the hyperbola of the top layer of reinforcing bars. The clearer the shape and the higher the level of brightness, the better the condition of the concrete, and vice versa. The experienced analyst inspecting the profiles gives the final evaluation of bridge deck corrosion independent of any numerical value. This eliminates the relativity of the numerical amplitude method scale and means that each bridge deck is evaluated based on the shape of the hyperbola of the top reinforcing bars rather than on numerical (amplitude) value.

In addition, the GPR profile analyst can detect any anomaly not related to the condition of the concrete, such as structural elements (beams or columns under the slab) or water puddling on the surface of the deck. GPR profile analysis using this method does not require a depth correction because it does not deal with numerical values. One more advantage over the numerical amplitude method is that the image-based method maps the corroded areas with exact limits rather than by interpolating the contour line of amplitudes as in the

numerical amplitude method. This method is more accurate for evaluating bridge decks and more closely represents their real and exact condition than does the numerical amplitude method. However, the image-based method has an important limitation: data interpretation is subjective because it depends completely on the GPR profile analyst's experience and judgment. Thus, there is no systematic way to inspect the profiles of the bridge deck under investigation.
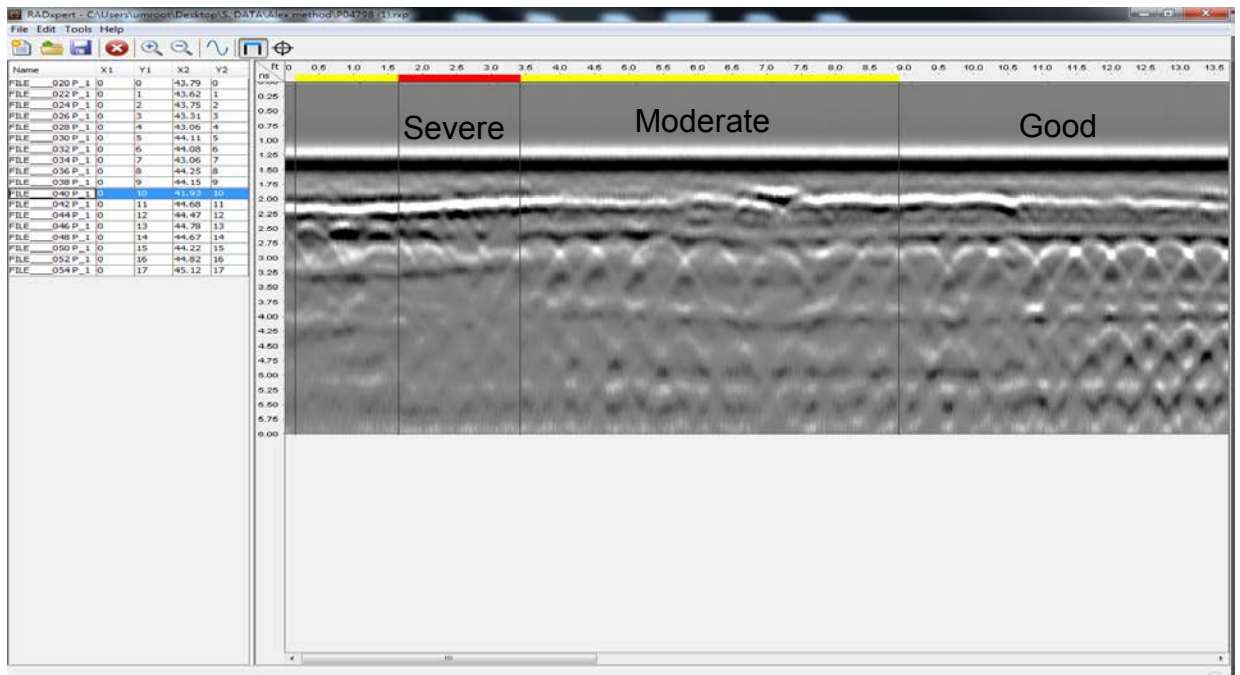
Figure 2-6 Visually marking the anomalies using RADxpert software

2.8.3 CLUSTERING-BASED THRESHOLD CALIBRATION

Although the amplitude analysis is an objective method, it has a limitation related to threshold determination. In addition, the image-based analysis method is considered a subjective method. Therefore, Dinh (2014) presented a method that combines both numerical amplitude and image-based analysis. After selecting the reinforcing bars through amplitude analysis, the analyst is asked to examine the GPR profiles visually. The visual examination allows the analyst to

determine the number of corrosion categories that the bridge deck should have. After identifying the categories, the amplitude data will be divided into groups according to the number of the categories using K-means clustering. The K-means clustering will determine the thresholds of each category. Figure 2-7 illustrates an example of a three-category bridge deck using this method. Figure 2-7 shows that, after inspecting the bridge profiles visually, the analyst decided that this bridge should have three categories (good, moderate, and severe). Category limits are defined by k-means clustering (-1.9581dB, -5.5591dB). The areas for each category are 42.5%, 47.5%, and 10%, respectively.

2.8.4 CORRELATION ANALYSIS

Dinh (2014) introduced a new method to assess concrete bridge deck corrosion, based primarily on comparing A-scan profiles of a newly constructed bridge with the same A-scan profiles of the same bridge taken at a different time (inspection time): in other words, comparing the scans based on the difference between time-series data rather than comparing them based on the relative difference between the amplitude values. Figure 2-8 shows the comparison between two A-scans done at different times. The closer the correlation coefficient to one, the more similar the scans are and the less change there is in concrete condition.
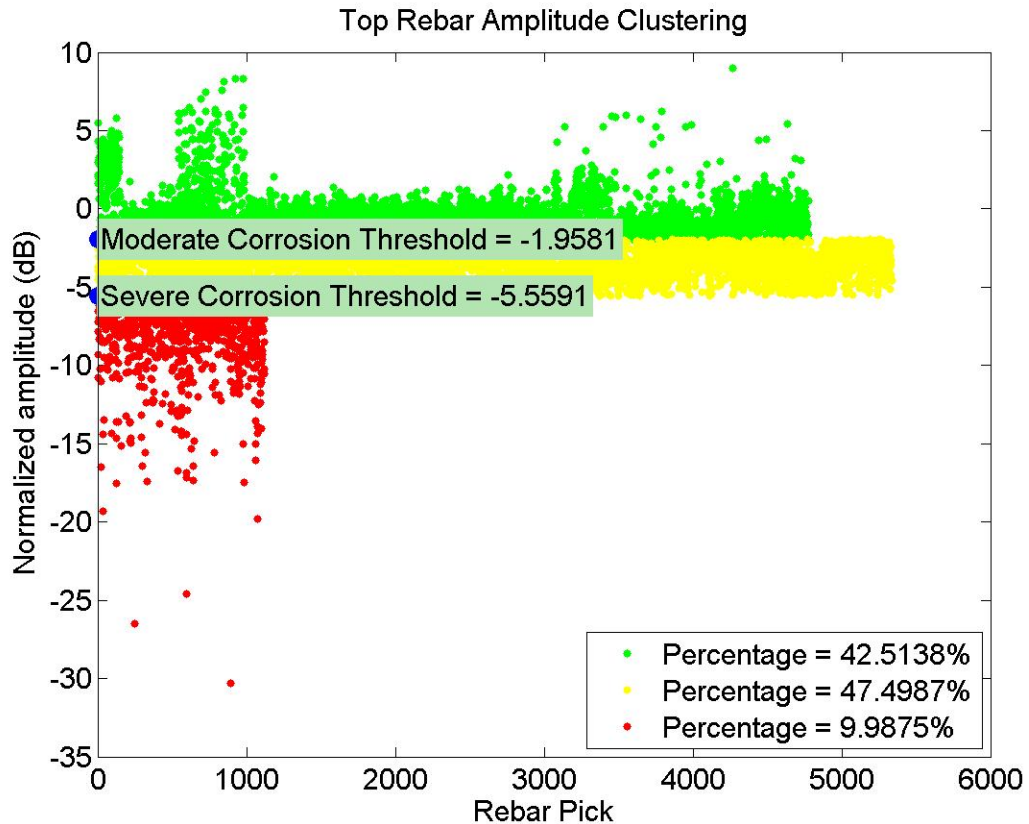
Figure 2-7. Thresholds and areas of each category

However, this method has some limitations, one of which is that the bridge deck should be surveyed when newly constructed. The profiles from the newly constructed bridge provide the reference point to which future profiles will be compared. Another limitation is that, for the purpose of comparing both scans, the location of the scans should be recorded exactly. Aside from these limitations, this method is advantageous in that it allows observing and differentiating between abnormal signals related to structural variation and abnormal signals caused by corrosion defects.
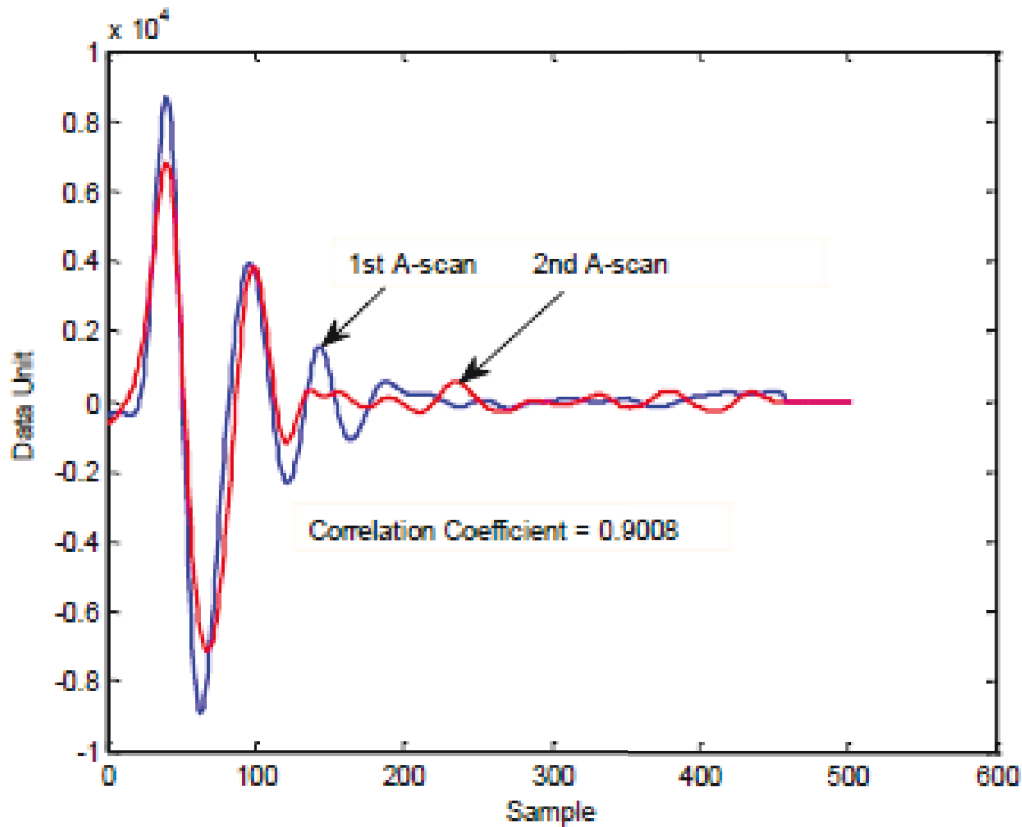
Figure 2-8. Comparison of two A-scans (Dinh 2014)

2.9 K-MEANS CLUSTERING

The difference between clustering (unsupervised learning) and classification (supervised learning) is that clustering analysis does not have prior identifiers such as category labels, while classification use identifiers to distinguish the data (Duda et al. 2001). K-means clustering is the most popular type of clustering algorithm because of its ease of implementation, efficiency, empirical clustering, and simplicity (Jain 2010). There are two classifications of data analysis techniques for K-means clustering: exploratory and descriptive (i.e., understanding the structure and the characteristic without a pre-specified

hypotheses) and confirmatory or inferential, a type used to validate a hypothesis or assumption (Tabachnick and Fidell 2007).

Webster defines cluster analysis as "a statistical classification technique for discovering whether the individuals of a population fall into different groups by making quantitative comparisons of multiple characteristics". The main purposes of data clustering include

- Underlying structure: to gain insight into data, generate hypotheses, detect anomalies, and identify salient features.

- Natural classification: to identify the degree of similarity among forms or organisms (phylogenetic relationship).

- Compression: as a method for organizing the data and summarizing it through cluster prototypes.

The number of clusters K, cluster initialization, and distance metric are the main three user-defined parameters required to perform K-means clustering (Jain 2010). Although there are great advantages to K-means clustering, it has some weaknesses:

- Parameter k must be chosen in advance.

- Data must be numerical and comparable via Euclidean distance.

- The algorithm works best on data containing spherical clusters.

- The algorithm is sensitive to points that do not belong to any cluster (outliers). These can distort the centroid positions and ruin the clustering.

2.10 STATISTICAL ANALYSIS

2.10.1　　Chi-Squared Test

The chi-squared test is used to test whether the data follow a specific distribution (Snedecor et al. 1989). The advantage of the chi-squared test is that it could be applied to any univariate distribution where the cumulative distribution function could be calculated. Another advantage of the chi-squared test over the Anderson-Darling and Kolmogorov-Smirnov tests is that it can be applied to a discrete distribution. A-D and K-S tests can be applied only to continuous distribution. However, the chi-squared test has a disadvantage: to make the test valid, the sample size must be sufficient.

The chi-squared test is defined by the following characteristics:

H_0: The data follow a specified distribution.

H_a: The data do not follow the specified distribution.

If the test statistic is greater than the critical value at specific significance level, then the null hypothesis will be rejected.

2.10.2　　Anderson-Darling Test

The Anderson-Darling test, used to decide if the data follow a specific distribution (Stephens 1974), makes use of the specific distribution in calculating critical values. This has the advantage of allowing a more sensitive test and the disadvantage that critical values must be calculated for each distribution.

The A-D test is defined by the following characteristics:

H_0: The data follow a specified distribution.

H_a: The data do not follow the specified distribution.

The critical values for the Anderson-Darling test depend on the specific distribution being tested. The hypothesis that the distribution is of a specific form is rejected if the test statistic is greater than the critical value.

2.10.3 Kolmogorov-Smirnov Test

The Kolmogorov-Smirnov test is used to decide whether the data follow a specific distribution (Chakravart et al. 1967). The K-S test has some advantages, one of which is that the distribution of the K-S test statistic itself does not depend on the underlying cumulative distribution function being tested. Another advantage is that it is an exact test. However, the K-S test has several critical limitations:

- It only applies to continuous distributions.

- It tends to be more sensitive near the center of the distribution than at the tails.

- The distribution must be fully specified. That is, if location, scale, and shape parameters are estimated from the data, the critical region of the K-S test is no longer valid. It typically must be determined by simulation.

The K-S test is defined by

H_0: The data follow a specified distribution.

H_a: The data do not follow the specified distribution.

If the test statistic is greater than the critical value at specific significance level, then the hypothesis will be rejected regarding the distributional form.

2.10.4 Critical Values and P-Values

Critical values for a hypothesis test depend upon a test statistic, which is specific to the type of test, and the significance level α, which defines the test's sensitivity. A value of α = 0.1 implies that the null hypothesis is rejected 10% of the time when it is, in fact, true. The choice of α is somewhat arbitrary, although in practice values of 0.1, 0.05, and 0.01 are common. Critical values are essentially cut-off values that define regions where the test statistic is unlikely to lie. For example, a region where the critical value is exceeded with probability α if the null hypothesis is true. The null hypothesis is rejected if the test statistic lies within this region that is often referred to as the rejection regions.

Another quantitative measure for reporting the result of a hypothesis test is the p-value. The p-value is the probability of obtaining the observed sample results when the null hypothesis is true. If this p-value is very small, usually less than or equal to a previously chosen threshold value called the significance level (traditionally 5% or 1%), it suggests that the observed data are inconsistent with the assumption that the null hypothesis is true and thus that the hypothesis must be rejected and the other hypothesis accepted as true. In other words, a small p-value is an indication that the null hypothesis is false (Nuzzo 2014). Table 2-2 represents the different p-values and their corresponding degree of acceptance.

Table 2-2 P-values and Their Acceptance Degree

P-value	Acceptance Degree
P > 0.1	No evidence against the null hypothesis. The data appear to be consistent with the null hypothesis
0.05 < P < 0.1	Weak evidence against the null hypothesis in favor of the alternative
0.01 < P < 0.05	Moderate evidence against the null hypothesis in favor of the alternative
P < 0.01	Strong evidence against the null hypothesis in favor of the alternative

2.11 MEAN VERSUS MEDIAN

The terms "mean" and "median" are the most commonly used in statistics to find the central tendency. Therefore, this section will explain these terms from a statistical point of view with regard to their differences, their applicability, etc. "Mean" can simply be defined as the average of a set of data, while the "median" is the numerical value separating the higher half of a data or probability distribution from the lower half. Consider, for example, a set of data: 2, 3, 4, 4, 5, 8, 10, 12, and 15. The mean equal to the summation of all these values divided by the number of these values is $\bar{x} = \frac{2+3+4+4+5+8+10+12+15}{9} = \frac{63}{9} = 7$, while the median is equal to the middle value, which is 5.

Usually, there is a misunderstanding with regard to which parameter is better, whether mean or median. There is no specific answer; each of these has its advantages and disadvantages. For example, means is more appropriate for data with a normal distribution, while the median is more suitable for a distribution that is skewed either positively or negatively. Meanwhile, mean cannot be applied to all distributions because values that are too small or too large (outliers) have a great impact on the value of the mean. Therefore, in the

case of outliers, it is better to use the median to derive the central tendency.

Table 2-3 summarizes the difference between the mean and the median.

Table 2-3 Mean vs. Median

	Mean	Median
Definition	Arithmetic average of a set of numbers or distribution	Middle value in a sample sorted into ascending order
Applicability	Suitable for normal distributions	Suitable for skewed distributions
Relevance to the data set	It is not powerful because the outliers have a great effect on the data	Because it is more suitable for skewed distribution, it could be used to find the central tendency
Calculation	Summation of values divided by the number values	The exact middle number of the set of values

2.12 MONTE CARLO SIMULATION

Monte Carlo statistical tests can be used to define the most probabilistic modeling as a stochastic simulation (Ripley 1987). Sawilowsky (2003) differentiates between the Monte Carlo simulation and the Monte Carlo method. Simulation is an imaginary representation of the reality, so the Monte Carlo simulation uses repeated sampling to identify the properties of a phenomenon; whereas the Monte Carlo method can be used to solve a mathematical or statistical problem. Monte Carlo tests can be used in applied statistics in two ways: first, to compare competing statistics for small samples under realistic data conditions; and, second, to provide executions of hypothesis tests that are more effective than exact tests (Sawilowsky et al. 2003). It is not necessary for a Monte Carlo simulation to be useful to have truly random numbers. However, sometimes it is important for the simulation of some application to be

31

unpredictable. To have a good simulation, only the quality of the pseudo-random sequence should be random enough.

2.13 PREVIOUS RESEARCHES ON THRESHOLDS

The relationship between the GPR measurements and the condition of decks is still not understood well, which limits complete acceptance of GPR as an inspection tool. Maser et al. (2012) attempt to understand the relationship better between the GPR output and the condition of decks, which would give decision makers more confidence to use GPR to assess bridge deck corrosion. The model developed by Maser attempts to find a threshold to determine whether the concrete is sound or deteriorated by making a correlation between GPR and half-cell potential. The scale of GPR is from 0 to 1, where 0 represents deterioration and 1 represents sound concrete. Based on ASTM C876, a threshold for half-cell potential was set at -350 mV, the best value for the GPR threshold that have the highest percentage of matching (90.2%) between GPR and half-cell potential was 0.45 (Maser et al. 2012). Martino et al. (2014) developed a model based on a correlation between GPR and half-cell potential whose threshold is to determine whether the condition of the bridge deck is sound or corroded. Martino et al. (2014) attempt to make GPR a standalone assessment tool by trying to find a threshold for GPR that can differentiate sound from corroded areas. The model is developed based on the observation that the histogram of a sound bridge deck's amplitude is compacted and symmetric and has almost a normal distribution (Figure 2-9a), while for the corroded bridge deck is quite spread out and skewed to one side (Figure 2-9b). Based on statistical parameters such as

mean, standard deviation, skew, and kurtosis, a linear regression formula is used to calculate the corroded area, which is equal to skew multiplied by the mean of the amplitude values (Figure 2-10). After the percentage of corroded area is calculated, GPR threshold is found by trial and error to have almost the same area of corrosion. Although these studies seem promising in the effort to make GPR a standalone assessment tool, they nevertheless have some limitations, one of which is that both studies depend on half-cell potential to make a correlation with GPR related to corrosion, while even half-cell potential can only detect the potential for corrosion, not the corrosion itself. Another shortcoming is that there is only one threshold, which means it can differentiate only between sound and corroded areas. Moreover, the developed or calculated threshold varies from one deck to another and is not constant for all decks like with other technologies such as half-cell potential, which has a constant threshold of -350 mV.
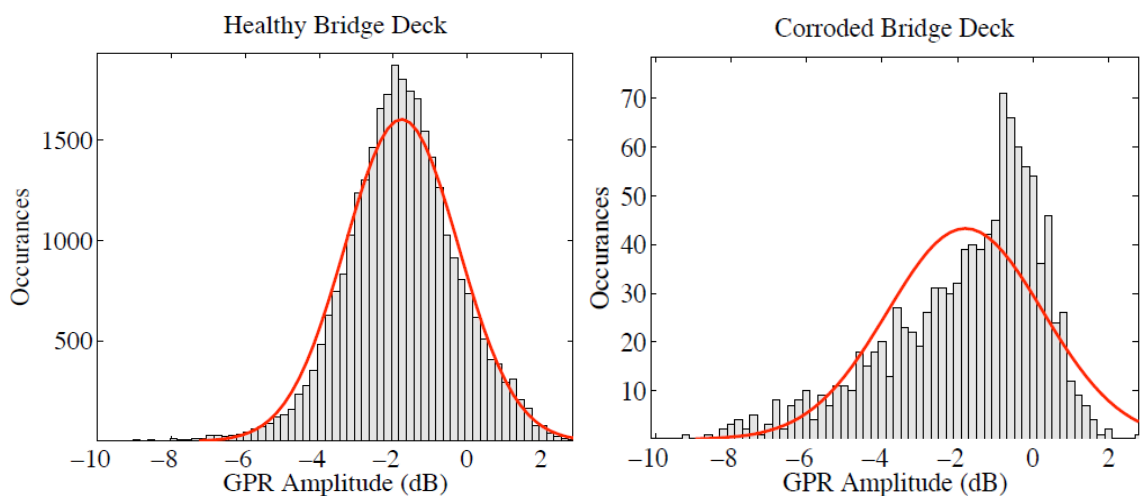
Figure 2-9. a) Histogram of sound bridge deck b) Histogram of a corroded bridge deck (Martino et al. 2014)

2.14 LIMITATIONS OF PREVIOUS RESEARCH

As described earlier, each method mentioned has its advantages and limitations, the latter of which will be summarized in this section as illustrated in Table 2-4.

Table 2-4 Limitation of Current Methods

Method	Limitations
Numerical Amplitude	• No exact thresholds that define the limits of different categories of corrosion
Image-based	• Subjective interpretation
Clustering-based Threshold Calibration	• Number of categories depends on the analyst decision • Thresholds values vary from one bridge to another
Correlation Analysis	• Two inspections required • Second scan should be in the exact same location of the previous scan • Availability of data
GPR threshold	• Based only on half-cell potential • Only one threshold • Thresholds vary from one deck to another
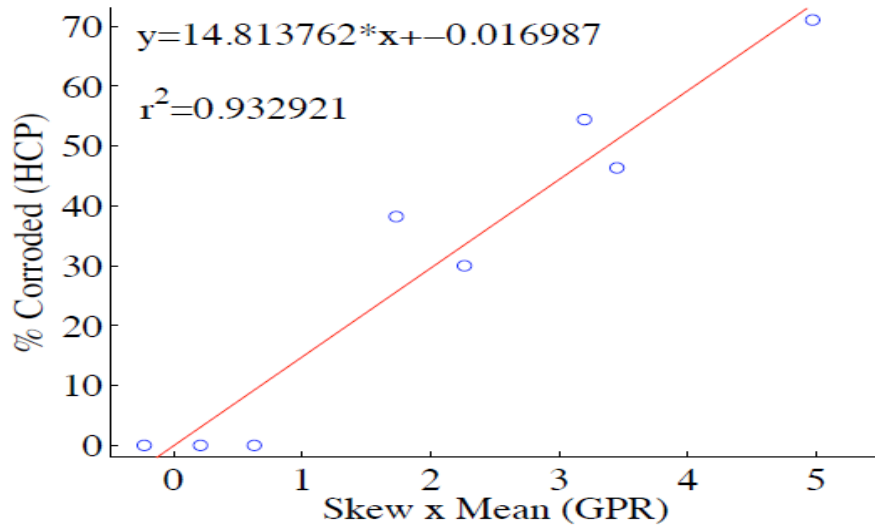
Figure 2-10. Linear regression formula (Martino et al. 2014)

CHAPTER 3 RESEARCH METHODOLOGY

This chapter explains the methodology used to achieve the objectives of this research. Figure 3-1 presents the overall methodology followed in this research. The methodology can be divided into three main sections: literature review, data collection and data analysis, and model development. The literature review is explained in the previous chapter and will not be discussed in this chapter. Data collection and analysis and model development will be explained in sections 3.2 and 3.3, respectively. Section 3.1 illustrates the process of collecting data, the sources of these data, and how these data have been divided and used. Section 3.2, "Data Analysis and Model Development," shows how these data have been analyzed to develop the appropriate fixed numerical scale for GPR.

3.1 DATA COLLECTION

Data collection was one on the most challenging process in the research process. As discussed earlier, GPR is a new technique compared to other NDTs. Therefore, that availability of data is low, especially for old bridges. Data could be obtained either by surveying bridge decks or by using data from previous research. Figure 3-2 illustrates both data collection methods. More than half of bridge decks used in this research are from bridge decks surveying; the detailed procedure followed to survey bridge decks and the reasons for following that procedure are explained in section 4.1. Additionally, section 4.2 describes the data collected from previous research, the types of sources used, the information

related to the machine frequency, and the type of antenna used (either ground-coupled or air-coupled).
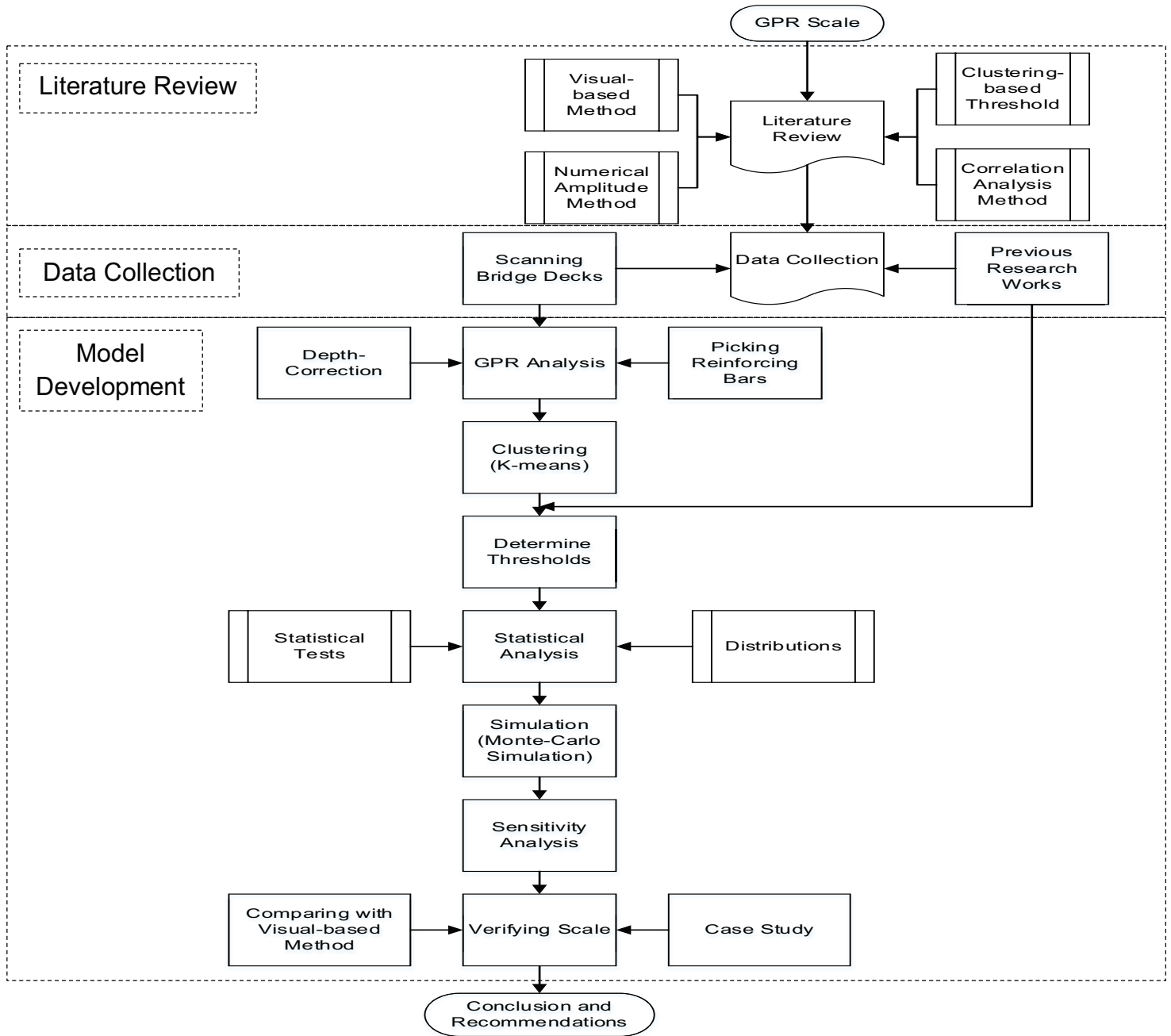
Figure 3-1. Overall research methodology
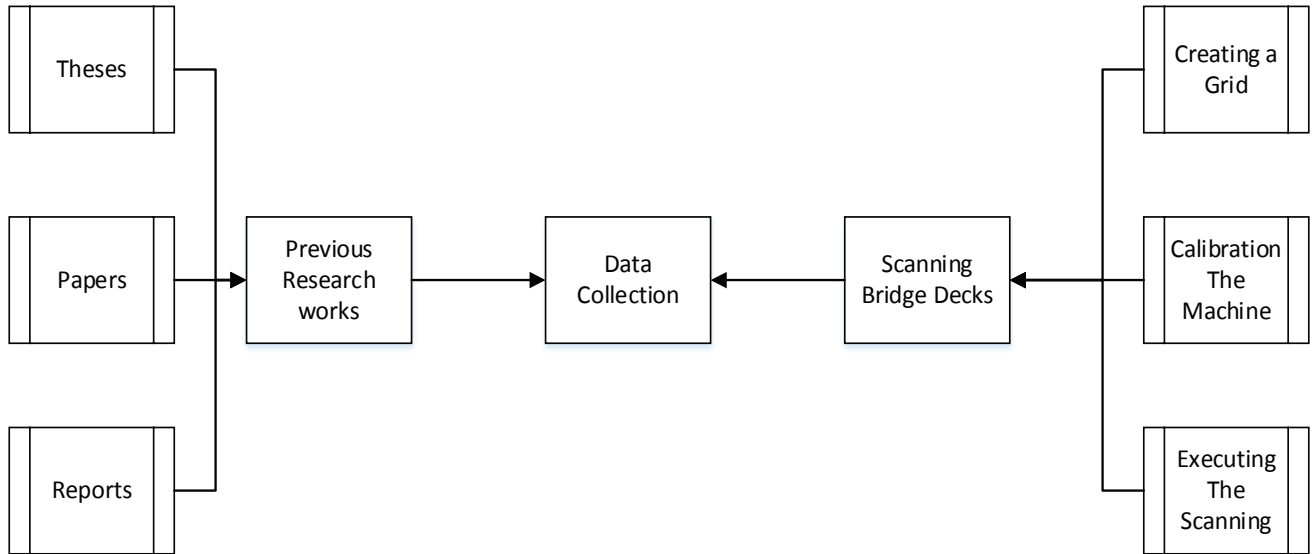
Figure 3-2. **Data collection flow chart**

3.2 DATA ANALYSIS AND MODEL DEVELOPMENT

After the data collection process, many analysis procedures were performed to draw a relationship between bridge deck corrosion and the frequency with which the machine is able to generate a standard scale with fixed numerical thresholds. The procedures and techniques used to analyze that data are explained in detail in CHAPTER 5.

Figure 3-3 shows the methods, techniques, and software used to analyze the data. First, the profiles are imported to a software application called RADAN 7® to extract the amplitude values of the top reinforcing bars; these amplitude values are the core data on whose values the whole technique is performed. These values required much analysis in order to be useful for developing a standardized scale. After extracting the amplitude values for the whole surveyed bridge decks and performing a depth correction for these amplitudes to make a normalization, the values were divided into categories using the K-means

clustering technique, with the limits of each category used as thresholds to define the different categories of corrosion. The reasons for using k-means clustering to divide the amplitude values into four groups are that 1) it is fast, robust, and easy to understand, 2) it produces tighter cluster than hierarchical clustering, and 3) it gives the best result when the data are well separated from each other. After the process of grouping and clustering was completed, statistical analysis was performed to check which distribution that each threshold followed is the best-fit distribution, and three statistical tests were performed while only the chi-squared test had been used to check the data. The median of each distribution was used as the value of the corresponding threshold because the best fit distributions have relatively high skewness and the amplitude values have some outliers; thus median should be chosen for any other parameters.

Next, a Monte-Carlo simulation was executed to simulate that data and make it more reliable; Monte-Carlo simulations have many important advantages, one of which is that the probability distribution within the model can be flexibly and easily used. Furthermore, Monte-Carlo simulations can model interdependent relationships between input variables, and the changes in the model can be investigated easily and quickly. After the simulation was performed, a sensitivity analysis was done to check the effect of changing the thresholds on the areas of each category. Sensitivity analysis was done seven times for each bridge by changing the thresholds one unit at a time. Finally, the most appropriate scale was chosen based on the analysis performed regarding

the areas of the four categories and the scale that related to these areas. The area of each category is calculated by using Equation 3-1, 3-2, 3-3, and 3-4.

$$Area\ of\ Good = \frac{G}{T}x100 \qquad\qquad\text{Equation 3-1}$$

$$Area\ of\ Fair = \frac{F}{T}x100 \qquad\qquad\text{Equation 3-2}$$

$$Area\ of\ Poor = \frac{P}{T}x100 \qquad\qquad\text{Equation 3-3}$$

$$Area\ of\ Critical = \frac{C}{T}x100 \qquad\qquad\text{Equation 3-4}$$

Where T represents the number of total points, G represents the number of points above the Good-Fair threshold; F represents the number of points between Good-Fair and Fair-Poor thresholds, P represents the number of points between Fair-Poor and Poor-Critical thresholds, and C represents the number of points below the Poor-Critical threshold. After calculating the area of each category for each bridge deck, following steps had been done to find the most appropriate scale:

- Tabulate the area of each category of corrosion for each bridge deck.

- Calculate the average and the standard deviation for the whole seven scales and the four category of corrosion.

- Find the absolute value of the area for the specific scale of a specific category for the bridge deck minus the average value divided by the standard deviation.

- The most appropriate scale for that bridge deck is the minimum summation of the four categories of that scale.

- Repeat this step for all bridge decks, and choose the scale that occurs most frequently as the most appropriate scale.

After finding the most appropriate scale, the deterioration curve of the corrosion of reinforcing bars is drawn using the Weibull distribution, whose probability distribution function is defined by Equation 3-5:

$$f(t) = \frac{\delta}{\tau}(\frac{t-\alpha}{\tau})^{\delta-1} \; x \; e^{-(\frac{t-\alpha}{\tau})^{\delta}}$$

Equation 3-5

where α = location parameter, τ = scale parameter, δ = shape parameter, and t = time.

The reasons behind using Weibull distribution function to draw the deterioration curves are: first, it has been proven to be one of best functions to represent the deterioration of concrete. Based on its parameters, the function starts at maximum level of performance and remains constant for a certain time, and this is the case in concrete structures which at first their condition is excellent for a certain time after construction. After a while the condition of concrete starts decreasing and similarly the Weibull function starts decreasing as well. Finally the speed of deterioration in concrete decrease near the end of its service life, also the slope of the Weibull function will decrease at the end. Second reason for using Weibull function is that it does not require a lot of historical inspection data to draw a deterioration curve. Finally, the Weibull function parameters are calculated easily and are also significant figures.

The cumulative Weibull distribution function is defined in Equation 3-6

$$\boldsymbol{f(t) = 1 - e^{-(\frac{t-\alpha}{\tau})^{\delta}}}$$

Equation 3-6

The Weibull reliability function of distribution is equal to the cumulative distribution function subtracted from one (Equation 3-7).

$$R(t) = 1 - f(t) = e^{-(\frac{t-\alpha}{\tau})^{\delta}}$$
<div align="right">Equation 3-7</div>

In order to draw the ideal condition curve, the listed below condition must be met (Semaan 2011):

- In the beginning (t=0) the condition is equal to 1 (maximum), so:

$$1 = \alpha \cdot e^{-(\frac{0}{\tau})^{\delta}} \Rightarrow \alpha = 1$$

- δ = 3 provides the smoothest inclination (Gkountis 2014)

- At time = service life = 100 years, the condition equals 0.2 (minimum), thus:

$$0.2 = e^{-(\frac{100}{\tau})^{3}} \Rightarrow \ln 0.2 = \ln 1 - (\frac{100}{\tau})^{3}$$

$$\tau = \frac{100}{(-\ln 0.2)^{1/3}} = 85.33 \; years$$
<div align="right">Equation 3-8</div>

Thus when assuming the service life for the bridge deck is equal to 100 years, then the useful service life (condition = 0.4) is 85.33 years. By substituting 75 and 50 years in Equation 3-8 instead of 100 years, t will be 64 and 42.67 years respectively. The curves drawn in this way represent the ideal condition curves for bridge decks that have a service life of 100, 75, and 50 years respectively.

Another curve is drawn at the time of inspection; in this case, we have the age of the bridge deck and the percentage of good condition at that time. Then the curve can be drawn by using Equation 3-9:

$$R(t) = e^{\ln Ci(\frac{t}{t_i})^{3}}$$
<div align="right">Equation 3-9</div>

where ti is the time of inspection and Ci is the percentage of good condition at time ti. This curve will be compared with ideal condition curves at different times. From this comparison the expected service life for that bridge deck will be known.
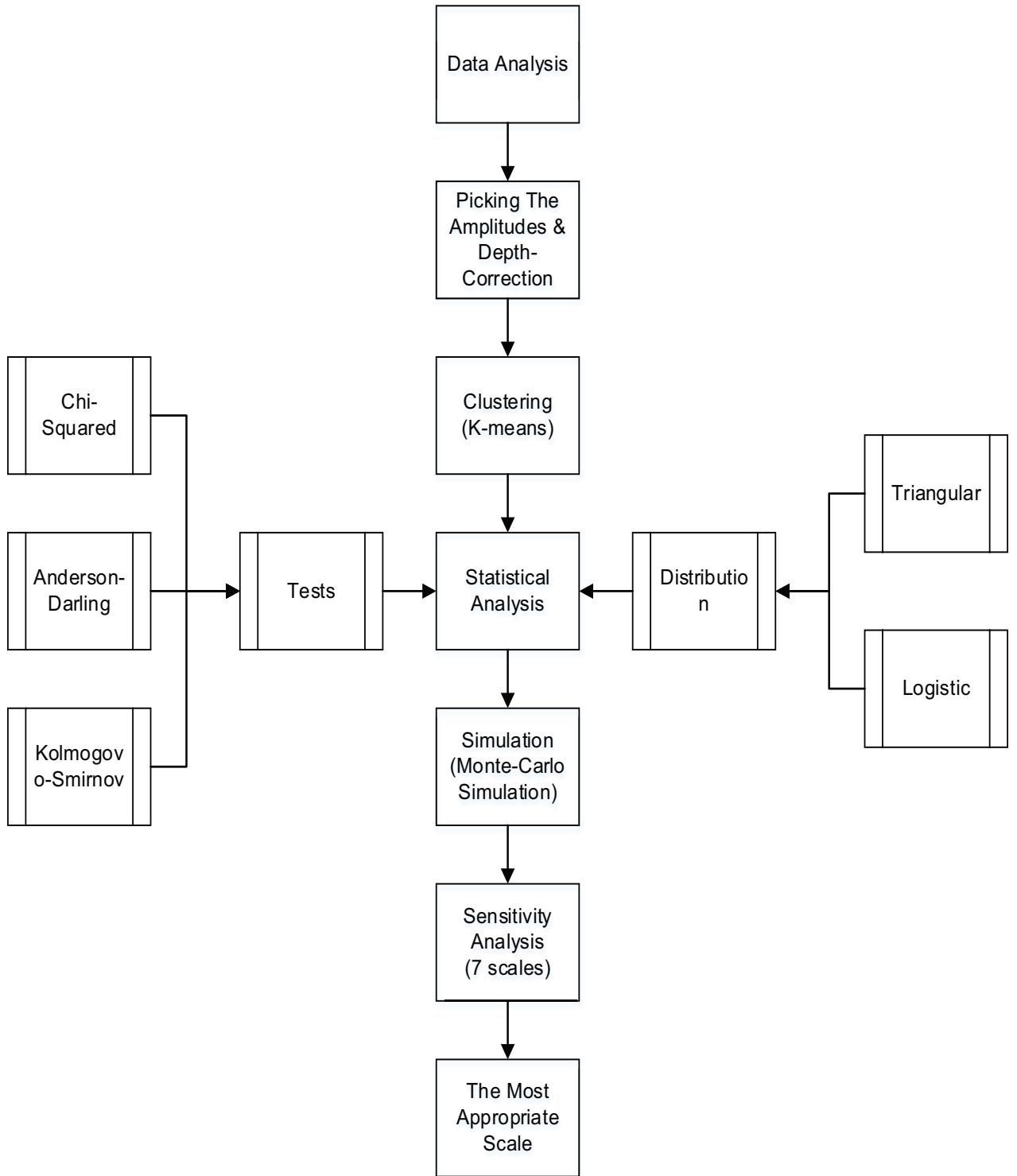
Figure 3-3. Model development flow chart

CHAPTER 4 DATA COLLECTION

Data from 61 bridges were collected either from surveying or from previous research works. From these 61 bridges, 14 bridges were measured by a 1.0 GHz-frequency machine, 34 bridges were measured by a 1.5 GHz-frequency machine, and 12 bridges were measured by a 2.6 GHz-frequency machine as shown in Figure 4-1. However, only the bridge decks measured by the 1.5 GHz-frequency machine were used in this research because the numbers of the bridge decks for other machines were not sufficient to perform analysis for them, and the machine frequency of 1.5 GHz is the one most commonly used.
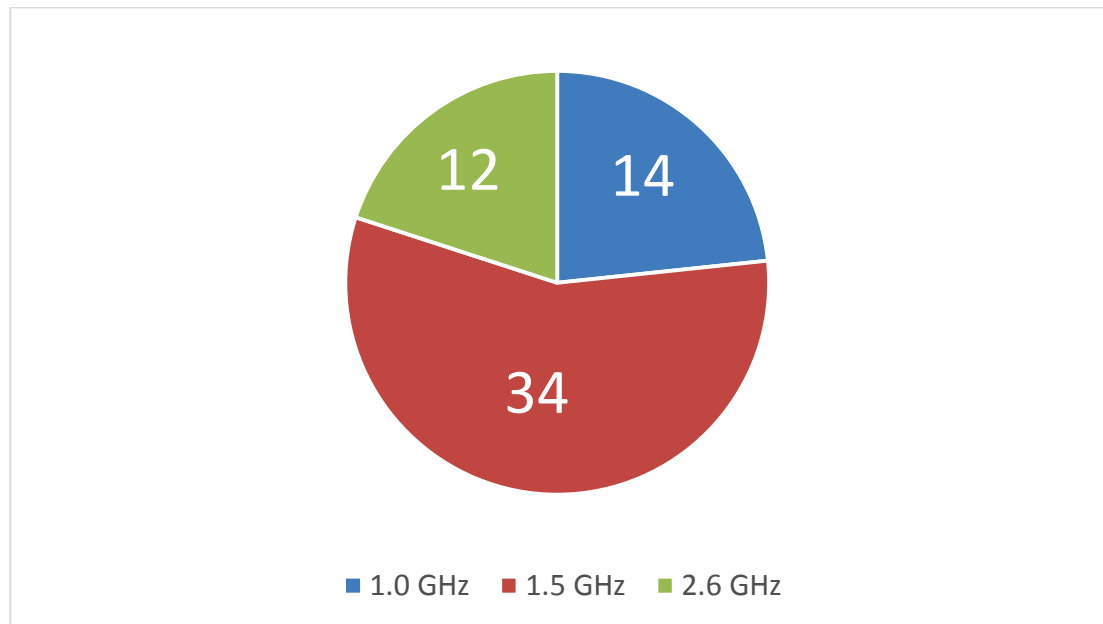
Figure 4-1. Number of bridge decks for each machine

Figure 4-2 shows that out of 34 bridge decks, 20 bridge decks were surveyed, and 14 were collected from previous research.
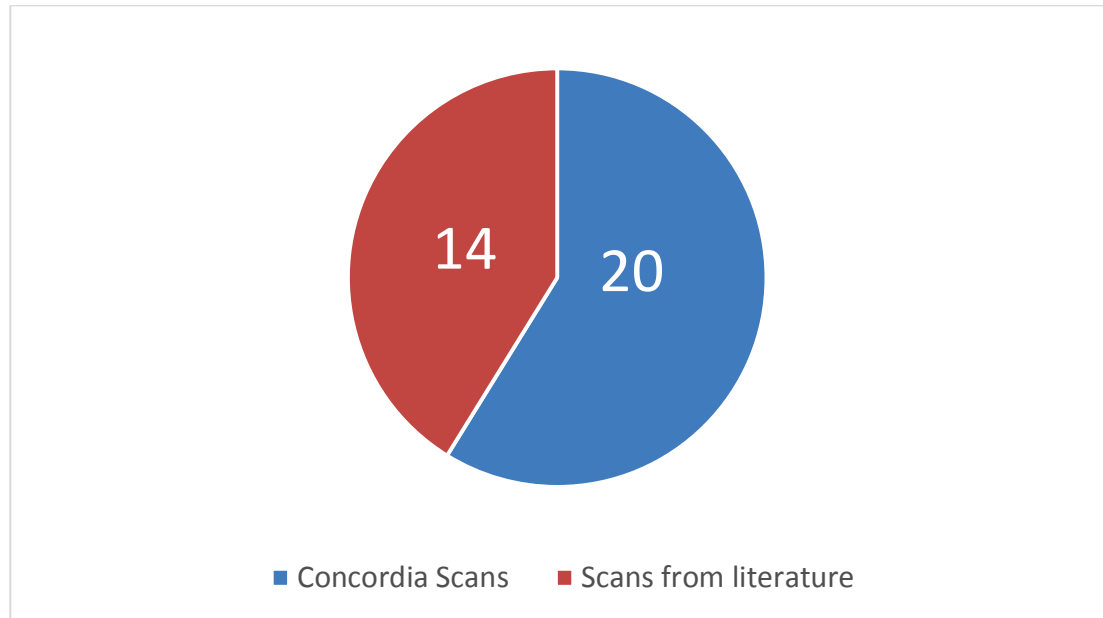
Figure 4-2. Number of surveyed bridge decks vs. decks collected from previous researches

These data from either surveyed bridge decks or previous studies are incomplete. Much information is not known such as; bridge decks age, whether the deck has asphalt layer or not, the amount of moisture content, etc. However, the available information had been used as much as possible in order to find a standardized scale for the whole bridge decks using 1.5 GHz GPR machine.

4.1 BRIDGE SURVEYS

Data collection via bridge surveys consists of simple procedures that must be followed in order to have accurate results: marking a grid, calibrating the GPR machine, and executing the survey. A detailed explanation of how these procedures were done is described in the following sections.

4.1.1 Marking A Grid

The first step of surveying the bridge is to make a grid on the deck surface. Usually, this involved marking off a 2 ft. x 2 ft. orthogonal grid. Sometimes, in order to increase the survey's accuracy, a 1 ft. x 1 ft. grid is marked off. The bridge deck resembles that shown in Figure 4-1. The purpose of making a grid is to help and guide the inspector to move the machine in straight line. Moreover, the gird is marked by numbers and letters such as A5, B8, etc., that will help the inspectors to locate the damage on the bridge deck and compare its location with the map.

Figure 4-3. 2 ft. x 2 ft. grid (Gucunski et al. 2011)

4.1.2 GPR Calibration

The GPR machine must be calibrated in order to make it able to measure the exact length of the bridge deck during the surveying.

The calibration process is done as following:

- A known distance is marked (10 ft., for example).

- The calibration option will be chosen in the GPR machine, based on the distance (another calibration option based on the time could be used if the machine is moving at a constant speed).

- The GPR machine is moved from the starting mark to the end mark.

Once these steps have been completed, the GPR machine is calibrated and is ready to start surveying the bridge deck.

4.1.3 Surveying the bridge

When the machine is calibrated, we start surveying the bridge by moving the GPR machine over the marking dots in straight lines in the long direction. To finish this process quickly, we scan one line in one direction and the next in the reverse direction as shown in Figure 4-2. However, the profiles done in the reverse direction should be reversed again by using the RADAN 7® software in order to generate the map to represent the real and the exact corrosion of the bridge deck.
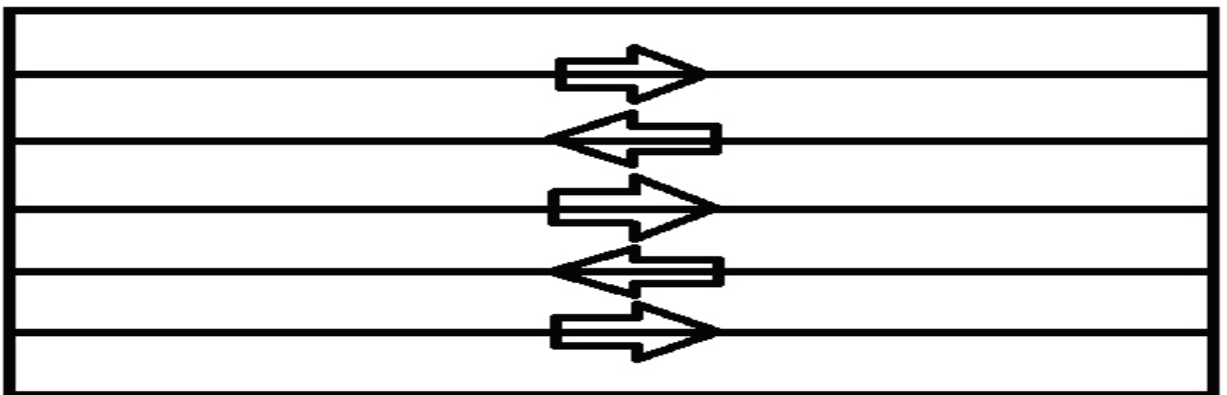
Figure 4-4. Surveying bridge process

4.2 BRIDGE DATA FROM PREVIOUS RESEARCH

48

Data used in this study from bridge decks other than surveyed bridges are collected from previous studies such as reports, papers, and theses. However, the data collected from these studies are not complete and are missing much relevant information. Nevertheless, they were used to enrich the database. Data from approximately fourteen bridges was collected; the GPR scale for each bridge was inserted in a table to identify the threshold of each category. Nine bridges are from the final report of a project done by the Iowa Highway Research Board, the Iowa Department of Transportation, and the Federal Highway Administration in January 2011. The title of the report is "Comprehensive Bridge Deck Deterioration Mapping of Nine Bridges by Non-destructive Technologies". These nine bridge decks had been studied and investigated using different NDTs such as 1) ground-penetrating radar (GPR), both ground- and air-coupled; 2) half-cell potential; 3) impact-echo (IE); 4) ultrasonic surface wave (USW); and 5) electrical resistivity (ER). Moreover, these non-destructive tests had been validated using the coring technique. However, only the tests and the results from the GPR technique had been used in this thesis. Figure 4-3 shows the thresholds of GPR scale that was added to the data base in the interests of this research, whereas the data from other bridge decks were gathered from many other different sources. Data that had been collected from surveying bridge decks and previous research works are tabulated in Table 4-1. All bridge deck data collected in this research are shown in Appendix 7.1.
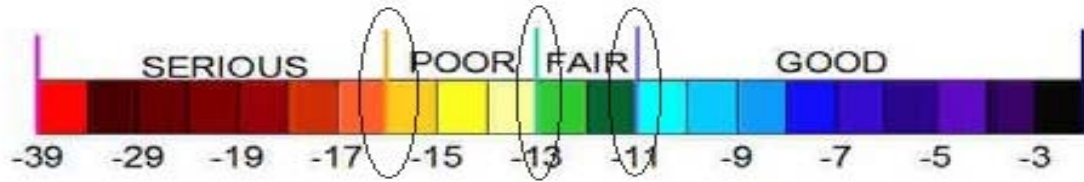
Figure 4-5. Thresholds of GPR scale (Gucunski et al. 2011)

Table 4-1 Sample of Collected Data

Frequency (GHz)	Machine	Good-Fair	Fair-Poor	Poor-Critical	Scale
1.5	ground-coupled	-11.00	-13.00	-16.00	
1.5	ground-coupled	-11.00	-13.00	-16.00	
1.5	ground-coupled	-10.50	-12.50	-15.50	

CHAPTER 5 DATA ANALYSIS AND MODEL DEVELOPMENT

This chapter will explain in details the flowchart shown in Figure 3-3. Each section shows the procedures for every important step done to analyze the data and develop the model. First, it shows how the data was extracted from the GPR profiles to make the analysis useful and the techniques and the software used. Next, it explains the different techniques used to perform the analysis and the reasons for using each technique. Finally, it shows the ways in which the developed model was verified.

5.1 PICKING THE AMPLITUDES

After surveying the bridge deck, scanning profiles are imported to the RADAN 7® software for analysis and the extraction of useful information. First, the profile is cut down to remove the extremes and just include the bridge deck. Next, the peak of the parabolic shape, which represents the top reinforcing steel bar, is selected (Figure 5-1). When the whole bars are selected, an excel sheet is generated containing the scan number, amplitude, and two-way travel time for each point (bar). This step is repeated again for the whole bridge deck's profiles. The reason for selecting the peak of the parabolic shapes is that it represents the exact location of the top bar. These red points shown in Figure 5-1 represent the location of top reinforcing bars and their amplitudes.
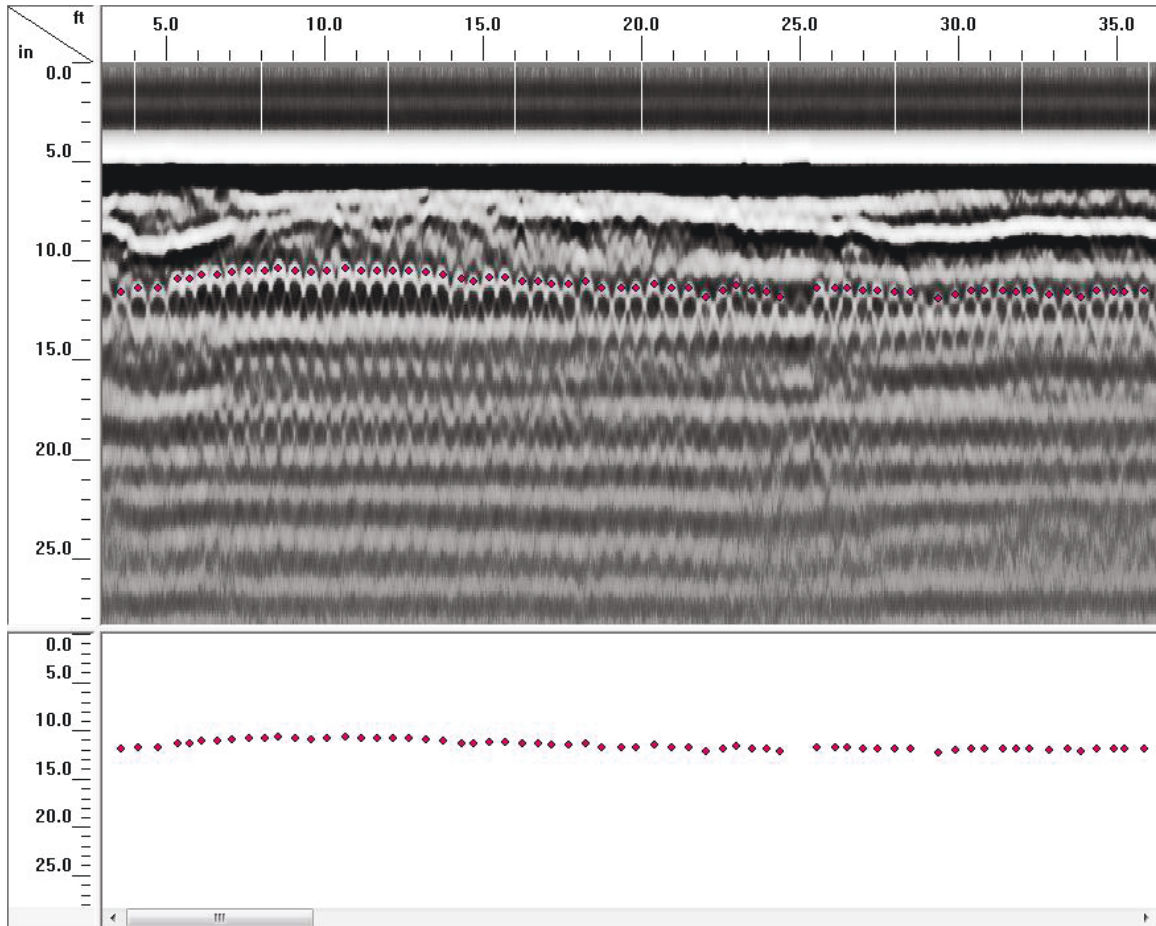
Figure 5-1. Selection of top reinforcing steel bars

5.2 DEPTH CORRECTION

After the whole bars for the whole profiles of the bridge deck are selected and Excel sheets are generated for all profiles, these excel sheets are imported to software in order to perform a depth correction for the reinforcing bars. The principle of the depth correction is to normalize the depth of the reinforcing bar. Reinforcing bars have different depth even for a new bridge, this will lead to a difference in the amplitude of the reflected wave because, as discussed earlier, there is a relationship between the amplitude and the depth. Therefore, the amplitudes of reflected waves are plotted versus the two-way travel time, after

which a quantile linear regression fitting is drawn at the 90th percentile as shown

in Figure 5-2. This regression line is subtracted from depth-dependent amplitude

in order to normalize the depth.
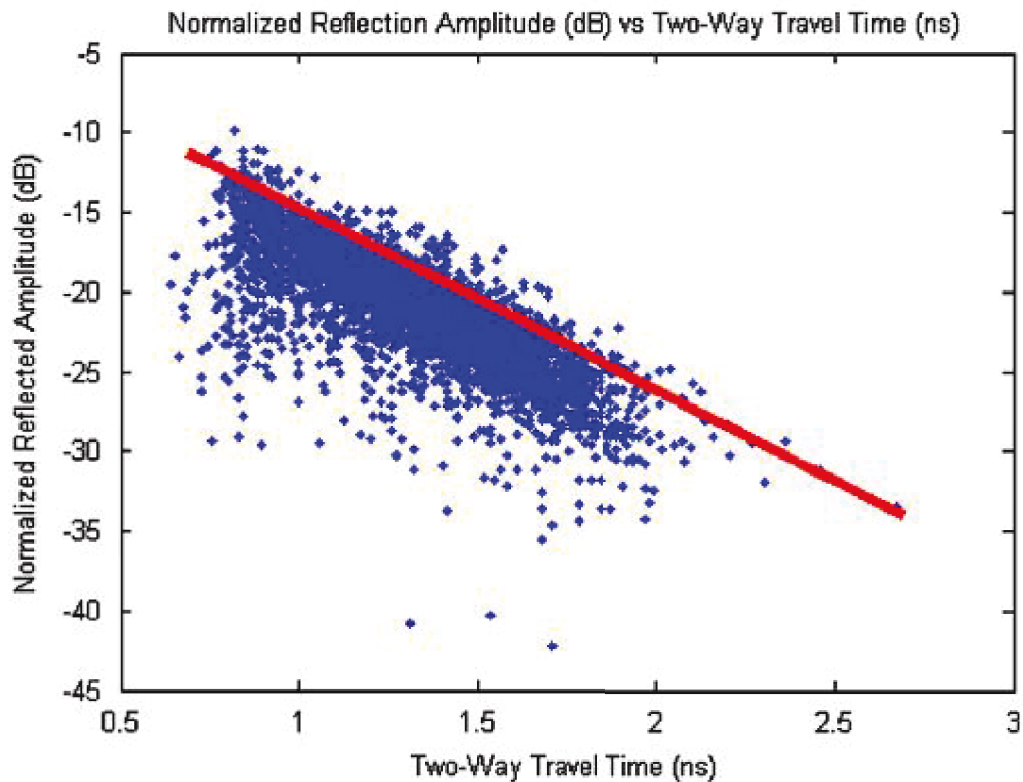
Figure 5-2. Quantile linear regression fitting at 90th percentile (Barnes et al.

2008)

5.3 CLUSTERING THE AMPLITUDES

After finishing the depth-correction process, a new excel sheet is

generated containing the new amplitude values. MATLAB is used to cluster the

new amplitude values for bridge deck into four categories using K-means

clustering. The limits of each category of surveyed bridge decks and the limits

used from bridge decks collected from previous studies are entered in an Excel

sheet as illustrated in Table 5-1. This table had the three limits of 34 different

bridge decks. These limits are ready for statistical analysis to find the most appropriate thresholds for the GPR scale.

Table 5-1 Category Limits of Bridge Decks

Bridge	Good-Fair	Fair-Poor	Poor-Critical
A	-11.00	-13.00	-16.00
B	-11.00	-13.00	-16.00
C	-10.50	-12.50	-15.50
D	-11.50	-13.50	-16.50
E	-11.50	-13.50	-16.50
F	-11.50	-13.50	-16.50
G	-11.00	-13.00	-16.00
H	-10.75	-12.75	-15.75
I	-10.75	-12.75	-15.75
J	-23.00	-25.00	-28.00
K	-13.00	-15.00	-18.00
L	-19.50	-21.50	-24.50
M	-23.00	-25.00	-28.00
N	-24.00	-26.00	-29.00
O	-23.00	-29.00	-33.00
P	-4.00	-8.00	-12.00
Q	-2.00	-8.00	-12.00
R	-1.00	-5.00	-8.00
S	-0.99	-3.38	-6.24
T	0.12	-2.24	-4.40
U	0.67	-1.97	-4.14
V	0.21	-1.81	-3.70
W	-1.05	-3.50	-7.19
X	-1.37	-3.62	-7.00
Y	-0.94	-2.84	-5.48
Z	-1.12	-3.59	-7.71
AA	-2.61	-7.37	-16.81
AB	-2.87	-7.57	-14.24
AC	-3.57	-9.68	-20.29
AD	-3.32	-9.22	-18.92
AE	-3.17	-7.89	-14.51
AF	-2.97	-7.65	-13.99
AG	-3.78	-9.93	-19.94
AH	-0.80	-3.01	-6.37

5.4 STATISTICAL ANALYSIS

These data are imported into a statistical software application called Crystal-Bal for analysis. The software checks the distributions followed by each threshold. Statistical tests and their corresponding P-values, including the chi-squared, Anderson-Darling, and Kolmogorov-Smirnov tests, were used to check which distribution is most suitable for the data. The distribution for each threshold is assigned based on the smallest test value of the chi-squared test. Moreover, in order to have the highest confidence level that the data follow specific distribution, P-values were calculated; the closer the P-value to one the more confidence we have. Table 5-2 represents a summary of the statistical analysis and statistical tests. From Table 5-2, it is noticeable that the Good-Fair threshold has a triangular distribution, which considers a continuous probability distribution with min equal to -28.38, likeliest 0.67, and max 1.03. Even though, the value of the chi-squared test is relatively high and the p-value is equal to zero, this distribution was the most suitable one among the other distributions, which included normal, logistic, lognormal, etc. However, for the fair-poor threshold, the logistic distribution was the most appropriate based on the value of the chi-squared test (3.7647). In addition, the p-value of 0.288 means that the null hypothesis (data follow logistic distribution) cannot be rejected. Finally, for the third threshold (poor-critical), it also follows the logistic distribution, although not in the same degree of acceptance. This threshold has less degree of acceptance than the fair-poor threshold in terms of the value of the chi-squared test and its corresponding p-value.

Table 5-2 Summary of Statistical Analysis and Statistical Tests

	Good-Fair	Fair-Poor	Poor-Critical
Distribution	Triangular	Logistic	Logistic
Mean	-7.63	-10.74	-14.94
Median	-7.71	-10.04	-14.63
Mode	0.67	-10.04	-14.63
Standard Deviation	6.89	7.6	7.82
Variance	47.48	57.68	61.16
Skew	-0.5654	0	0
Kurtosis	5.4	4.2	4.2
Chi-Squared Test	16.8235	3.7647	7.2941
P-Value	0.000	0.288	0.063
A-D Test	2.1746	0.9305	0.7076
P-Value	-	0.000	0.035
K-S Test	0.2546	0.1281	0.1172
P-Value	-	0.128	0.168
Min	-28.38		
Likeliest	0.67		
Max	1.03		

The logistic distribution is like the normal distribution but with higher kurtosis (longer tails). After verifying that the data follow a specific distribution, and because the data used has some outliers, the median of each limit is used as limits for the required scale, giving it three thresholds (-7.71 dB, -10.04 dB, -14.63 dB) and four categories (good, fair, poor, critical). Figure 5-3 illustrates the created scale after a statistical analysis.

Figure 5-3. GPR scale for 1.5 GHz machine

5.5 SIMULATION-BASED SCALE

A Monte Carlo simulation was performed using Crystal Ball. The simulation was done on the three thresholds (good-fair), (fair-poor), and (poor-critical). The statistical analysis shows that best-fit distribution for the threshold (good-fair) is the triangular, while for the other two thresholds (fair-poor) and (poor-critical) is logistic. Therefore, these three distributions were assumed in the simulation. After 1,000,000 trials, the simulation results were accurate and close to the original data. The medians for the three thresholds (good-fair), (fair-poor), and (poor-critical) are (-7.71), (-10.06), and (-14.64), respectively. Figures 5-4 to 5-6 show the graph of the thresholds being simulated while the result of the simulation is presented in the Appendix 7.5.
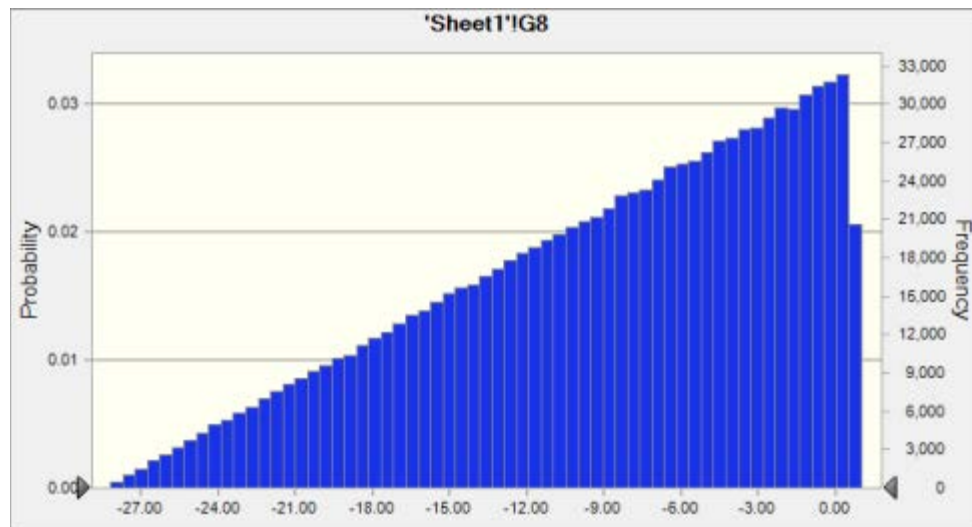
Figure 5-4. Plot of good-fair threshold
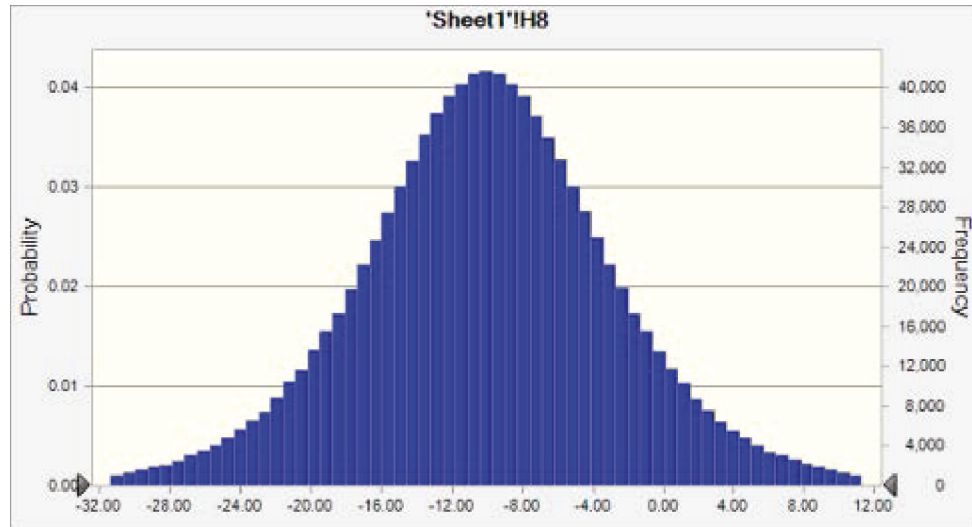
Figure 5-5. Plot of fair-poor threshold
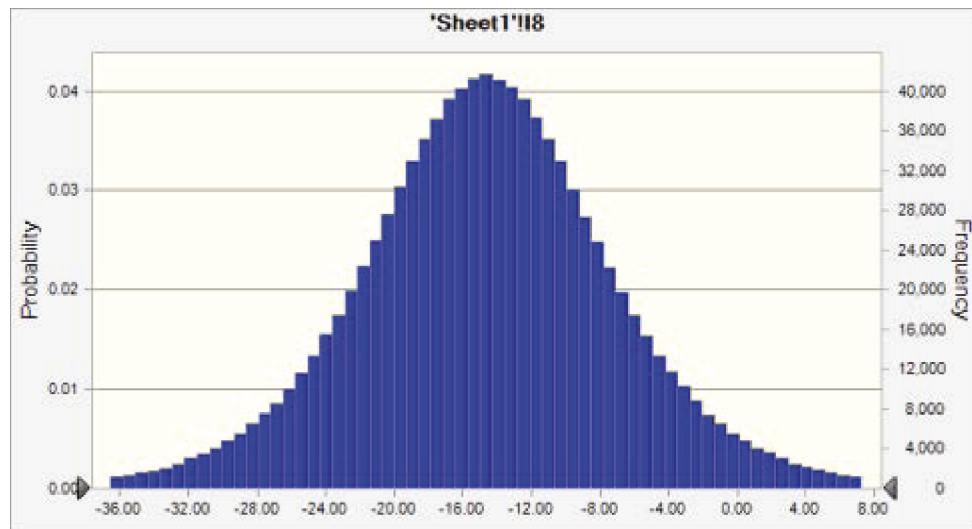
Figure 5-6. Plot of poor-critical threshold

5.6 SENSITIVITY ANALYSIS

After executing the simulation for the three thresholds, a sensitivity analysis was performed to check the effect of changing the thresholds values on the areas of each category. The thresholds for the three categories were changed simultaneously. The ranges of the thresholds that had been utilized are shown in Table 5-3. The corrosion maps for one bridge deck with different ranges

of thresholds will be shown in this section from Figure 5-7 up to Figure 5-13. The maps of another bridge deck will be in appendix 7.2. It is apparent from these maps that when the thresholds are shifted up, the areas of good concrete decrease and the areas of critical category increase. The area of each category is calculated precisely by using count and COUNTIF equation in Excel. The count equation is used to find the total number of points (top reinforcing bars), COUNTIF is used to find number of points that fall between the two specified thresholds. For example, for a bridge with a total of 13624 points, 6320 points above -7.71, 4385 points between -7.71 and -10.04, 2579 points between -10.04 and -14.63, and 340 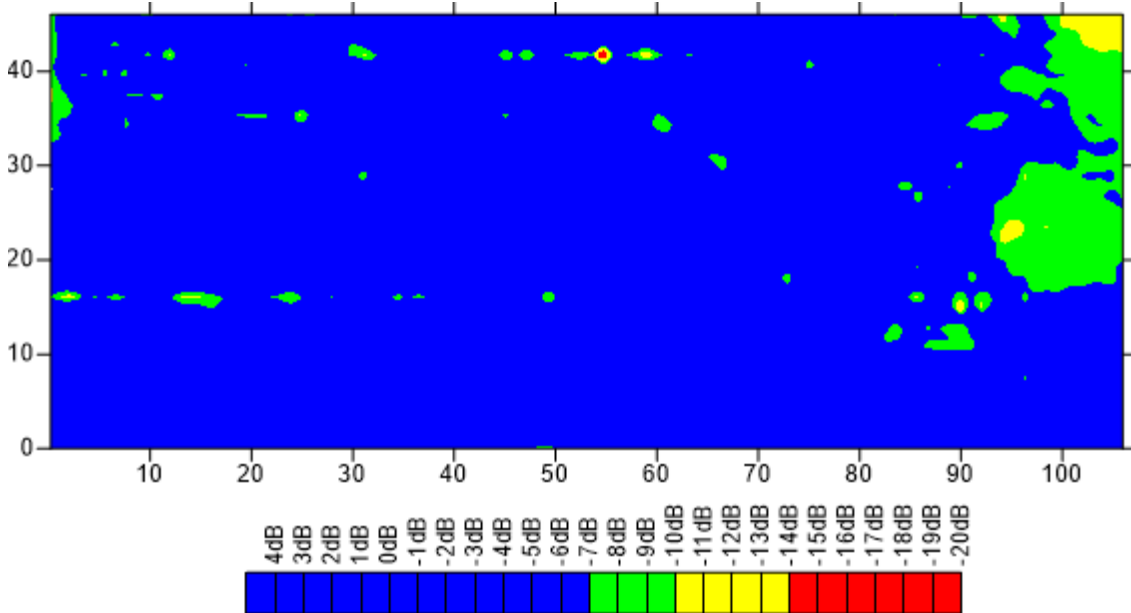points below -14.63, the "good" area equals $\frac{6320}{13624}x100\% =$ 46.39%. Areas of fair, poor, and critical are 32.19%, 18.93%, and 2.50% respectively.

Table 5-3. Thresholds Values for Sensitivity Analysis

SCALE	GOOD-FAIR	FAIR-POOR	POOR-CRITICAL
A	-7.71	-10.04	-14.63
B	-6.71	-9.04	-13.63
C	-5.71	-8.04	-12.63
D	-4.71	-7.04	-11.63
E	-3.71	-6.04	-10.63
F	-2.71	-5.04	-9.63
G	-1.71	-4.04	-8.63

Bridge 206

GOOD	FAIR	POOR	CRITICAL
96.13%	2.82%	0.95%	0.10%

Figure 5-7. Corrosion map using scale A
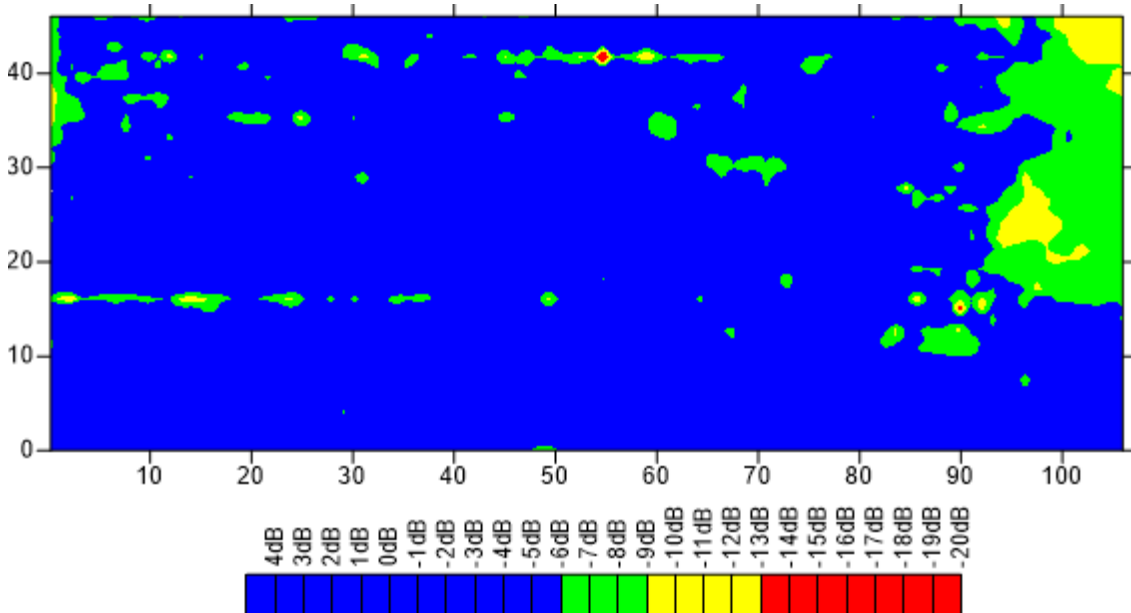
GOOD	FAIR	POOR	CRITICAL
93.50%	4.64%	1.70%	0.15%

Figure 5-8. Corrosion map using scale B

GOOD	FAIR	POOR	CRITICAL
88.48%	8.37%	2.87%	0.28%
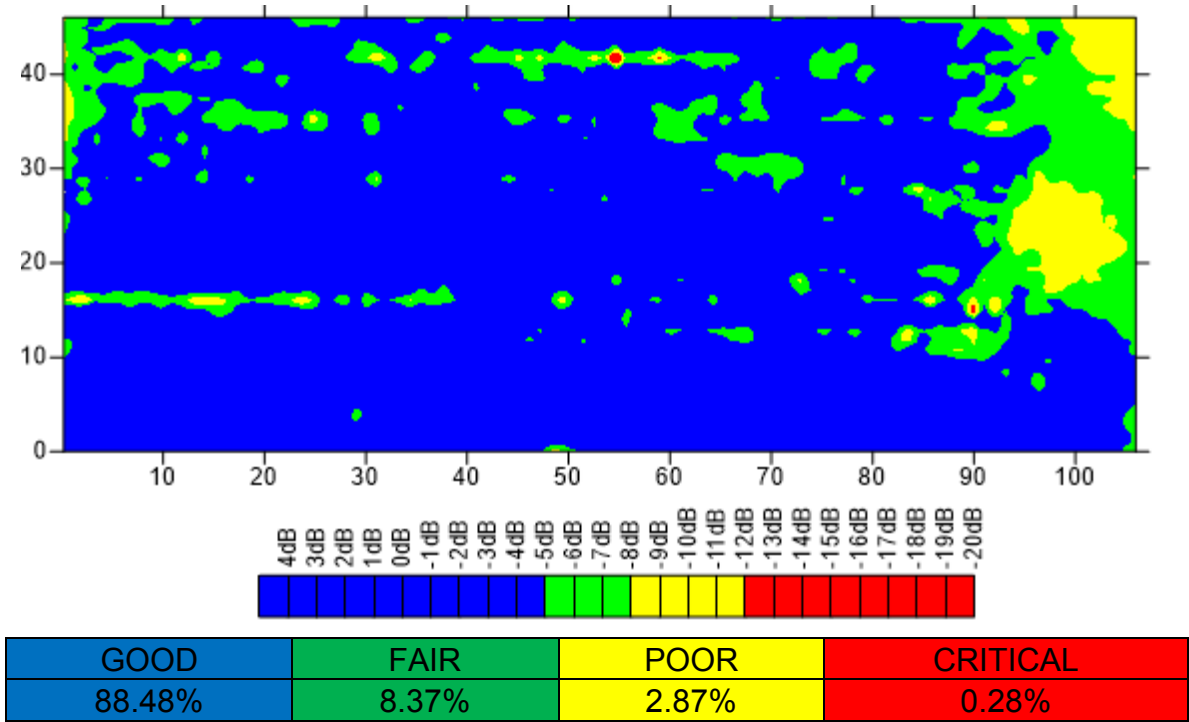
Figure 5-9. Corrosion map using scale C

GOOD	FAIR	POOR	CRITICAL
79.88%	14.74%	4.95%	0.43%
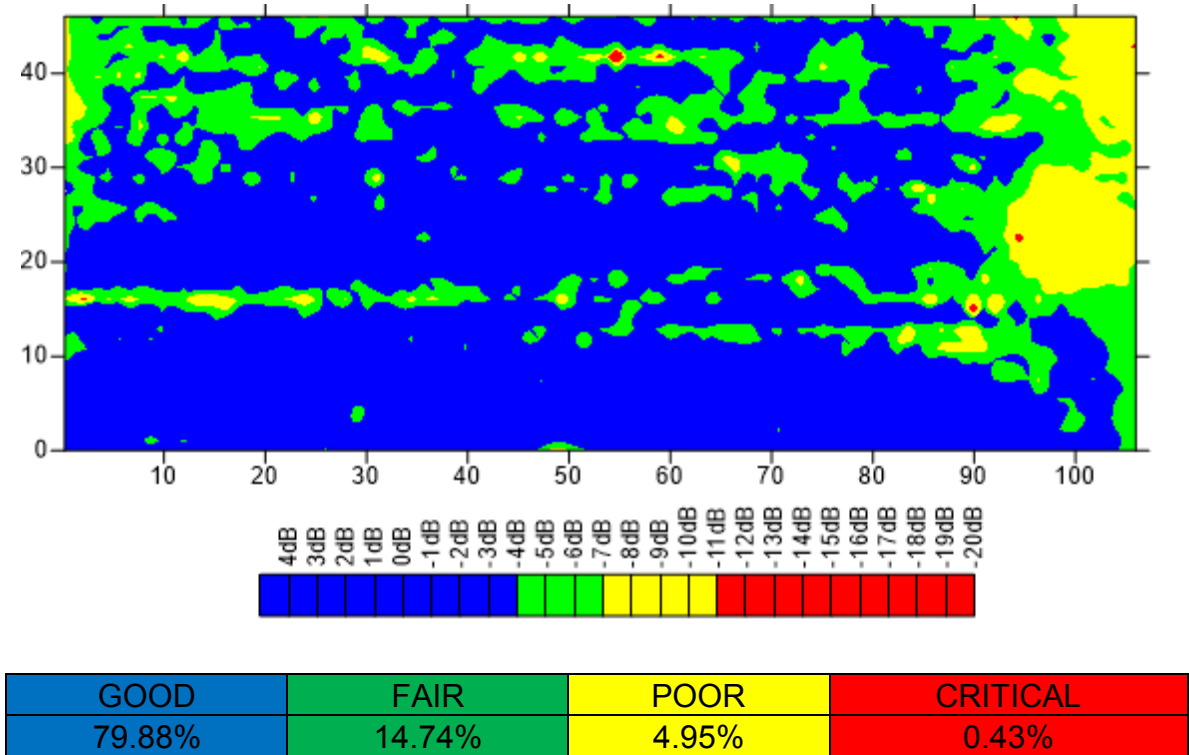
Figure 5-10. Corrosion map using scale D
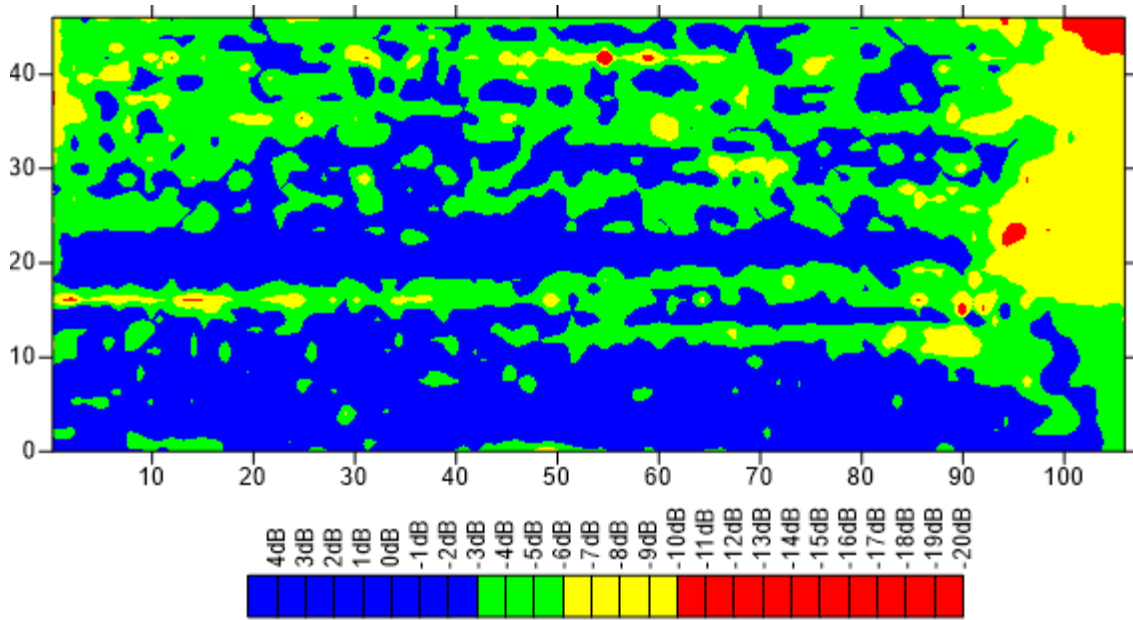
GOOD	FAIR	POOR	CRITICAL
65.53%	24.66%	9.13%	0.69%

Figure 5-11. Corrosion map using scale E
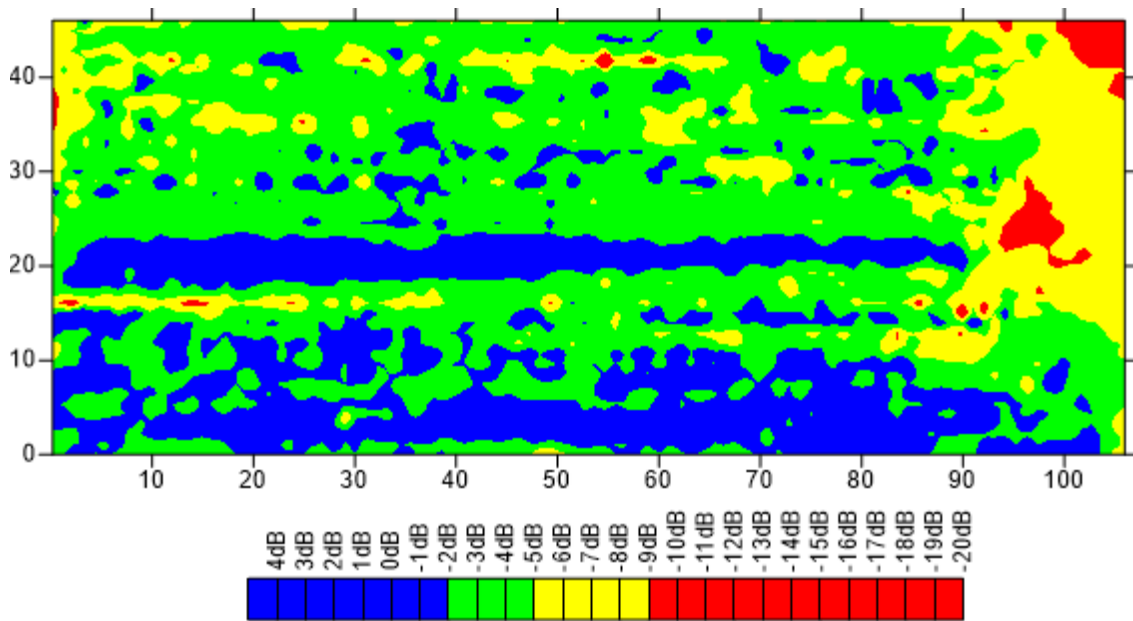
GOOD	FAIR	POOR	CRITICAL
46.46%	36.88%	15.34%	1.32%

Figure 5-12. Corrosion map using scale F

GOOD	FAIR	POOR	CRITICAL
27.48%	43.93%	26.32%	2.27%
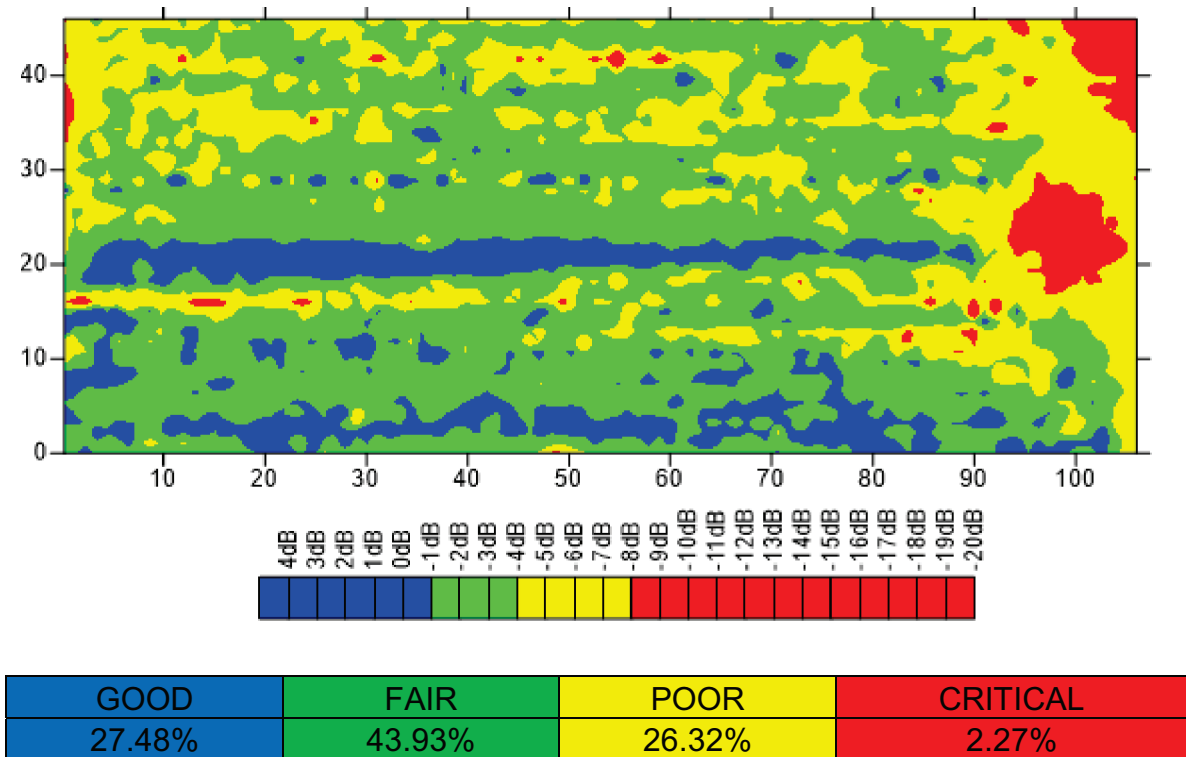
Figure 5-13. Corrosion map using scale G

From these maps it can be observed that the shapes and locations of the deteriorations are approximately the same. However, the area and the extent of these deteriorations increases from one scale to another.

5.7   CHOOSING THE MOST APPROPRIATE SCALE

After finding the area of each category for each bridge based on scales discussed in Section 5.6, the areas for the whole surveyed bridges were tabulated. Only one bridge deck sample is shown in this section; analyses of other bridge decks are provided in Appendix 7.3. Table 5-4 shows the areas of the four categories from scale A up to scale G.

Table 5-4. Areas of Bridge (1)

Scale	GOOD (G1)	FAIR (F1)	POOR (P1)	CRITICAL (C1)
		Bridge 1		
G	37.77%	38.87%	21.03%	2.32%
F	56.20%	30.67%	11.66%	1.47%
E	72.24%	20.11%	6.67%	0.98%
D	84.16%	11.22%	3.95%	0.67%
C	90.88%	6.15%	2.48%	0.49%
B	94.54%	3.50%	1.60%	0.36%
A	96.59%	2.13%	1.05%	0.23%

While the areas for all bridges are tabulated as well, a table including the average of each area for each scale for each bridge was drawn as shown in Table 5-5. In addition, Table 5-6 provides standard deviation.

Table 5-5. Averages of Areas for each Scale

Scale	GOOD (GA)	FAIR (FA)	POOR (PA)	CRITICAL (CA)
		Average		
G	33.88%	36.97%	21.42%	7.73%
F	52.10%	27.21%	14.76%	5.93%

E	66.97%	17.73%	10.65%	4.66%
D	76.93%	11.46%	7.90%	3.71%
C	83.12%	7.90%	6.07%	2.91%
B	87.28%	5.77%	4.62%	2.33%
A	90.23%	4.40%	3.51%	1.86%

Table 5-6. Standard Deviation

Standard Deviation				
Scale	GOOD (GS)	FAIR (FS)	POOR (PS)	CRITICAL (CS)
G	0.098	0.117	0.103	0.110
F	0.170	0.061	0.113	0.088
E	0.202	0.050	0.108	0.070
D	0.202	0.058	0.095	0.056
C	0.184	0.061	0.081	0.045
B	0.159	0.059	0.066	0.036
A	0.133	0.054	0.051	0.029

When the averages and the standard deviation are calculated, the absolute difference between the area of each category for each bridge and the corresponding average value is divided by the corresponding standard deviation as shown in Table 5-7.

Table 5-7. Absolute Difference

Scale	ABS((G1-GA)/GS)	ABS((F1-FA)/FS)	ABS((P1-PA)/PS)	ABS((C1-CA)/CS)
G	0.395	0.163	0.038	0.492
F	0.241	0.564	0.275	0.508
E	0.261	0.478	0.370	0.529
D	0.358	0.042	0.414	0.542
C	0.422	0.285	0.443	0.544
B	0.456	0.381	0.460	0.547
A	0.480	0.422	0.483	0.553

Then the summation of these values for each scale for each bridge is calculated as illustrated in Table 5-8. The corresponding scale of the minimum summation is selected; for example, in this bridge deck scale, G has the minimum summation and has been therefore been selected as the most appropriate scale.

Table 5-8. Selected Scale

1.088	G
1.589	F
1.638	E
1.356	D
1.695	C
1.844	B
1.937	A

After this step is repeated on all bridges, the number of occurrences for each scale is plotted on a histogram as shown in Figure 5-14. From this figure it can

be concluded that the scale A occurs most frequently. Therefore, this scale with its corresponding thresholds will be the most appropriate scale for assessing bridge deck corrosion using a frequency setting of 1.5 GHz.
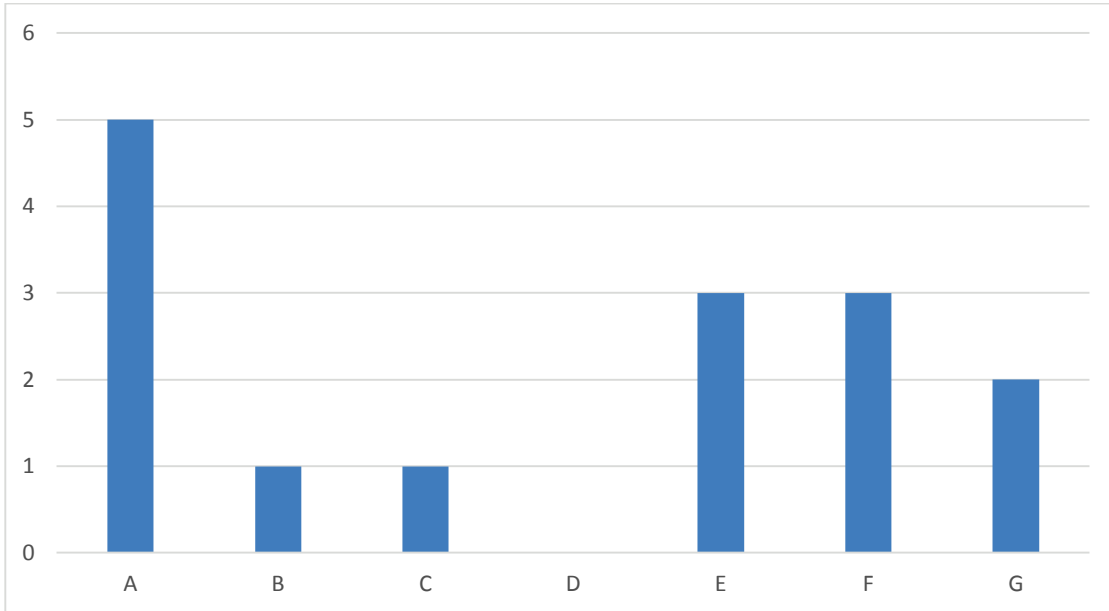
Figure 5-14. Plot of Scale vs. Occurrence

5.8   VERIFYING THE NEW SCALE

In order to verify the developed scale, a new bridge was surveyed, and the developed scale was applied to that bridge. As can be seen from Figure 5-15, most of the area (99 %) of bridge falls into the "good" category while very small or even neglected areas fall under either "poor" or "critical." From the GPR map of the bridge it can be concluded that the developed scale is accurately and precisely representing the real and exact corrosion of the bridge deck.

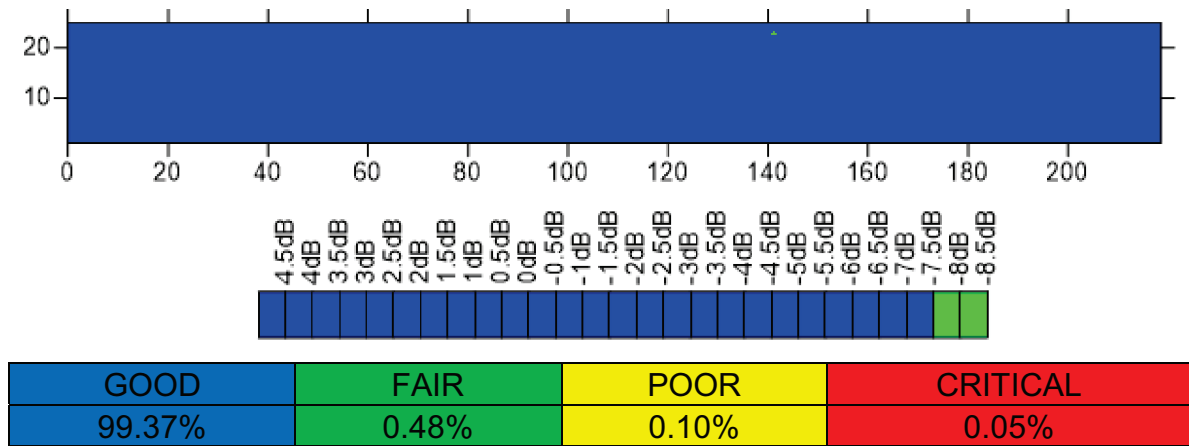| GOOD	FAIR	POOR	CRITICAL
99.37%	0.48%	0.10%	0.05%

Figure 5-15. GPR map of a brand new bridge using the developed scale

5.9 COMPARISON WITH OTHER METHODS

Another way to verify or validate the accuracy of the developed scale, GPR corrosion maps for the same bridge deck developed by different methods are compared with the corrosion map generated by the developed scale. The first four maps (Figure 5-16 to Figure 5-19) are for an old bridge deck and are generated via developed scale, image-based method, clustering-based threshold calibration method, and numerical amplitude method, respectively; the second four maps (Figure 5-20 to Figure 5-23) are for the same bridge deck, but after demolishing and constructing a new one. The map created by the developed scale shows some similarities among the maps created by image-based and clustering-based threshold calibration; zones are labelled A and B. However, areas identified as "good" in maps generated by developed scale and image-based techniques are close to each other, while critical areas are similar in the image-based and clustering-based threshold calibration maps.

However, the the map created by the image-based method (Figure 5-21) of the newly constructed bridge deck (surveyed after 2 weeks of construction),

which is supposed to be completely in good condition, exactly shows the deck's corrosion, while the only map that has numerical value and represents the real and exact corrosion of the bridge deck is the map created using the developed scale (Figure 5-20). The map created via the clustering-based threshold calibration method (Figure 5-22) shows that more than 20% of the total area is in severe condition and less than 10% in good condition, which is implausible for a new deck. Moreover, the map created by the numerical amplitude method has some red areas (Figure 5-23). It therefore can be concluded that the maps created using the developed scale technique are the most accurate, precise, and representative of the exact corrosion of the deck under investigation.

GOOD	FAIR	POOR	CRITICAL
71.40%	13.45%	11.02%	4.13%
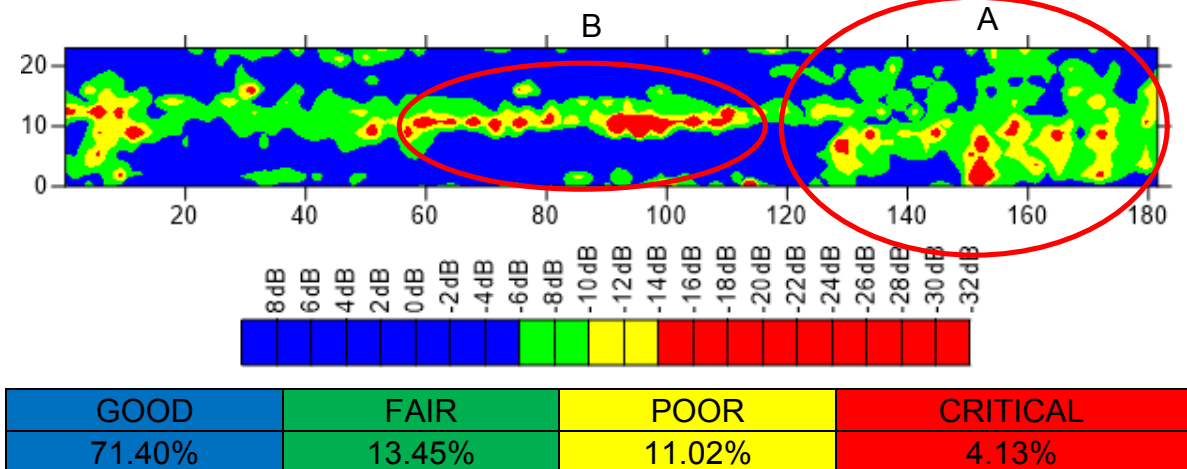
Figure 5-16. GPR corrosion map by developed scale (Old)

Good	Moderate	Severe
72%	14%	14%
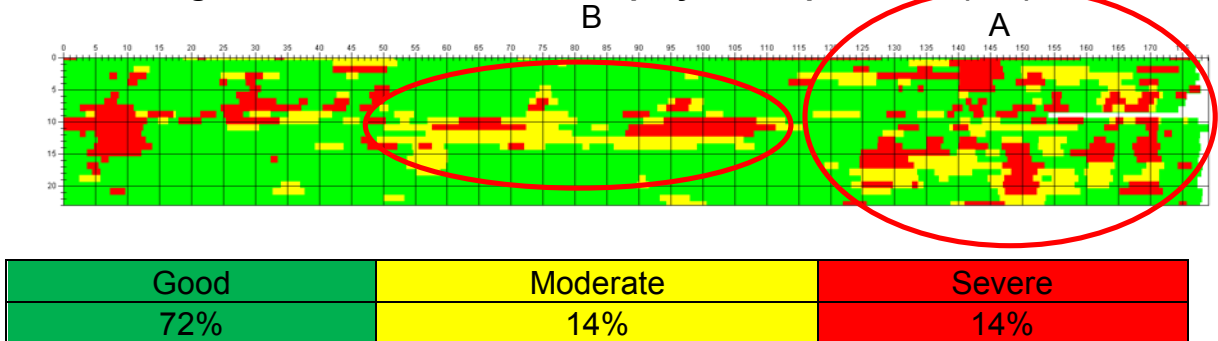
Figure 5-17. GPR corrosion map by RAXpert® software (Old)

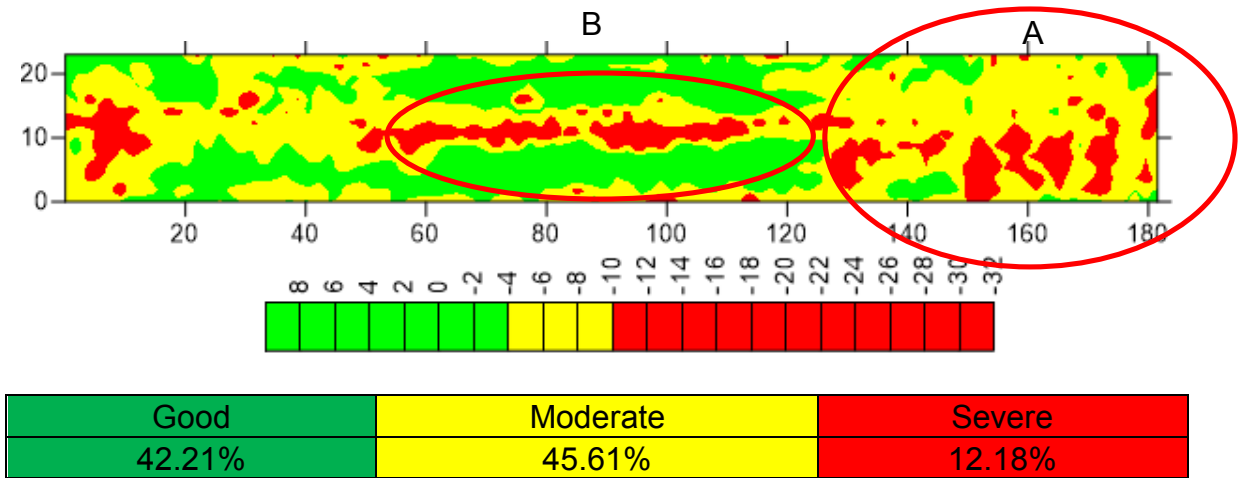| Good	Moderate	Severe
42.21%	45.61%	12.18%

Figure 5-18. GPR corrosion map by clustering-based threshold calibration

method (Old)
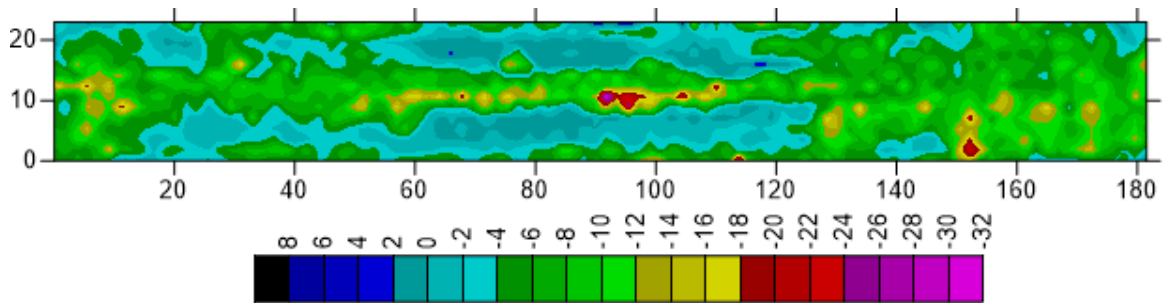
Figure 5-19. GPR corrosion map by numerical amplitude method (Old)

GOOD	FAIR	POOR	CRITICAL
99.37%	0.48%	0.10%	0.05%

Figure 5-20. GPR corrosion map by developed scale (New)

Good	Moderate	Severe
100%	0%	0%
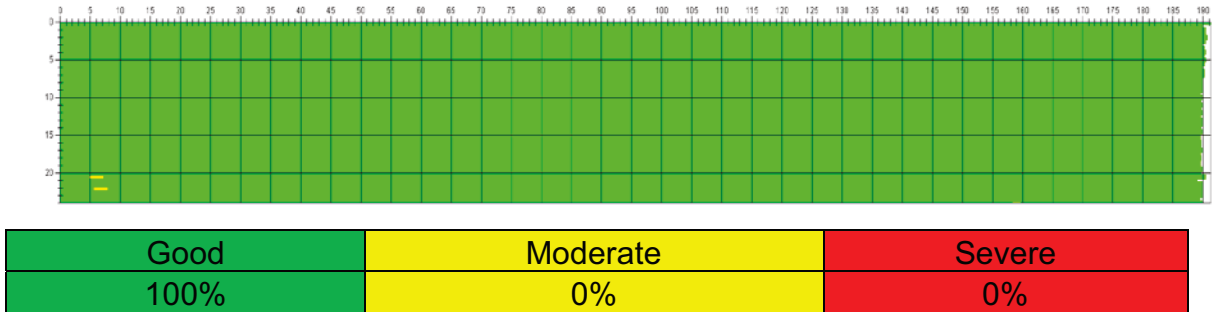
Figure 5-21. GPR corrosion map by RAXpert® software (New)

Good	Moderate	Severe
9.50%	65.62%	24.88%
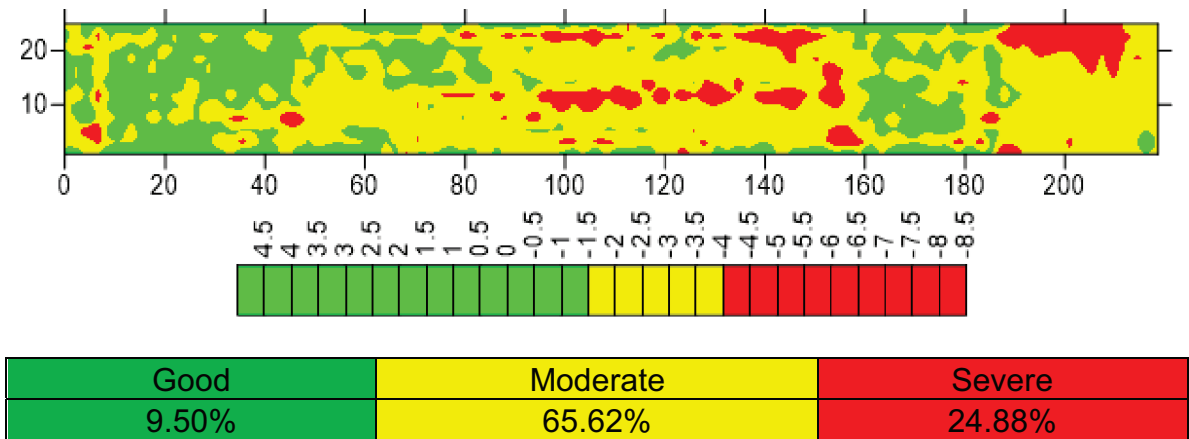
Figure 5-22. GPR corrosion map by clustering-based threshold calibration

method (New)

Figure 5-23. GPR corrosion map by numerical amplitude method (new)
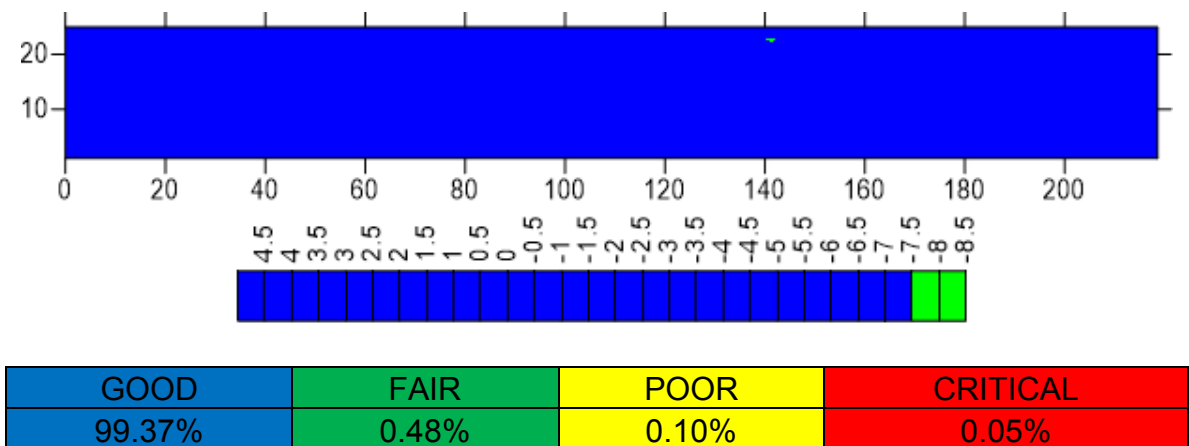
5.10 COMPARING WITH OTHER TECHNIQUES
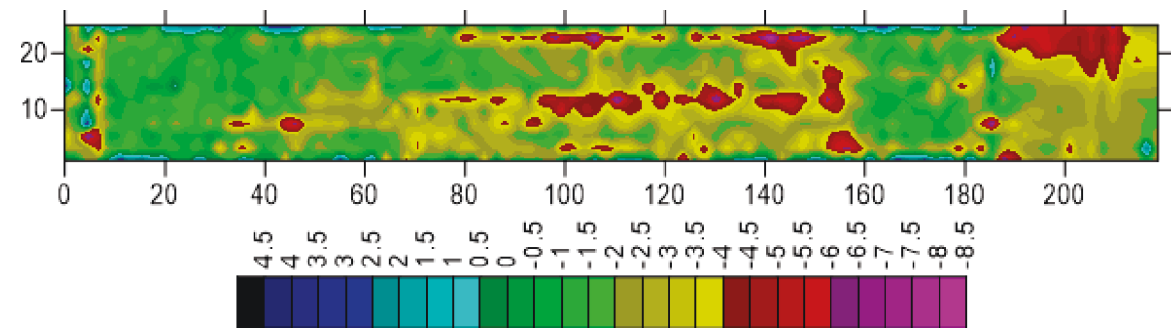
In order to validate the resulted model, a correlation with half-cell potential test and coring test which are done by a specialized company. A correlation can be noticed between Figure 5-24 and Figure 5-25, these two maps show some

similarity that related to corrosion. Zones A, B & C in both maps are similar in the extent to each other. Therefore, by comparing a map drawn by the developed scale and another one drawn by using half-cell potential and they show a correlation and similarity, this will strength the validity of the developed scale.
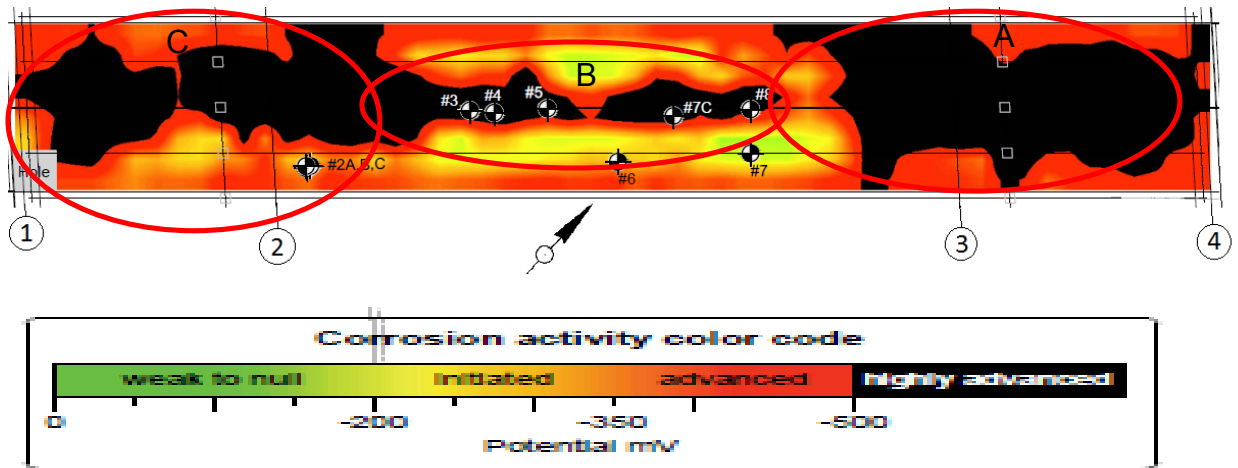
Figure 5-24 Corrosion map by half-cell potential
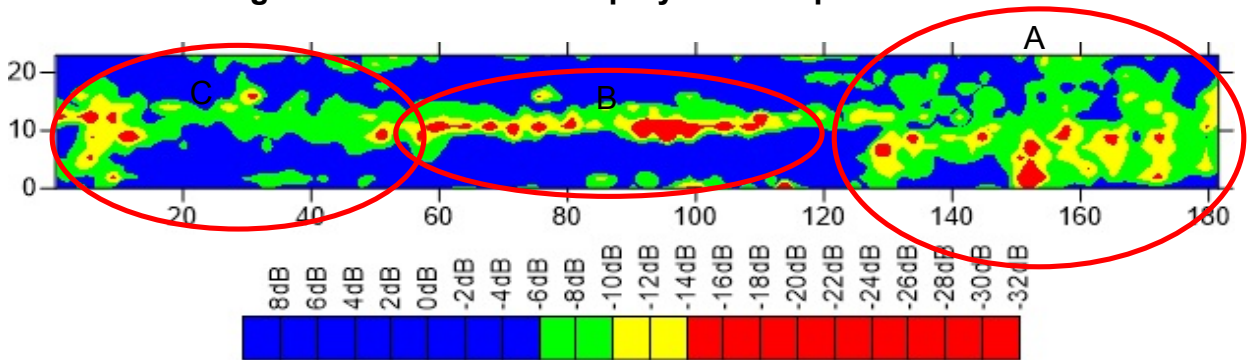
Figure 5-25 Corrosion map by GPR

While for coring test, in order to show the correlation between the developed scale and the coring sample, two samples will be utilized, one is corroded one is not. Based on both techniques, the half-cell potential and the GPR (Figure 5-24 & Figure 5-25), it is illustrated that the sample (2A) is non-corroded sample. The result and the image that submitted by the specialized

company shows that the coring sample is non-corroded as shown in Figure 5-26. On the other hand, the sample (7C) which represents a corroded sample based on the half-cell potential and GPR tests, also Figure 5-27 shows the image of the coring sample that done by the company confirms the result of the developed scale which indicates that this core is in a corroded condition.

Figure 5-26 Non-corroded coring sample

Figure 5-27 Corroded coring sample

5.11 DETERIORATION CURVES FOR CORROSION OF REINFORCING BARS

After verifying the developed scale as the most appropriate scale for representing the exact and real bridge deck corrosion level, deterioration curves for the corrosion of reinforcing bars are drawn for two bridge decks using the Weibull distribution. Four curves are drawn for each bridge deck, of which three, called ideal curves, are developed by assuming the following conditions:

- At the beginning (t=0), the condition of the bridge deck is equal to 1.

- Service Life (SL) of the bridge deck are 100, 75, and 50 years.

- The condition threshold is equal to 0.4.

- The minimum condition is equal to 0.2.

These three curves were drawn using Equation 3-7, but with different SL (100, 75, and 50 years). The less SL the bridge deck has, the steeper the slope of the curve will be and vice versa.

The fourth curve is drawn using Equation 3-9 at the time of inspection and is based on the good condition of the bridge deck. Figure 5-24 shows that the status of the bridge deck corrosion at inspection time follows the curve of ideal condition when assuming that the service life (SL) of that bridge deck is equal to 100 years; nevertheless, the useful SL of that bridge deck is about 85 years when the condition is equal to 0.4. However, Figure 5-25 illustrates that this bridge deck will stand for 75 years because the curve at inspection time follows the curve of ideal condition of 75 years, while the useful service life is about 60 years (at condition equals to 0.4).
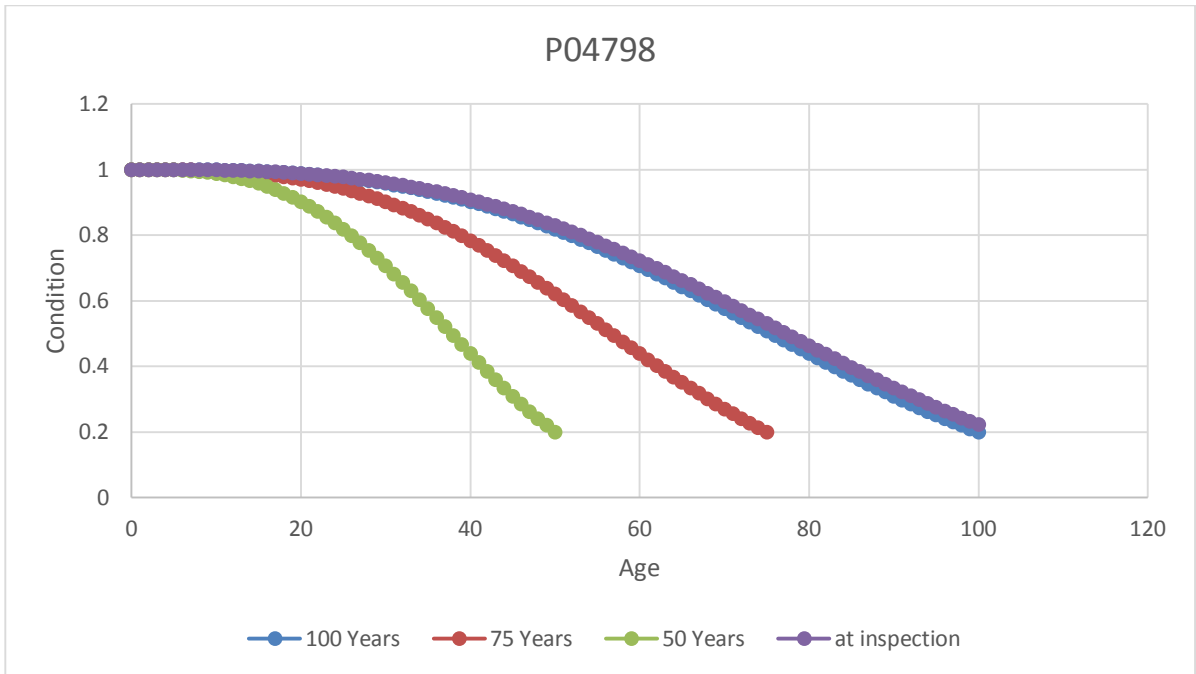
Figure 5-28. Deterioration curves for corrosion of reinforcing bars for bridge P04798
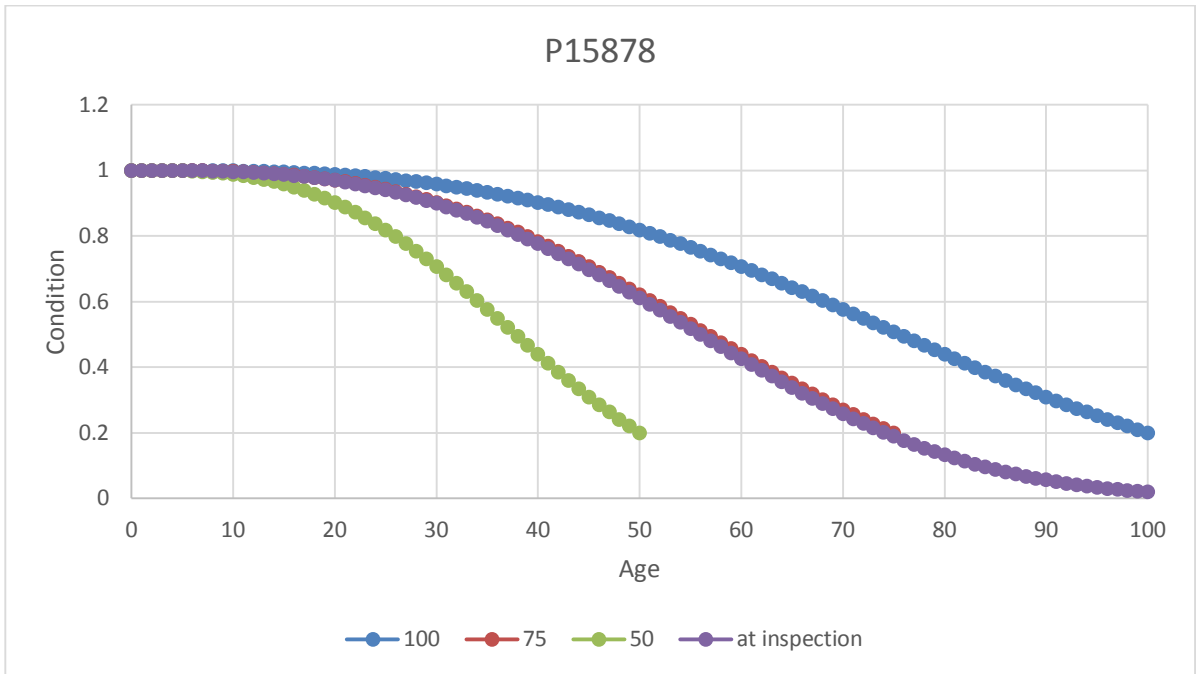

Figure 5-29. Deterioration curves for corrosion of reinforcing bars for bridge P15878

CHAPTER 6 CONCLUSIONS, LIMITATIONS, AND RECOMMENDATIONS

6.1 SUMMARY AND CONCLUSIONS

Numerical amplitude analysis is the most commonly used method for assessing bridge deck corrosion as surveyed by GPR. Despite this method's various advantages, however, it has an important and critical shortcoming related to its scale. The scale used in numerical amplitude method varies from one bridge deck to another and is not constant for all bridge decks, which can lead to misinterpretation. This research focuses on solving this limitation by developing a four-category scale with fixed thresholds defining the different categories.

The scale used in this research has been developed by collecting data on more than 30 bridge decks. GPR analysis has been performed on the collected data to find the top reinforcing bars' amplitude values, which have been divided into four groups using k-means clustering. Statistical analysis has been executed to check the best-fit distribution for the thresholds, on which Monte Carlo simulations have been performed to verify their values.

The final result of this research is a GPR scale that has four categories (good, fair, poor, and critical) and three fixed numerical thresholds that define these categories (-7.71 dB, -10.04 dB, -14.63 dB). This scale has been validated through application to a brand-new bridge, resulting in a correlation between the map generated by the developed scale and the real corrosion of the bridge deck, which should be in a good condition. Moreover, an agreement between bridge analyses performed using both developed scale and image-based software (RADxpert) demonstrates that these two methods support the accuracy and the

validity of the scale. We can therefore conclude that this scale is the most appropriate for assessing the corrosion of concrete bridge decks using a 1.5 GHz-frequency GPR machine.

6.2   RESEARCH CONTRIBUTIONS

The scale developed over the course of this research is expected to provide more accurate inspection results and more precisely assess bridge deck corrosion. The main contributions of this research are listed as follows:

- Analyzing the most common methods used to assess the corrosion of the concrete bridge decks using GPR.

- Mapping the corrosion of concrete bridge decks seven times with different values of thresholds and seeing the changes in the areas of different categories of corrosion by changing the values of the thresholds.

- Developing a fixed numerical scale with four categories of corrosion (good, fair, poor, critical).

- Building a deterioration model for a concrete bridge deck.

6.3   LIMITATIONS

This research has some limitations that can be summarized as follows:

- Availability of data. The ages of the bridges used in this research are missing, making it difficult to classify the bridges based on their ages. Moreover, the effects of different types of bridge deck cover (e.g., whether or not a bridge has an asphalt layer) are not considered.

- Time of surveying. As mentioned earlier, moisture has a great effect on the result of GPR scan. However, it is unknown whether the surrounding environmental conditions for the bridge deck included in this research are for summer or winter.

- Different Machine. For this study only results from a ground-coupled 1.5 GHz-frequency machine are used. However, the effects of using different machine types (air-coupled) or different frequencies (1.0 GHz or 2.6 GHz) are not included.

6.4 RECOMMENDATIONS AND FUTURE WORK

As mentioned earlier, GPR technology is a recent NDT as compared to other NDTs for assessing bridge deck corrosion. Therefore, this area of research and field of technology is wide open for continued study.

- **Research Enhancements:**

1. One of the most important recommendations for future work is to automate the analysis processes to expedite and increase their accuracy. For example, the process of manually selecting the amplitude of the top reinforcing bar for each bridge deck requires more than 6-7 hours. Moreover, no automated tool or software application exists that can run the whole analysis process at once. Analysts use a specific software application to find the amplitude values of the top reinforcing bars and another application to perform the depth correction for these amplitude values, and a third to draw a corrosion

map of the bridge deck. Developing software capable of performing all three tasks task will be beneficial.

2. Collect more data related to or affecting the GPR, such as the age of the deck, type of GPR machine, or frequency.

- **Research Extensions:**

    1. Link the ages, location, moisture content, amount of traffic, and other factors that affect bridge deck corrosion with the developed scale and build a deterioration model for bridge decks based on these factors to help decision makers manage bridges effectively and wisely.

    2. Most research focuses on bridge decks and comparatively little on these other structural elements. Extending the application of GPR surveying technology to structural elements other than bridge decks, such as beams and columns will lead to the creation of a comprehensive index or grade for the entire bridge.

    3. Use GPR technology to assess corrosion of structural elements other than concrete, such as steel structures.

    4. Develop a Bridge Deck Corrosion Index (BDCI) based on the developed scale. This could done by fuzzifying a different area of corrosion for each bridge deck, then defuzzifying it to create a grade or index for that bridge deck.

References

Anonymous (2010). "Half Cell Electrical Potential Method." http://civil-online2010.blogspot.ca/2010/09/half-cell-electrical-potential-method.html (Nov. 10, 2014).

Abujarad, F. (2007). "*Ground Penetrating Radar Signal Processing for Landmine Detection*". PhD Thesis. Otto-von-Guericke-Universität Magdeburg, Universitätsbibliothek, Magdeburg, Germany.

Abujarad, F., Nadim, G., and Omar, A. (2005). "Clutter reduction and detection of landmine objects in ground penetrating radar data using singular value decomposition (SVD)." *Advanced Ground Penetrating Radar, 2005. IWAGPR 2005. Proceedings of the 3rd International Workshop on May 2-3,* IEEE, 37-42.

Alani, A. M., Aboutalebi, M., and Kilic, G. (2013). "Applications of ground penetrating radar (GPR) in bridge deck monitoring and assessment." *J.Appl.Geophys.,* 97 45-54.

Al-Nuaimy, W. (1999). "*Automatic Feature Detection and Interpretation in Ground-Penetrating Radar Data*". PhD Thesis. University of Liverpool, Liverpool, United Kingdom.

I. L. Al-Qadi, Lahouar, S. and Loulizi, A. (2003). "GPR: From the State-Of-the-Art to the State-Of-the-Practice." http://www.ndt.net/article/ndtce03/papers/v110/v110.htm (Dec. 7, 2014).

Annan, A. (2009). *Electromagnetic principles of ground penetrating radar.* Elsevier, Amsterdam, The Netherlands.

Barnes, C. L., Trottier, J., and Forgeron, D. (2008). "Improved concrete bridge deck evaluation using GPR by accounting for signal depth–amplitude effects." *NDT E Int.,* 41(6), 427-433.

Belli, K. M. (2008). "Ground penetrating radar bridge deck investigations using computational modeling". PhD. Northeastern University, Boston, USA.

Bostanudin, N. (2013). "*Computational methods for processing ground penetrating radar data*". PhD Thesis. University of Portsmouth, England.

Cardimona, S., Willeford, B., Wenzlick, J., and Anderson, N. (2000). "Investigation of bridge decks utilizing ground penetrating radar." *International Conference on the Application of Geophysical Technologies to Planning, Design, Construction, and Maintenance of Transportation Facilities,* St. Louis, Missouri, USA, .

Chakravarty, I., Roy, J., and Laha, R. (1967). *Handbook of methods of applied statistics.* McGraw-Hill, New York, USA.

Conyers, L. B. (2013). *Ground-penetrating radar for archaeology.* AltaMira Press, Maryland, USA.

Daniels, D. J. (2004). *Ground penetrating radar.* The Institution of Engineering and Technology, London, United Kingdom.

Daniels, D. J. (1996). "Surface-penetrating radar." *Electronics & Communication Engineering Journal,* 8(4), 165-182.

Dinh, K., and Zayed, T. (2013). "Correlation-based model for evaluating ground penetrating radar (GPR) data of concrete bridge decks." *Proceedings of the 30th ISARC on Aug 11-15,* Montreal, Canada, 44-53.

Dinh, K. (2014). "*Condition Assessment of Concrete Bridge Decks using Ground Penetrating Radar*". PhD Thesis. Concordia University, Montreal.

Dinh, K., and Zayed, T. (2014). "Innovative Method for Interpreting Ground-Penetrating Radar (GPR) Data from Concrete Bridge Decks." *Transportation Research Board 93rd Annual Meeting on Jan 12-16,* Washington, DC, USA, 11.

Dinh, K., Zayed, T., Moufti, S., Shami, A., Jabri, A., Abouhamad, M., and Dawood, T. (2015). "Clustering-based Threshold Model for Condition Assessment of Concrete Bridge Decks using Ground Penetrating Radar." *Transportation Research Board 94th Annual Meeting on Jan 11-15,* Washington, DC, USA, 11.

Dinh, K., Zayed, T., Romero, F., and Tarussov, A. (2014). "Method for Analyzing Time-Series GPR Data of Concrete Bridge Decks." *Journal of Bridge Engineering,* 20(6),.

Dojack, L. (2012). "Ground Penetrating Radar Theory, Data Collection, Processing, and Interpretation: A Guide for Archaeologists." *Rep. No. ANTH 545,* The University of British Columbia, British Columbia, Canada.

Duda, R. O., Hart, P. E., and Stork, D. G. (2001). *Pattern classification.* Wiley-Interscience, New York, USA.

Feller, W. (2008). *An introduction to probability theory and its applications.* John Wiley & Sons, New York, USA.

Gkountis, I. (2014). "INFRASTRUCTURE PERFORMANCE ASSESSMENT OF SUBWAY NETWORKS". Master's Thesis. Concordia University, Montreal, Canada.

Goodman, S. N. (1999). "Toward evidence-based medical statistics. 1: The P value fallacy." *Annals of Internal Medicine,* 130(12), 995-1004.

Grealy, M. (2006). "Resolution of ground-penetrating radar reflections at differing frequencies." *Archaeological Prospection,* 13(2), 142-146.

Gucunski, N., Romero, F., Imani, A. S., and Fetrat, F. (2013). "NDE-Based Assessment of Deterioration Progression in Concrete Bridge Decks." *Transportation Research Board 92nd Annual Meeting on Jan 13-17,* Washington, DC, USA, .

Gucunski, N., Romero, F., Kruschwitz, S., Feldmann, R., and Parvardeh, H. (2011). "*Comprehensive Bridge Deck Deterioration Mapping of Nine Bridges by Nondestructive Evaluation Technologies*." *Rep. No. Project SPR-NDEB(90)--8H-00,* Iowa Highway Research Board, Ames, USA.

Hubbard, S. S., Zhang, J., Monteiro, P. J., Peterson, J. E., and Rubin, Y. (2003). "Experimental detection of reinforcing bar corrosion using nondestructive geophysical techniques." *ACI Materials Journal,* 100(6), 501-510.

Hugenschmidt, J. (2002). "Concrete bridge inspection with a mobile GPR system." *Construction and Building Materials,* 16(3), 147-154.

Huston, D., Gucunski, N., Maher, A., Cui, J., Burns, D., and Jalinoos, F. (2007). "Bridge deck condition assessment with electromagnetic, acoustic and automated methods." *Sixth international workshop on structural health monitoring,* Stanford, USA, .

Huston, D. R., Pelczarski, N. V., Esser, B., and Maser, K. R. (2000). "Damage detection in roadways with ground penetrating radar." *8th International Conference on Ground Penetrating Radar on April 27,* International Society for Optics and Photonics, Gold Coast, 91-94.

Huston, D., Cui, J., Burns, D., and Hurley, D. (2011). "Concrete bridge deck condition assessment with automated multisensor techniques." *Structure and Infrastructure Engineering,* 7(7-8), 613-623.

Jain, A. K. (2010). "Data clustering: 50 years beyond K-means." *Pattern Recognition Letters,* 31(8), 651-666.

Jol, H. M. (2008). *Ground penetrating radar theory and applications.* Elsevier, Oxford, United Kingdom.

Lai, W., and Poon, C. (2012). "Applications of Nondestructive Evaluation Techniques in Concrete Inspection." *HKIE Transactions,* 19(4), 34-41.

Lim, M. K., and Cao, H. (2013). "Combining multiple NDT methods to improve testing effectiveness." *Construction and Building Materials,* 38 1310-1315.

Loulizi, A. (2001). "*Development of Ground Penetrating Radar Signal Modeling and Implementation for Transportation Infrastructure Assessment*". PhD Thesis. Virginia Polytechnic Institute and State University, Virginia, USA.

Luo, Y., and Fang, G. (2005). "GPR clutter reduction and buried target detection by improved Kalman filter technique." *Machine Learning and Cybernetics, 2005. Proceedings of 2005 International Conference on Aug 18-21,* IEEE, Guangzhou, China, 5432-5436.

Maierhofer, C. (2003). "Nondestructive evaluation of concrete infrastructure with ground penetrating radar." *Journal of Materials in Civil Engineering,* 15(3), 287-297.

Maser, K., and Bernhardt, M. (2000). "Statewide bridge deck survey using ground penetrating radar." *Proceedings of structural materials technology IV: an NDT conference on Feb 28- Mar 3,* Technomic Publishing Company, Pennsylvania, USA, 31-37.

Maser, K. R. (2009). "Integration of ground penetrating radar and infrared thermography for bridge deck condition evaluation." *Non-Destructive Testing in Civil Engineering Conference on June 30-July 3,* Citeseer, Nantes, France, .

Maser, K. R. (1996). "Condition assessment of transportation infrastructure using ground-penetrating radar." *Journal of Infrastructure Systems,* 2(2), 94-101.

Maser, K. R., Holland, T. J., and Roberts, R. (2002). "Non-Destructive Measurement of Layer Thickness on Newly Constructed Asphalt Pavement "." *Proceedings of the Pavement Evaluation Conference on Oct. 21-25,* Virginia, USA, 21-25.

Maser, K., Martino, N., Doughty, J., and Birken, R. (2012). "Understanding and Detecting Bridge Deck Deterioration with Ground-Penetrating Radar." *Journal of the Transportation Research Board,* 2313(1), 116-123.

Morey, R. M. (1998). *Ground penetrating radar for evaluating subsurface conditions for transportation facilities.* Transportation Research Board, Washington, DC, USA.

Neubauer, W., Eder-Hinterleitner, A., Seren, S., and Melichar, P. (2002). "Georadar in the Roman civil town Carnuntum, Austria: an approach for archaeological interpretation of GPR data." *Archaeological Prospection,* 9(3), 135-156.

Orlando, L. (2007). "Using GPR to monitor cracks in a historical building." *Advanced Ground Penetrating Radar, 2007 4th International Workshop on June 27-29,* IEEE, Naples, Italy, 45-48.

Parrillo, R., Roberts, R., and Haggan, A. (2006). "Bridge deck condition assessment using ground penetrating radar." *Proceedings of the ECNDT on Sep. 25-29,* Citeseer, Berlin, Germany, 2526.

Rao, D. P., Kumar, V., Kishore, R., and Bhikshma, V. (2007). "Ground penetrating radar and its applications in civil engineering." *Indian Concrete Journal,* 81(11), 35.

Ripley, B. (1987). *Stochastic simulation.* Wiley, New York, USA.

Sato, M., and Yarovoy, A. (2008). "GPR (ground penetrating radar) into real world." *Proceedings 39th of URSI General Assemblies on Aug. 7-16,* Chicago, USA, .

Sawilowsky, S. S., and Fahoome, G. C. (2003). "Statistics via Monte Carlo simulation with fortran." *Journal of Modern Applied Statistical Methods,* .

Sbartaï, Z., Laurens, S., Balayssac, J., Arliguie, G., and Ballivy, G. (2006). "Ability of the direct wave of radar ground-coupled antenna for NDT of concrete structures." *NDT & E International,* 39(5), 400-407.

Scott, M., Rezaizadeh, A., Delahaza, A., Santos, C., Moore, M., Graybeal, B., and Washer, G. (2003). "A comparison of nondestructive evaluation methods for bridge deck assessment." *NDT & E International,* 36(4), 245-255.

Semaan, N. (2011). "*Structural Performance Model for Subway Networks*". PhD Thesis. Concordia University, Montreal, Canada.

Serma, A. I. A., and Setan, H. (2009). "Ground penetrating radar (gpr) for subsurface mapping: preliminary result." *Geoinformation Science Journal,* 9(2), 45-62.

Stephens, M. A. (1974). "EDF statistics for goodness of fit and some comparisons." *Journal of the American Statistical Association,* 69(347), 730-737.

Tarussov, A., Vandry, M., and De La Haza, A. (2013). "Condition assessment of concrete structures using a new analysis method: Ground-penetrating radar computer-assisted visual interpretation." *Construction and Building Materials,* 38 1246-1254.

Wollny, K., and Bertold, A. (1998). "GPR measurements on active, stabilized and potential landslides." *Proc. of the Seventh International Conference on GPR,* Lawrence, USA, 401-403.

Xu, X., Miller, E. L., Rappaport, C. M., and Sower, G. D. (2002). "Statistical method to detect subsurface objects using array ground-penetrating radar data." *Geoscience and Remote Sensing, IEEE Transactions on,* 40(4), 963-976.

Zhao, A., Jiang, Y., Wang, W., and Jiaotong, X. (2005). "Exploring independent component analysis for GPR signal processing." *Progress In Electromagnetics Research Symposium on Aug 22-26,* Hangzhou, China, 750-753.

CHAPTER 7 APPENDIX

7.1   Summary of Collected Data

NO.	Frequency (GHz)	Machine	Good-Fair	Fair-Poor	Poor-Critical	Scale
1	1.5	ground-coupled	-11.00	-13.00	-16.00	
2	2.6	ground-coupled	-15.50	-17.50	-20.50	
3	1.5	ground-coupled	-11.00	-13.00	-16.00	

4	2.6	ground-coupled	-16.00	-18.00	-21.00	
						SERIOUS POOR FAIR GOOD -44 -35 -24 -22 -20 -18 -16 -14 -12 -10 -8
5	1.5	ground-coupled	-10.50	-12.50	-15.50	
						SERIOUS POOR FAIR GOOD -33.5 -18.5 -15.5 -12.5 -9.5 -6.5 -3.5
6	2.6	ground-coupled	-15.00	-17.00	-20.00	
						SERIOUS POOR FAIR GOOD -39 -23 -20 -17 -14 -11 -8
7	1.0	air-coupled (dual polarized)	-20.00	-22.00	-25.00	
						SERIOUS POOR FAIR GOOD -48 -28 -24 -20 -16 -12
8	1.0	air-coupled (transversely polarized)	-24.00	-26.00	-29.00	
						SERIOUS POOR FAIR GOOD -52 -32 -28 -24 -20 -16

9	1.5	ground-coupled	-11.50	-13.50	-16.50	
10	2.6	ground-coupled	-18.00	-20.00	-23.00	
11	1.0	air-coupled (dual polarized)	-21.50	-23.50	-26.50	
12	1.0	air-coupled (transversely polarized)	-20.50	-22.50	-25.50	
13	1.0	air-coupled (longitudinally polarized)	-27.00	-29.00	-32.00	

14	1.5	ground-coupled	-11.50	-13.50	-16.50	
15	2.6	ground-coupled	-18.50	-20.50	-23.50	
16	1.5	ground-coupled	-11.50	-13.50	-16.50	
17	2.6	ground-coupled	-17.00	-19.00	-22.00	
18	1.0	air-coupled (dual polarized)	-23.50	-25.50	-28.50	

19	1.0	air-coupled (transversely polarized)	-23.50	-25.50	-28.50	
20	1.0	air-coupled (longitudinally polarized)	-23.50	-25.50	-28.50	
21	1.5	ground-coupled	-11.00	-13.00	-16.00	
22	2.6	ground-coupled	-16.00	-18.00	-21.00	
23	1.5	ground-coupled	-10.75	-12.75	-15.75	

24	2.6	ground-coupled	-16.00	-18.00	-21.00	
25	1.0	air-coupled (dual polarized)	-23.50	-25.50	-28.50	
26	1.0	air-coupled (transversely polarized)	-23.50	-25.50	-28.50	
27	1.0	air-coupled (longitudinally polarized)	-23.50	-25.50	-28.50	
28	1.5	ground-coupled	-10.75	-12.75	-15.75	
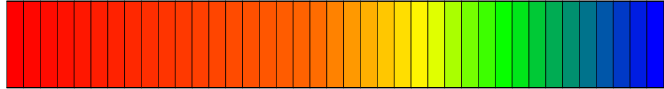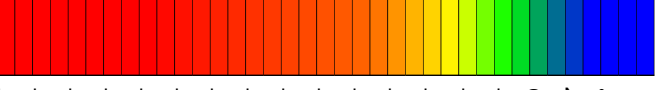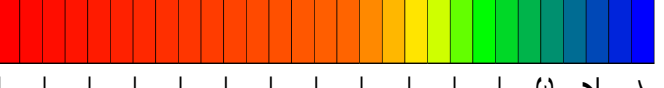
29	2.6	ground-coupled	-16.25	-18.25	-21.25	
30	1.5	ground-coupled	-23.00	-25.00	-28.00	
31	1.5	ground-coupled	-13.00	-15.00	-18.00	
32	1.5	ground-coupled	-19.50	-21.50	-24.50	
33	1.5	ground-coupled	-23.00	-25.00	-28.00	
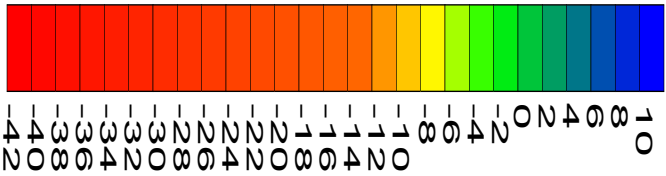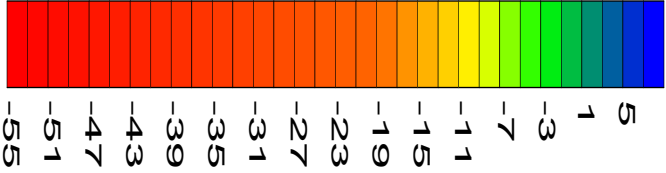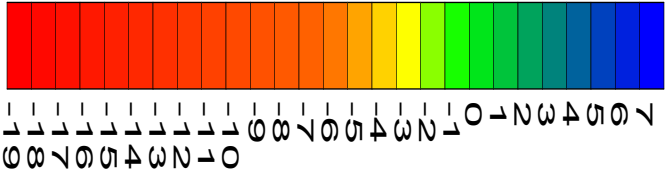
34	1.0	air-coupled	-20.00	-22.00	-25.00	
35	1.0	air-coupled	-17.00	-19.00	-22.00	
36	1.5	ground-coupled	-24.00	-26.00	-29.00	
37	2.0	air-coupled	-29.00	-31.00	-34.00	
38	1.0	ground-coupled	-40.00	-48.00	-54.00	

39	1.5	ground-coupled	-23.00	-29.00	-33.00	-45dB -43dB -41dB -39dB -37dB -35dB -33dB -31dB -29dB -27dB -25dB -23dB -21dB -19dB -17dB -15dB
40	1.5	ground-coupled	-4.00	-8.00	-12.00	-21dB -20dB -19dB -18dB -17dB -16dB -15dB -14dB -13dB -12dB -11dB -10dB -9dB -8dB -7dB -6dB -5dB -4dB -3dB -2dB -1dB 0dB 1dB 2dB 3dB 4dB
41	1.5	ground-coupled	-2.00	-8.00	-12.00	-24dB -22dB -20dB -18dB -16dB -14dB -12dB -10dB -8dB -6dB -4dB -2dB 0dB 2dB 4dB 6dB 8dB
42	1.5	ground-coupled	-1.00	-5.00	-8.00	-14dB -13dB -12dB -11dB -10dB -9dB -8dB -7dB -6dB -5dB -4dB -3dB -2dB -1dB 0dB 1dB 2dB 3dB 4dB
43	2.6	ground-coupled	-12.00	-14.00	-17.00	SERIOUS POOR FAIR GOOD; -35 -20 -17 -14 -11 -8 -5; GPR Attenuation-Based Grading (dB)

44	1.5	ground-coupled	-0.99	-3.38	-6.24	
45	1.5	ground-coupled	0.12	-2.24	-4.40	
46	1.5	ground-coupled	0.67	-1.97	-4.14	
47	1.5	ground-coupled	0.21	-1.81	-3.70	
48	1.5	ground-coupled	-1.05	-3.50	-7.19	

49	1.5	ground-coupled	-1.37	-3.62	-7.00	
50	2.6	ground-coupled	-2.60	-7.71	-16.43	
51	1.5	ground-coupled	-0.94	-2.84	-5.48	
52	1.5	ground-coupled	-1.12	-3.59	-7.71	
53	2.6	ground-coupled	-2.77	-8.17	-19.02	

54	1.5	ground-coupled	-2.61	-7.37	-16.81	
55	1.5	ground-coupled	-2.87	-7.57	-14.24	
56	1.5	ground-coupled	-3.57	-9.68	-20.29	
57	1.5	ground-coupled	-3.32	-9.22	-18.92	
58	1.5	ground-coupled	-3.17	-7.89	-14.51	

59	1.5	ground-coupled	-2.97	-7.65	-13.99	
60	1.5	ground-coupled	-3.78	-9.93	-19.94	
61	1.5	ground-coupled	-0.80	-3.01	-6.37	

7.2 Sensitivity Analysis

Bridge P04798

GOOD	FAIR	POOR	CRITICAL
84.68%	6.70%	5.39%	3.23%
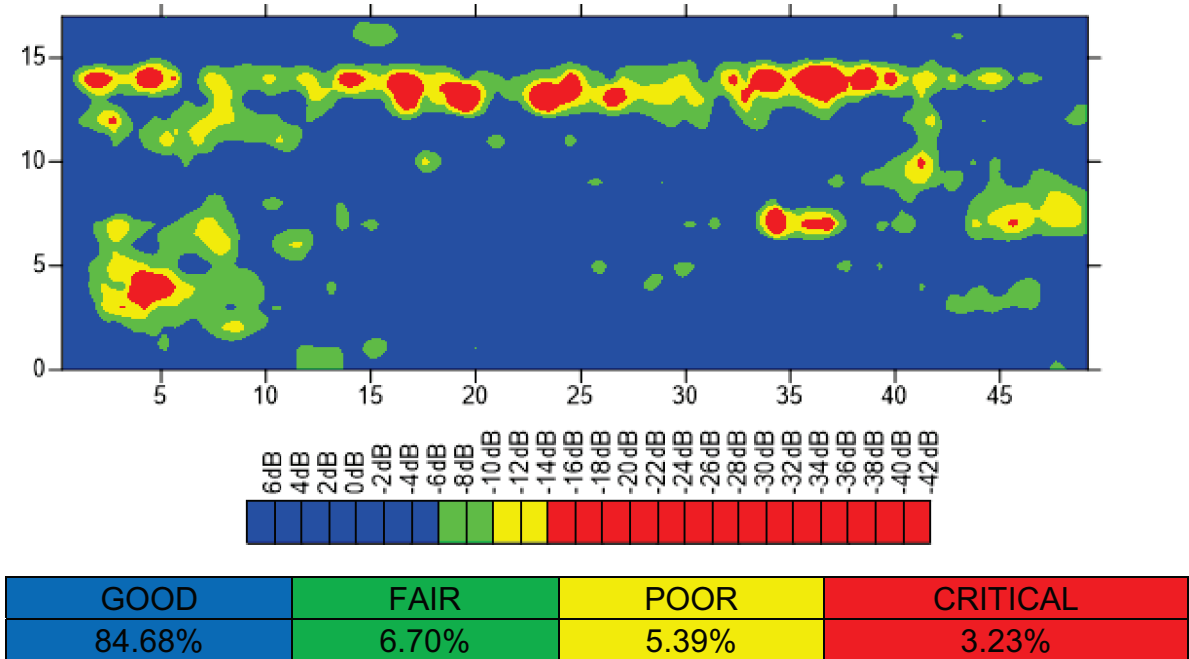
Figure 7-1 Corrosiveness map using scale A

GOOD	FAIR	POOR	CRITICAL
80.45%	8.31%	6.85%	4.39%
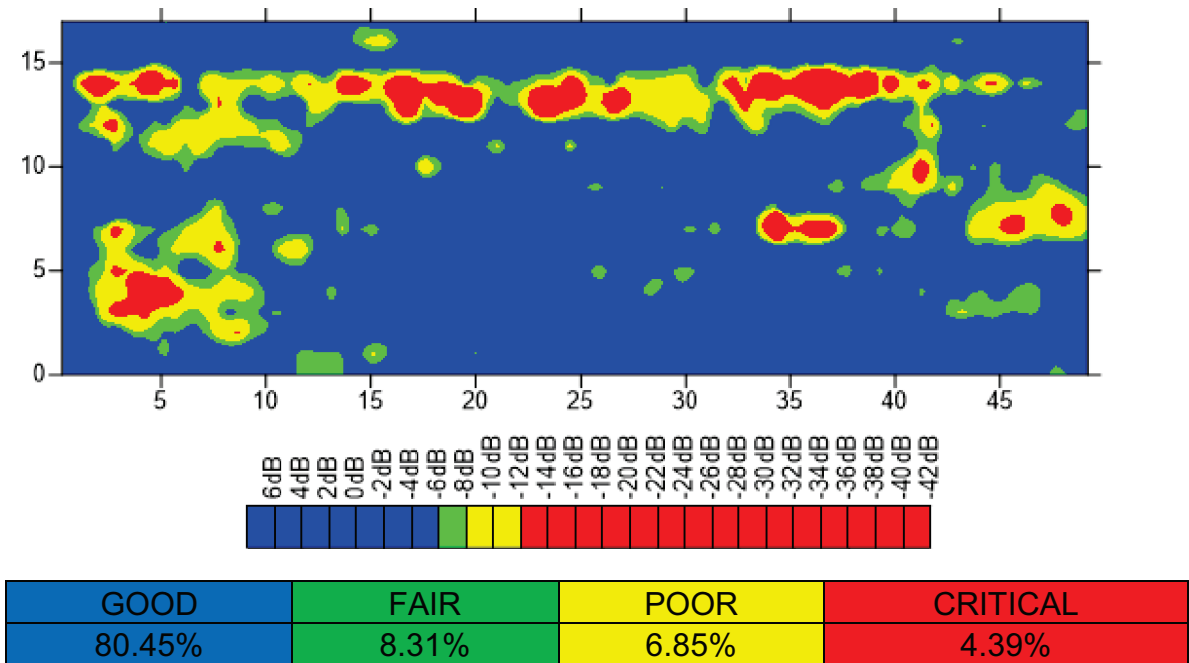
Figure 7-2 Corrosiveness map using scale B

GOOD	FAIR	POOR	CRITICAL
75.37%	10.39%	9.08%	5.16%
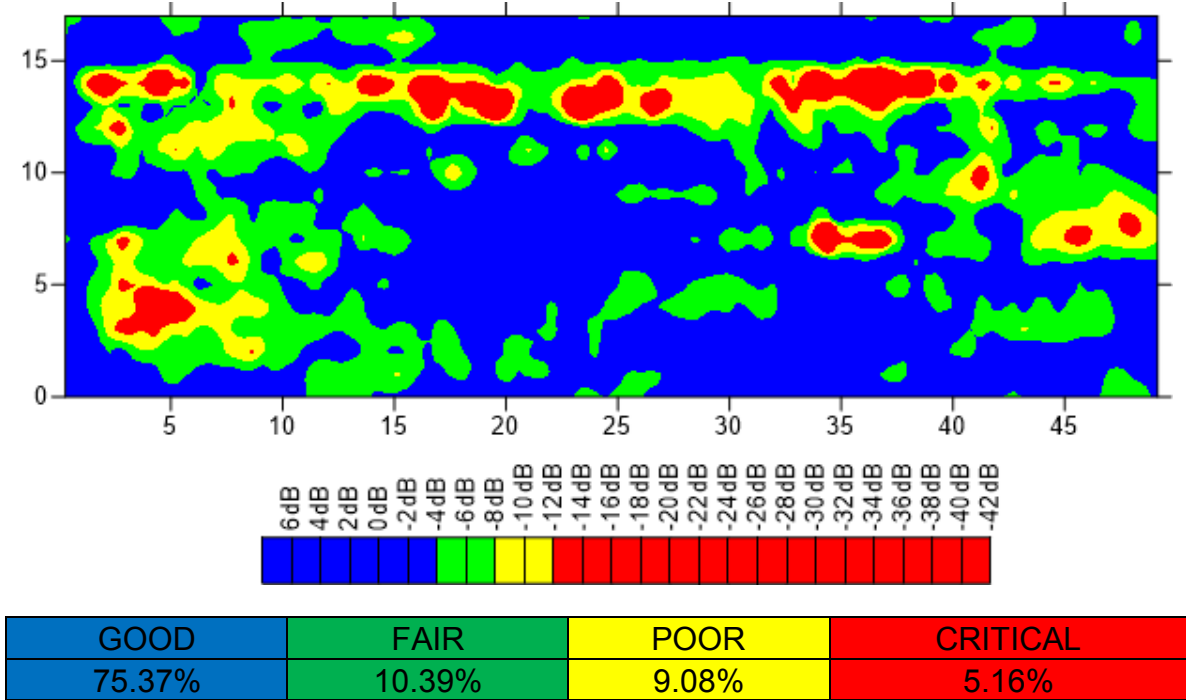
Figure 7-3 Corrosiveness map using scale C

GOOD	FAIR	POOR	CRITICAL
68.59%	13.47%	11.55%	6.39%
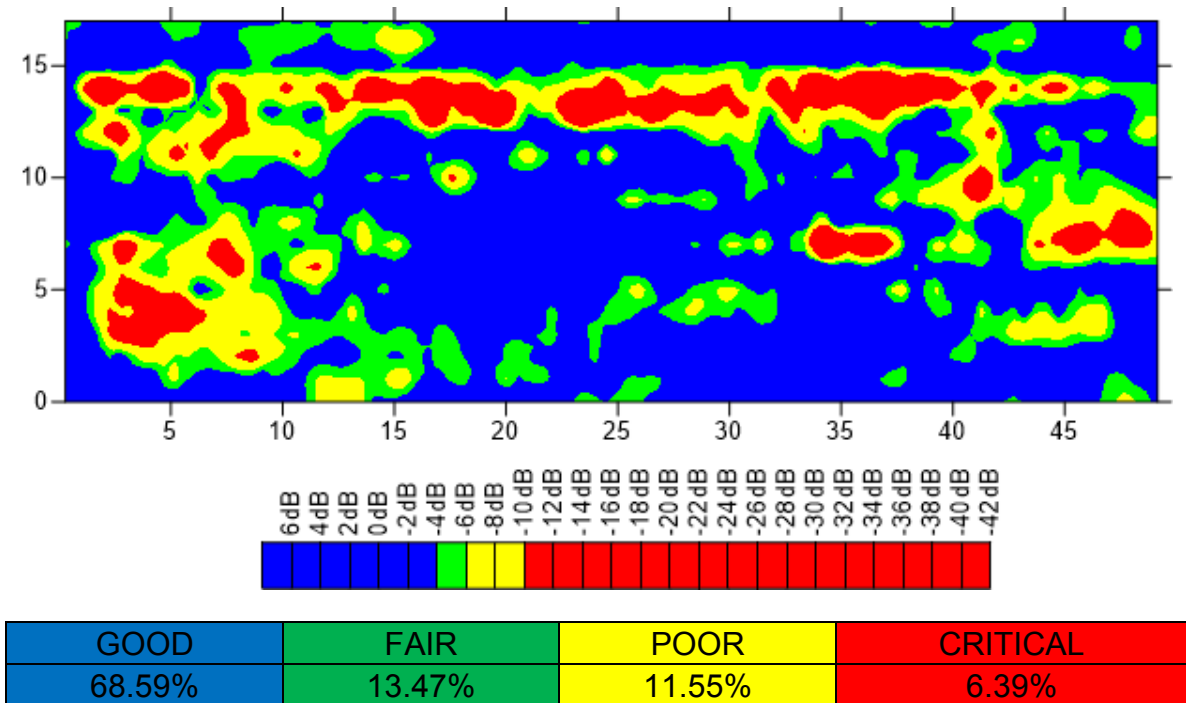
Figure 7-4 Corrosiveness map using scale D

GOOD	FAIR	POOR	CRITICAL
56.97%	20.48%	14.86%	7.70%
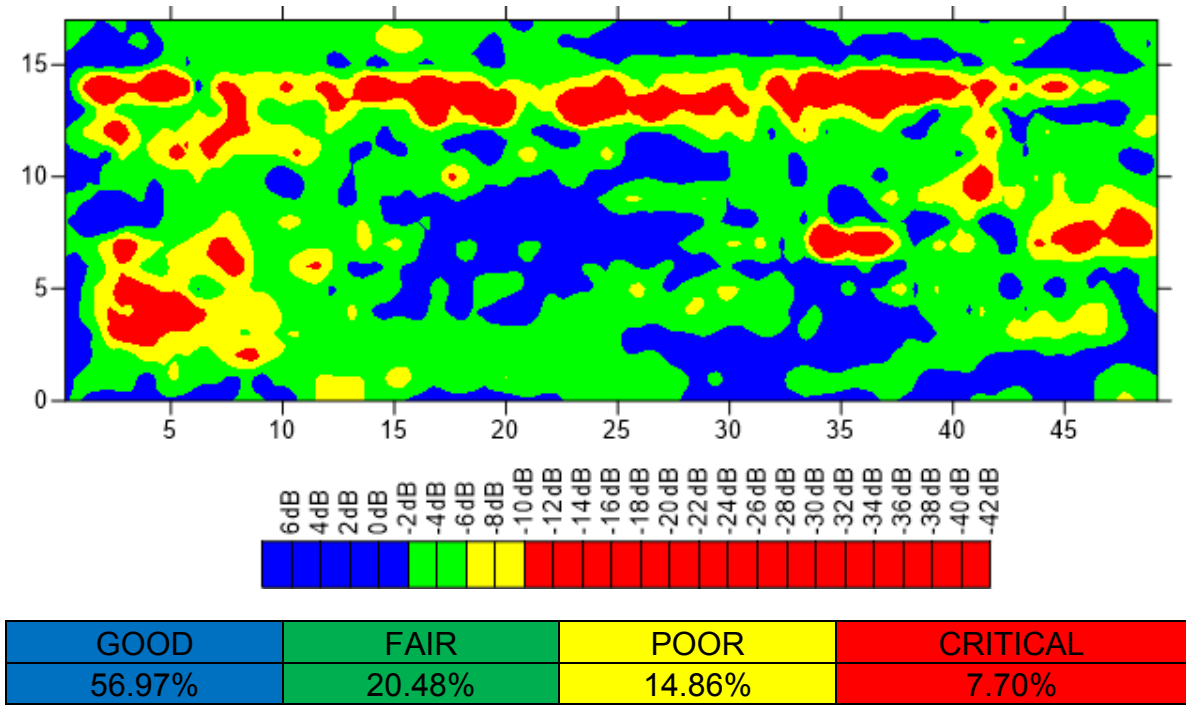
Figure 7-5 Corrosiveness map using scale E

GOOD	FAIR	POOR	CRITICAL
44.11%	27.64%	19.01%	9.24%
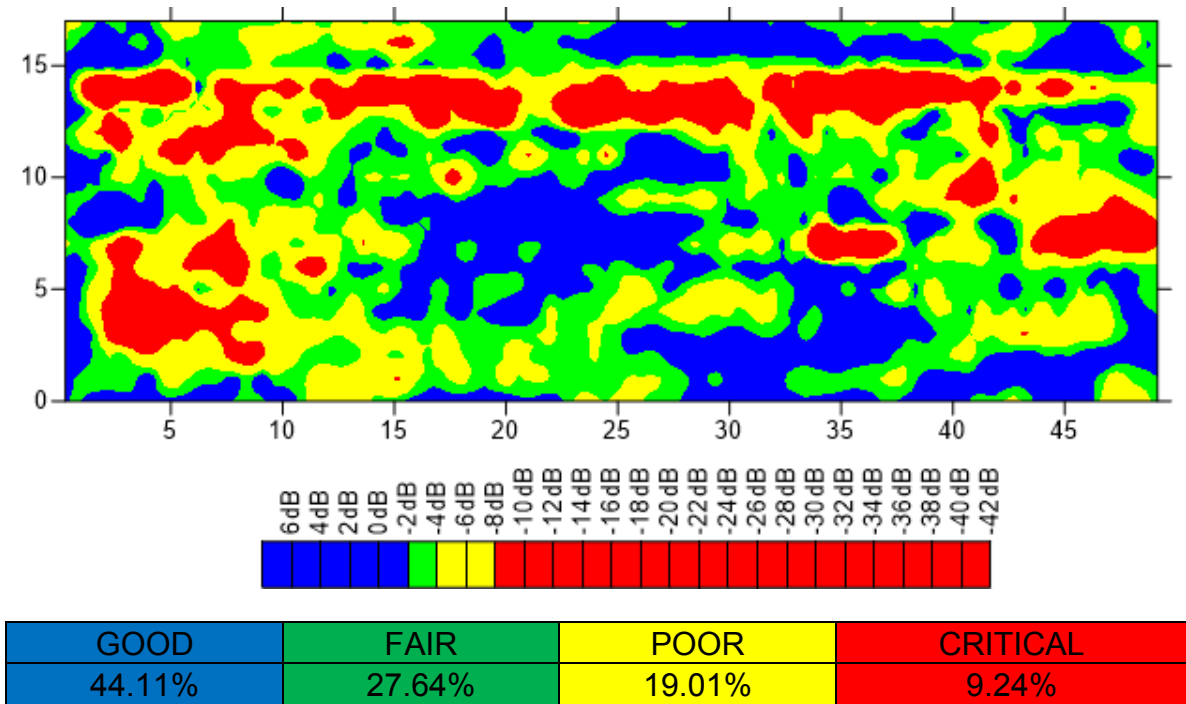
Figure 7-6 Corrosiveness map using scale F

GOOD	FAIR	POOR	CRITICAL
31.10%	30.02%	26.33%	12.55%
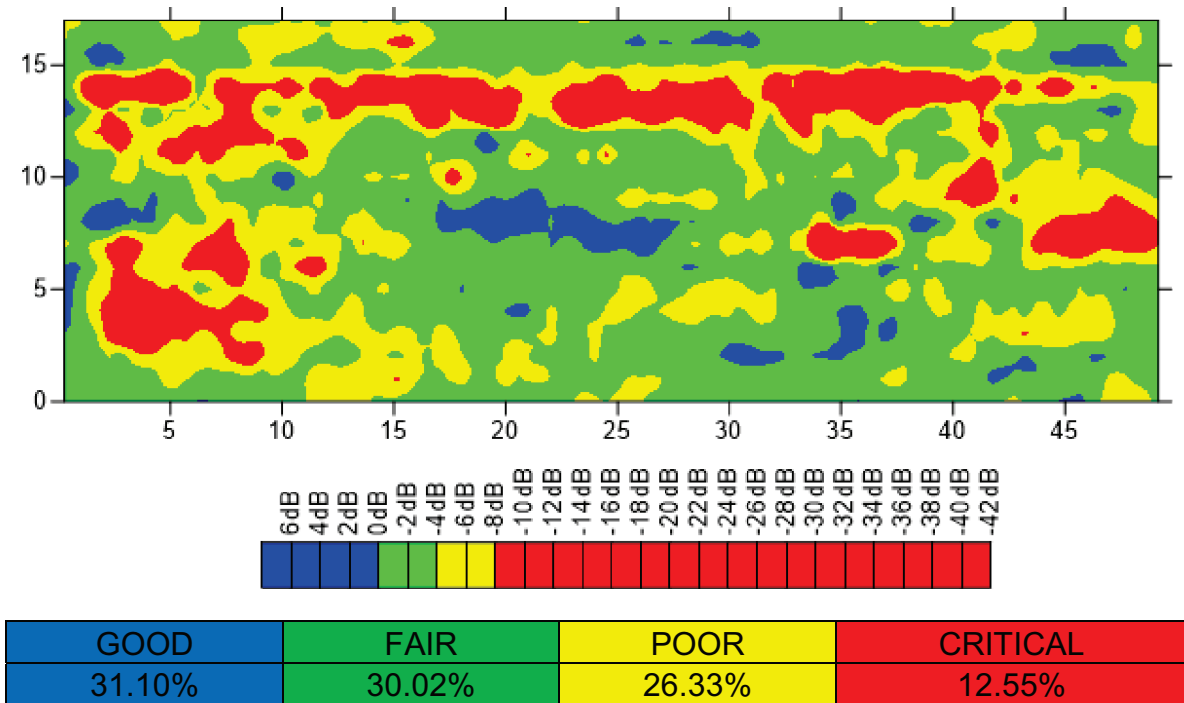
Figure 7-7 Corrosiveness map using scale G

7.3 AREAS OF FOUR CATEGORIES USING DIFFERENT SCALE FOR THE REMAINING BRIDGES

Table 7-1 Areas of Bridge (2)

Bridge 2				
Scale	GOOD	FAIR	POOR	CRITAICAL
G	27.48%	43.93%	26.32%	2.27%
F	46.46%	36.88%	15.34%	1.32%
E	65.53%	24.66%	9.13%	0.69%

	GOOD	FAIR	POOR	CRITAICAL
D	79.88%	14.74%	4.95%	0.43%
C	88.48%	8.37%	2.87%	0.28%
B	93.50%	4.64%	1.70%	0.15%
A	96.13%	2.82%	0.95%	0.10%

Table 7-2 Areas of Bridge (3)

Bridge 3				
Scale	GOOD	FAIR	POOR	CRITAICAL
G	33.35%	54.09%	12.11%	0.45%
F	61.46%	32.95%	5.36%	0.24%
E	83.29%	14.45%	2.05%	0.21%
D	92.83%	6.10%	0.94%	0.13%
C	96.93%	2.51%	0.46%	0.09%
B	98.63%	0.98%	0.33%	0.06%
A	99.27%	0.49%	0.18%	0.06%

Table 7-3 Areas of Bridge (4)

Bridge 4				
Scale	GOOD	FAIR	POOR	CRITAICAL
G	44.42%	47.13%	8.22%	0.23%
F	71.75%	25.05%	3.03%	0.17%
E	88.00%	10.65%	1.23%	0.11%
D	95.47%	3.91%	0.54%	0.07%
C	98.22%	1.42%	0.30%	0.06%
B	99.27%	0.52%	0.17%	0.04%
A	99.56%	0.30%	0.11%	0.03%

Table 7-4 Areas of Bridge (5)

Bridge 5				
Scale	GOOD	FAIR	POOR	CRITAICAL

	GOOD	FAIR	POOR	CRITICAL
G	47.43%	44.68%	7.42%	0.46%
F	74.04%	22.30%	3.38%	0.28%
E	88.91%	9.56%	1.34%	0.18%
D	95.31%	3.84%	0.75%	0.10%
C	97.76%	1.73%	0.44%	0.08%
B	98.97%	0.70%	0.34%	0.00%
A	99.41%	0.39%	0.21%	0.00%

Table 7-5 Areas of Bridge (6)

Bridge 6				
Scale	GOOD	FAIR	POOR	CRITAICAL
G	41.47%	35.20%	20.86%	2.47%
F	58.96%	26.92%	12.59%	1.54%
E	73.34%	17.15%	8.23%	1.28%
D	83.15%	11.13%	5.08%	0.64%

	GOOD	FAIR	POOR	CRITICAL
C	88.87%	7.72%	3.16%	0.26%
B	93.56%	4.44%	1.79%	0.21%
A	96.03%	2.52%	1.37%	0.09%

Table 7-6 Areas of Bridge (7)

Bridge 7				
Scale	GOOD	FAIR	POOR	CRITAICAL
G	46.10%	40.96%	12.60%	0.35%
F	69.68%	23.92%	6.23%	0.17%
E	83.99%	13.25%	2.64%	0.12%
D	91.90%	6.95%	1.07%	0.08%
C	96.29%	3.20%	0.44%	0.06%
B	98.45%	1.31%	0.19%	0.05%
A	99.37%	0.48%	0.10%	0.05%

Table 7-7 Areas of Bridge (8)

Bridge 8				
Scale	GOOD	FAIR	POOR	CRITAICAL
G	39.77%	45.59%	13.78%	0.85%
F	63.59%	28.79%	7.18%	0.44%
E	81.03%	14.59%	4.14%	0.24%
D	90.67%	6.92%	2.29%	0.12%
C	94.91%	3.65%	1.34%	0.10%
B	97.08%	2.26%	0.61%	0.05%
A	98.22%	1.41%	0.32%	0.05%

Table 7-8 Areas of Bridge (9)

Bridge 9				
Scale	GOOD	FAIR	POOR	CRITAICAL
G	31.81%	45.17%	20.94%	2.09%
F	52.89%	35.28%	10.35%	1.48%

	GOOD	FAIR	POOR	CRITICAL
E	72.00%	21.75%	5.26%	1.00%
D	85.18%	10.89%	3.22%	0.71%
C	92.28%	5.10%	2.12%	0.50%
B	95.41%	2.75%	1.49%	0.35%
A	97.03%	1.69%	1.02%	0.26%

Table 7-9 Areas of Bridge (10)

Bridge 10				
Scale	GOOD	FAIR	POOR	CRITAICAL
G	28.04%	30.64%	29.81%	11.51%
F	39.78%	30.04%	20.73%	9.45%
E	54.00%	24.20%	13.88%	7.92%
D	66.32%	17.35%	9.34%	7.00%
C	75.86%	10.99%	7.14%	6.01%
B	81.96%	7.37%	5.61%	5.06%

A	86.07%	5.12%	4.63%	4.19%

Table 7-10 Areas of Bridge (11)

Bridge 11				
Scale	GOOD	FAIR	POOR	CRITAICAL
G	31.10%	30.02%	26.33%	12.55%
F	44.11%	27.64%	19.01%	9.24%
E	56.97%	20.48%	14.86%	7.70%
D	68.59%	13.47%	11.55%	6.39%
C	75.37%	10.39%	9.08%	5.16%
B	80.45%	8.31%	6.85%	4.39%
A	84.68%	6.70%	5.39%	3.23%

Table 7-11 Areas of Bridge (12)

Bridge 12

111

Scale	GOOD	FAIR	POOR	CRITAICAL
G	22.52%	21.26%	33.51%	22.71%
F	30.96%	22.74%	27.87%	18.43%
E	40.38%	22.06%	22.45%	15.11%
D	50.42%	18.73%	18.28%	12.57%
C	59.58%	14.91%	15.02%	10.49%
B	66.83%	12.24%	12.50%	8.43%
A	72.85%	10.11%	9.99%	7.05%

Table 7-12 Areas of Bridge (13)

Bridge 13				
Scale	GOOD	FAIR	POOR	CRITAICAL
G	16.55%	13.73%	36.66%	33.06%
F	21.79%	15.59%	36.26%	26.36%
E	28.06%	17.46%	33.90%	20.58%

	GOOD	FAIR	POOR	CRITAICAL
D	35.17%	18.84%	29.71%	16.27%
C	43.08%	19.37%	24.98%	12.56%
B	51.09%	18.69%	20.05%	10.17%
A	59.66%	16.64%	15.43%	8.27%

Table 7-13 Areas of Bridge (14)

Bridge 14				
Scale	GOOD	FAIR	POOR	CRITAICAL
G	22.17%	18.43%	36.70%	22.70%
F	29.81%	19.09%	34.09%	17.01%
E	37.91%	20.45%	28.83%	12.81%
D	46.38%	20.22%	23.68%	9.73%
C	55.22%	18.61%	19.07%	7.10%
B	64.05%	15.78%	14.76%	5.41%
A	71.40%	13.45%	11.02%	4.13%

Table 7-14 Areas of Bridge (15)

Scale	GOOD	FAIR	POOR	CRITAICAL
		Bridge 15		
G	38.22%	44.79%	15.04%	1.95%
F	60.08%	30.34%	8.30%	1.28%
E	78.85%	15.07%	5.11%	0.96%
D	88.56%	7.58%	3.16%	0.69%
C	93.08%	4.40%	2.10%	0.42%
B	95.45%	2.99%	1.31%	0.25%
A	97.18%	1.70%	0.96%	0.15%

7.4 MAPS OF BRIDGE DECKS USING IMAGE-BASED METHOD

Bridge 206
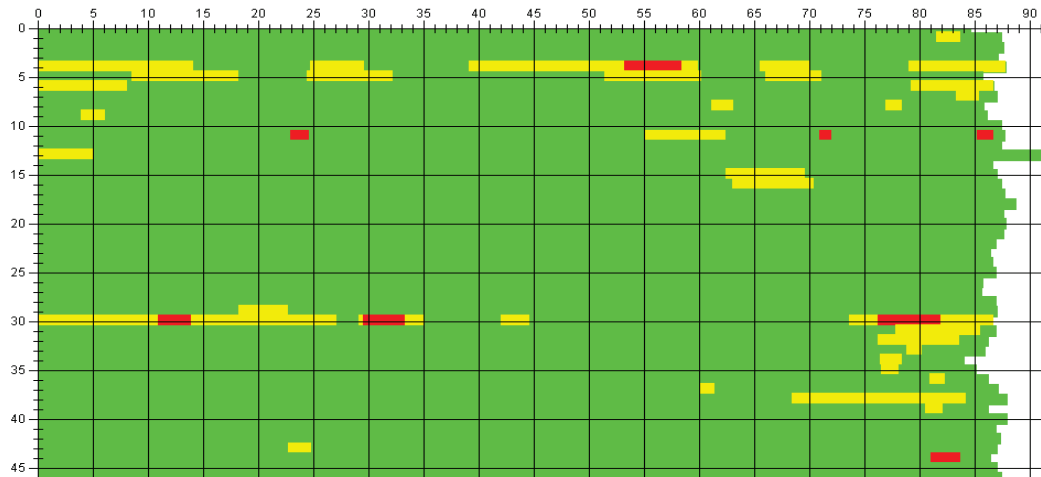
Good	Moderate	Severe
94%	5%	1%

212
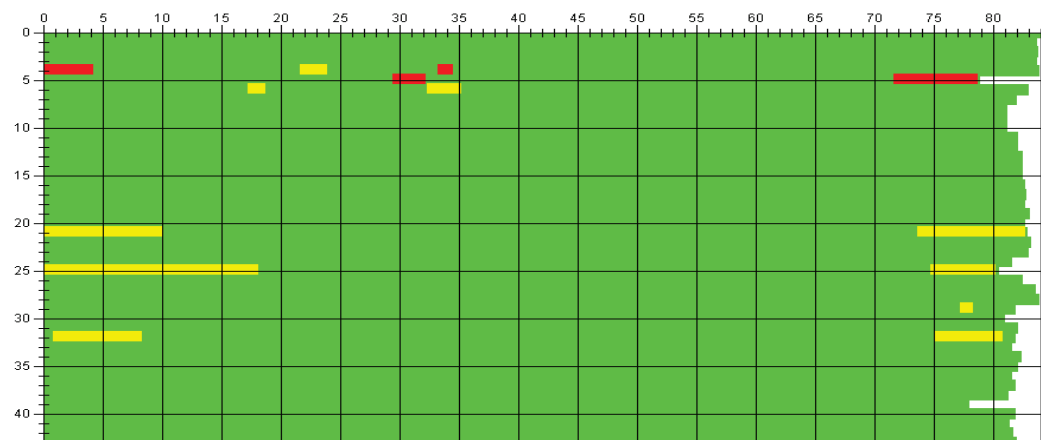
Good	Moderate	Severe
98%	2%	0%

219 CD
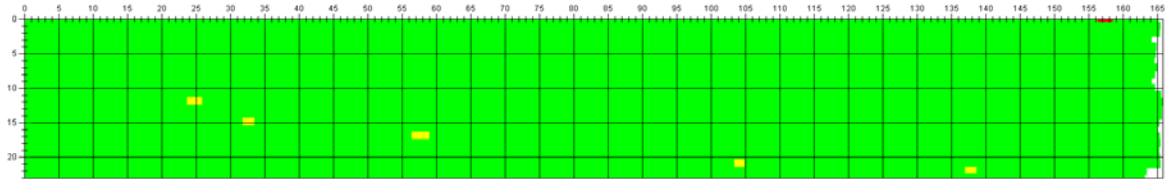
Good	Moderate	Severe
100%	0%	0%

219
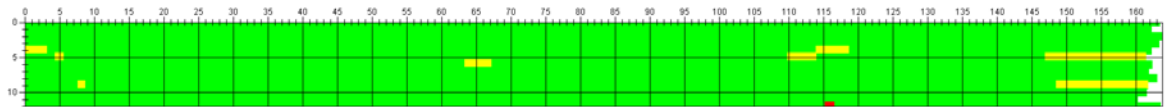
Good	Moderate	Severe
98%	2%	0%

220
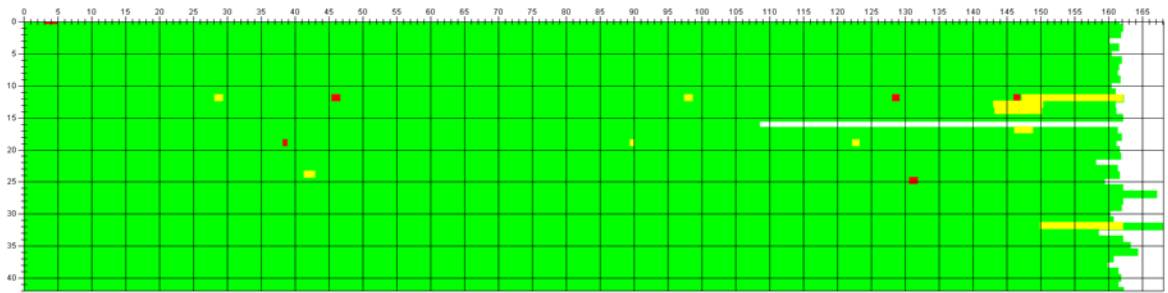
Good	Moderate	Severe
100%	0%	0%

Iowa 1.5
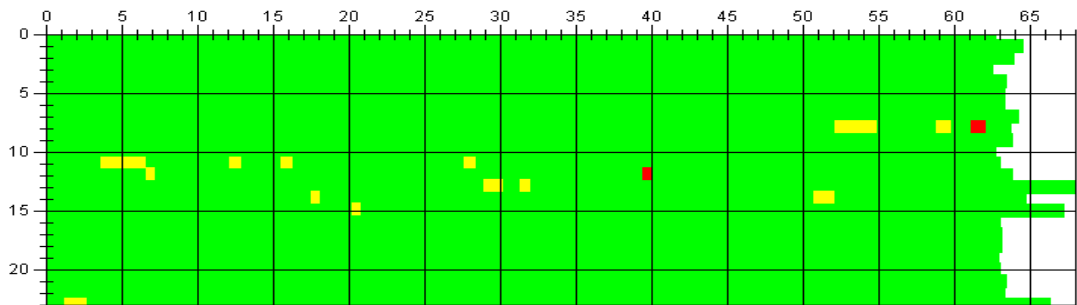
Good	Moderate	Severe
99%	1%	0%

Laval New
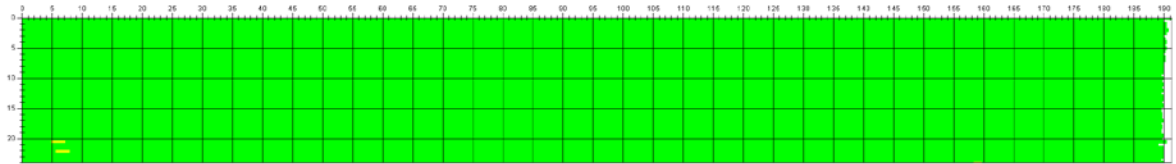
Good	Moderate	Severe
100%	0%	0%

New Jersey
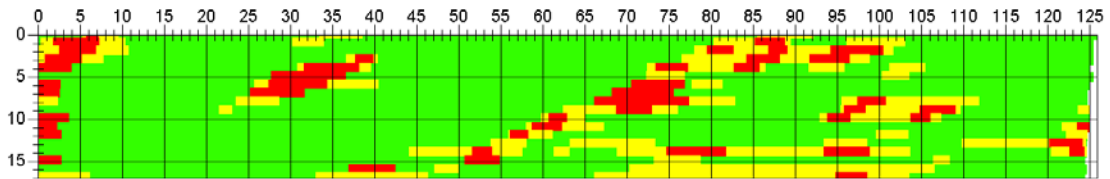
Good	Moderate	Severe
76%	15%	9%

Oakton
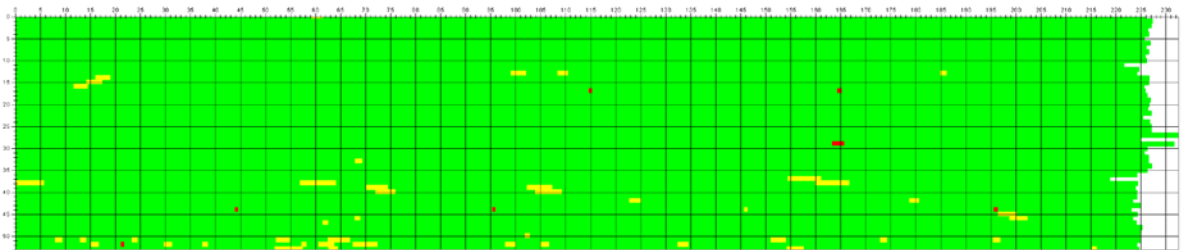
Good	Moderate	Severe
100%	0%	0%
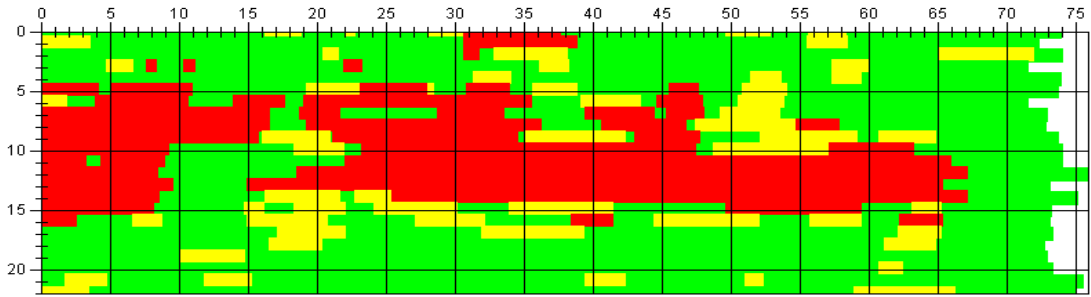
Good	Moderate	Severe
60%	13%	28%

P04798
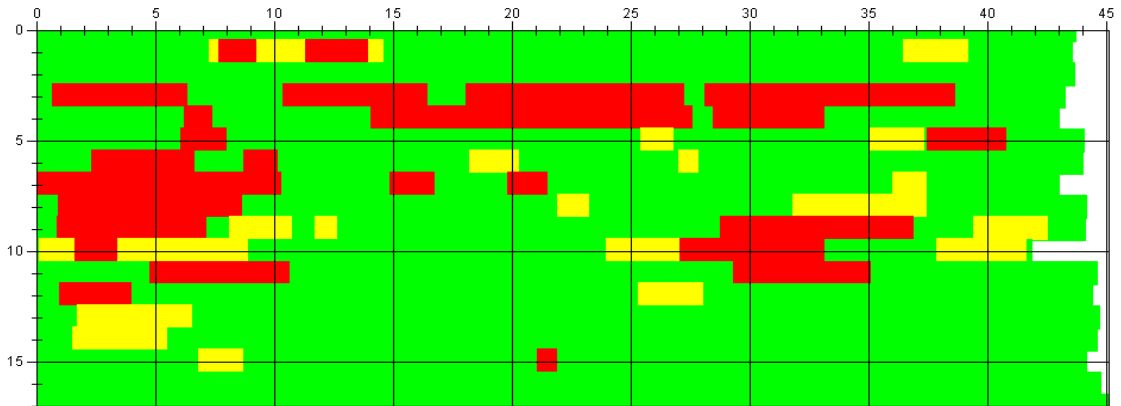
Good	Moderate	Severe
77%	7%	16%

P15878
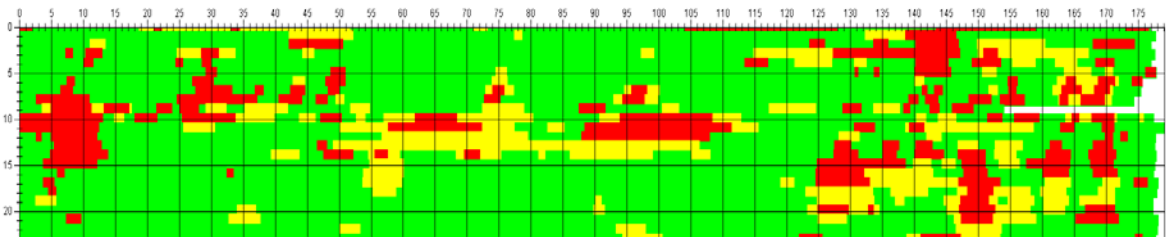
Good	Moderate	Severe
72%	14%	14%

P15878 (2014)
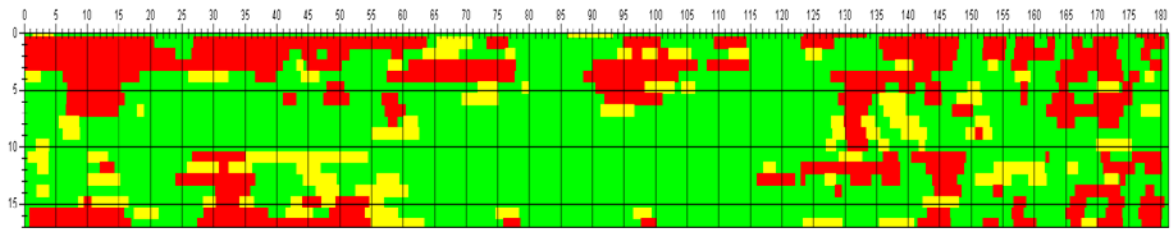
Good	Moderate	Severe
67%	10%	24%

Salt Creek
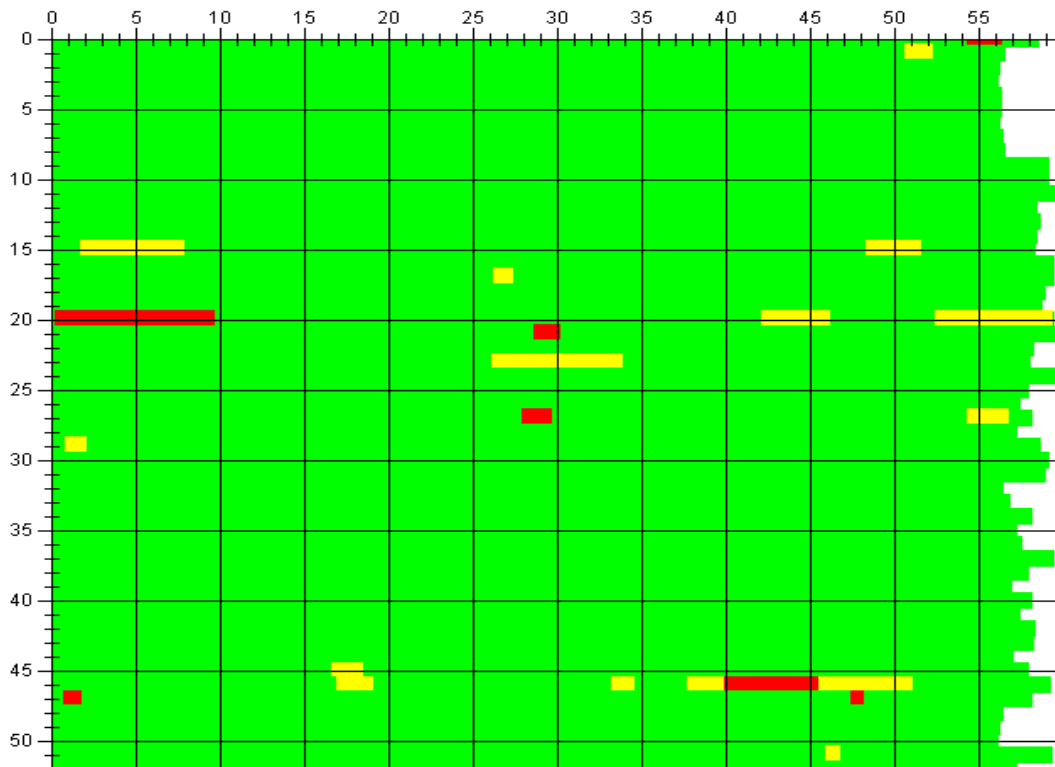
Good	Moderate	Severe
98%	2%	1%

7.5 Monte-Carlo Simulation Result

Crystal Ball Report - Full
Simulation started on
1/28/2015 at 2:26 PM
Simulation stopped on
1/28/2015 at 2:26 PM

Run preferences:
    Number of trials run   1,000,000
    Extreme speed
    Monte Carlo
    Seed   999
    Precision control on
      Confidence level   95.00%

Run statistics:
    Total running time (sec)   6.25
    Trials/second (average)   159,922
    Random numbers per sec   479,766

Crystal Ball data:
    Assumptions   3
      Correlations   0
      Correlation matrices   0
    Decision variables   0
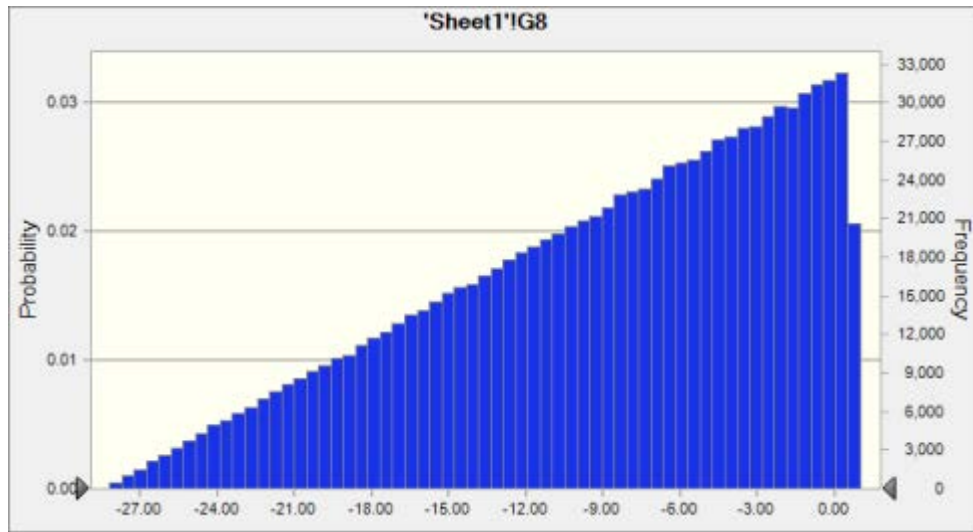   Forecasts   3

Forecasts

Worksheet: [Scale of bridges - Copy.xlsx]Sheet1

Forecast: G8

    Summary:
      Entire range is from 28.35 to 1.02
      Base case is 0.00
      After 1,000,000 trials, the std. error of the mean is 0.01

'Sheet1'!G8

	Forecast
Statistics:	values
Trials	1,000,000
Base Case	0.00
Mean	-8.89
Median	-7.71
Mode	---
Standard Deviation	6.89
Variance	47.49
Skewness	-0.5665
Kurtosis	2.40
Coeff. of Variation	-0.7749
Minimum	-28.35
Maximum	1.02
Range Width	29.37
Mean Std. Error	0.01

Forecast: G8 (cont'd)

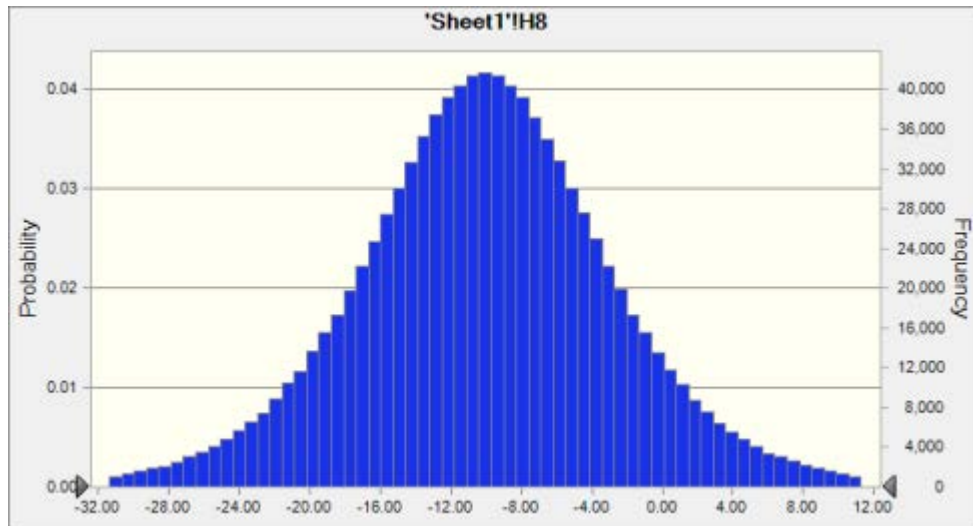|	Forecast
Percentiles:	values
0%	-28.35
10%	-19.15
20%	-15.31
30%	-12.37
40%	-9.89
50%	-7.71
60%	-5.74
70%	-3.93
80%	-2.24
90%	-0.65
100%	1.02

121

Forecast: H8

Summary:
    Entire range is from -66.65 to 50.16
    Base case is 0.00
    After 1,000,000 trials, the std. error of the mean is 0.01

Statistics:	Forecast values
Trials	1,000,000
Base Case	0.00
Mean	-10.05
Median	-10.06
Mode	---
Standard Deviation	7.60
Variance	57.81
Skewness	0.0013
Kurtosis	4.17
Coeff. of Variation	-0.7563
Minimum	-66.65
Maximum	50.16
Range Width	116.81
Mean Std. Error	0.01

Forecast: H8 (cont'd)

Percentiles: Forecast

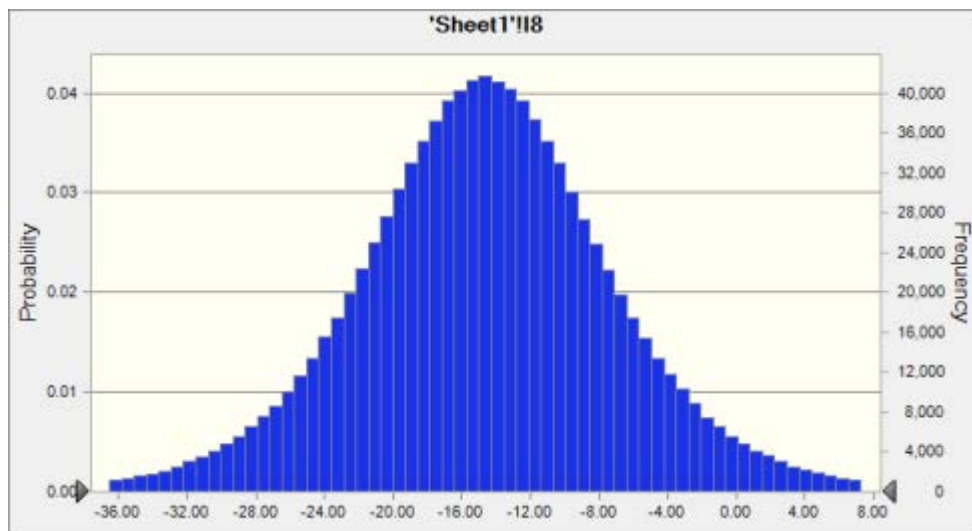|	values
0%	-66.65
10%	-19.29
20%	-15.87
30%	-13.60
40%	-11.76
50%	-10.06
60%	-8.36
70%	-6.50
80%	-4.23
90%	-0.83
100%	50.16

Forecast: I8

Summary:
Entire range is from -75.18 to 44.07
Base case is 0.00
After 1,000,000 trials, the std. error of the mean is 0.01

Statistics:	Forecast values
Trials	1,000,000
Base Case	0.00
Mean	-14.64
Median	-14.64
Mode	---

Standard Deviation	7.82
Variance	61.11
Skewness	-8.1462E05
Kurtosis	4.18
Coeff. of Variation	-0.5340
Minimum	-75.18
Maximum	44.07
Range Width	119.25
Mean Std. Error	0.01

Forecast: I8 (cont'd)

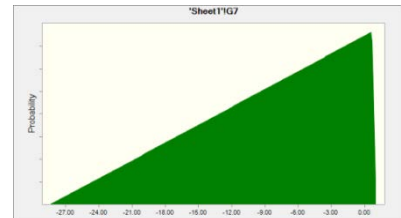| Percentiles:	Forecast values
0%	-75.18
10%	-24.10
20%	-20.62
30%	-18.31
40%	-16.39
50%	-14.64
60%	-12.89
70%	-10.99
80%	-8.66
90%	-5.15
100%	44.07

End of Forecasts

Assumptions

Worksheet: [Scale of bridges - Copy.xlsx]Sheet1

Assumption: G7

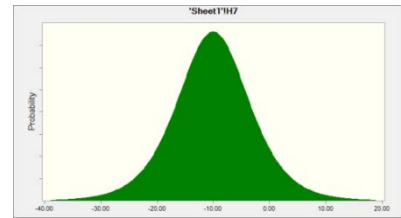| Triangular distribution with parameters:	
Minimum	-28.38
Likeliest	0.67
Maximum	1.03

Assumption: H7

Logistic distribution with parameters:

Mean   -10.04
Scale   4.19

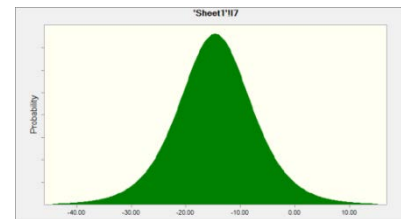## Assumption: I7

Logistic distribution with parameters:

Mean   -14.63
Scale   4.31

End of Assumptions